An *in vivo* RNAi screen identifies evolutionary conserved *Drosophila* fat storage regulators

Dissertation

zur Erlangung des mathematisch-naturwissenschaftlichen Doktorgrades

"Doctor rerum naturalium"

der Georg-August-Universität Göttingen

im Promotionsprogramm "Grundprogramm- Biologie"

der Georg-August University School of Science (GAUSS)

vorgelegt von

Jens Baumbach

aus Munster

Göttingen, den 27.03.2014

Betreuungsausschuss

PD Dr. Ronald P. Kühnlein,
Arbeitsgruppe Molekulare Physiologie, Max-Planck-Institut für biophysikalische Chemie

Prof. Dr. Herbert Jäckle,
Abteilung Molekulare Entwicklungsbiologie, Max-Planck-Institut für biophysikalische Chemie

Prof. Dr. Gregor Bucher,
Department of Developmental Biology, Georg August Universität Göttingen

Mitglieder der Prüfungskommission

Referent: PD Dr. Ronald P. Kühnlein,
Arbeitsgruppe Molekulare Physiologie, Max-Planck-Institut für biophysikalische Chemie

Korreferent: Prof. Dr. Herbert Jäckle,
Abteilung Molekulare Entwicklungsbiologie, Max-Planck-Institut für biophysikalische Chemie

....

Weitere Mitglieder der Prüfungskommission:

Prof. Dr. Gregor Bucher,
Department of Developmental Biology, Georg August Universität Göttingen

Prof. Dr. Reinhard Schuh,
Abteilung Molekulare Entwicklungsbiologie, Max-Planck-Institut für biophysikalische Chemie

Prof. Dr. André Fiala,
Abteilung Molekulare Neurobiologie des Verhaltens, Johann-Friedrich-Blumenbach-Institut für Zoologie und Anthropologie (Georg August Universität Göttingen)

Dr. Roland Dosch,
Department of Developmental Biochemistry, Universitätsmedizin Göttingen (Institut für Entwicklungsbiochemie)

Tag der mündlichen Prüfung: 22.04.2014

Vorveröffentlichungen der Dissertation

Teilergebnisse aus dieser Arbeit wurden mit Genehmigung des Betreuers in folgenden Beiträgen vorab veröffentlicht:

Publikationen

Baumbach, J. and Kühnlein, R.P. (2011). Body fat storage regulators revealed by an *in vivo* RNAi screen in *Drosophila.* MPIbpc News 11/12, 1-5

Baumbach, J., Hummel, P., Bickmeyer, I., Kowalczyk, K.M., Frank, M., Knorr, K., Hildebrandt, A., Riedel, D., Jäckle, H., and Kühnlein, R.P. (2014). A *Drosophila in vivo* screen identifies store-operated calcium entry as a key regulator of adiposity. Cell Metab. 19, 331–343.
Im Zusammenhang mit dieser Publikation wurden die Versuche zu Fig. 12B, 13C, 14B, 16N und 17B von Anja Hildebrandt durchgeführt und die Bilder zu Fig. 18D und 23C, D von Dr. Diemar Riedel aufgenommen.

Baumbach, J.*, Xu, Y.*, Hehlert, P., & Kühnlein, R. P. (2014). *Galphaq*, *Ggamma1* and *Plc21C* control *Drosophila* body fat storage. Journal of Genetics and Genomics, *accepted*
*geteilte Erstautorenschaft
Im Zusammenhang mit dieser Publikation wurden die Bilder zu den Fig. 31D und 32A von Yanjun Xu aufgenommen, der Grossteil der Versuche zu Fig. 33 von Yanjun Xu durchgeführt und die Versuche zu Fig 30B von Philip Hehlert durchgeführt.

Beiträge

Carmen Rotte (2014). Pressemitteilung- Neuer Regulator für Fettleibigkeit in Fliegen entdeckt*.* MPIbpc News 3, 3-4

Tagungsbeiträge

Regional *Drosophila* Meeting 2011- "An *in vivo* RNAi screen identifies evolutionary conserved *Drosophila* fat storage regulators" *(poster presentation)*

Workshop "Molecular Mechanisms of Development and Differentiation" (2011)- A body fat-based *in vivo* RNAi screen in *Drosophila* reveals conserved fat storage regulators *(talk)*

German Fly Metabolism Meeting 2011- A body fat-based *in vivo* RNAi screen in *Drosophila* reveals conserved fat storage regulators *(talk)*

Regional *Drosophila* Meeting 2012- "A body-fat based *in vivo* RNAi knockdown screen in *Drosophila* identifies the store-operated calcium entry as a fat storage regulatory pathway" *(talk)*

Bestätigung zur eigenständigen Anfertigung der wissenschaftlichen Arbeit:

Hiermit bestätige ich die folgendende Dissertation mit dem Titel "An *in vivo* RNAi screen identifies evolutionary conserved *Drosophila* fat storage regulators" selbstständig und ohne unerlaubte Hilfe/Hilfsmittel angefertigt zu haben.

……………………………………

(Jens Baumbach, Ort, Datum)

Table of contents

Table of Contents

Table of contents

Abbreviations

ACC	*Acetyl-CoA carboxylase*
ACS	*Acetyl Coenzyme A synthase*
Act5C	*Actin 5C*
ADP	adenosine diphosphate
AEL	after egg laying
Akh	Adipokinetic hormone
AkhR	AKH receptor
amp	ampulla
Arf79F	*ADP ribosylation factor at 79F*
ATGL	Adipose triglyceride lipase
ATP	adenosine triphosphate
BDSC	Bloomington *Drosophila* Stock Center
BMI	body mass index
Bmm	Brummer
bp	base pair
BSA	bovine serume albumin
c	Primary candidate
CAFE	capillary feeding
CaLexA	calcium-dependent nuclear import of *LexA*
Cam	Calmodulin
cAMP	3`-5`-cyclic Adenosine monophosphate
cc	corpora cardiaca
CCA	coupled colorimetric assay
Cct1	CTP:phosphocholine cytidylyltransferase
CDP	cytidine diphosphate
CDP-E	CDP-ethanolamine
cDNA	complementary DNA
cm	centimeter
co	cohorts
CoA	coenzyme A
cr	crop
CrebB	cyclic-AMP response element binding protein B
Crtc	CREB-regulated transcription coactivator
Cul-4	*Cullin-4*
d	day(s)
DAG	diacylglycerol
db	*diabetes*
dFOXO	*forkhead box, sub-group O*
Dgat1	Diacylglycerol transferase 1
Dm	*Drosophila melanogaster*
DN	dominant-negative
DNA	deoxyribonucleic acid
Drosophila	*Drosophila melanogaster*

Abbreviations

eas	*easily shocked*
e.g.	*exempli gratia*
eGFP	enhanced Green Fluorescent Protein
EM	electron microscopy
ER	endoplasmic reticulum
ey	*eyeless*
fa	*fatty a*
FA	fatty acids
Fas	*Fatty acid synthase*
FB	fat body
FC	body fat content
Fig.	figure
FLP	flipase
g	gramme
garz	*gartenzwerg*
gDNA	genomic DNA
GFP	Green Fluorescent Protein
GO	Gene Ontology
gof	gain of function
GPCR	G-protein coupled receptor
GRHR	gonadotropin-releasing hormones
h	hour(s)
HLH106	Helix loop helix protein 106
hpRNA	hairpin RNA
hs	heat shock
iCa^{2+}	intracellular Ca^{2+}
i.e.	*id est*
IGF	insulin-like growth factors
IIS	insulin/IGF-signaling
InR	Insulin receptor
IP3	Inositol-1,4,5,-tris-phosphate
IPC	insulin producing cells
Itp-r83A	Inositol-1,4,5,-tris-phosphate receptor
kb	kilo base pair
KD	knockdown
kDa	kilo Dalton
kg	kilogramme
kJ	kilojoule
kcal	kilocalories
L1	first instar larvae
L2	second instar larvae
L3	third instar larvae
lacZ	β-Galactosidase
LD	lipid droplet
LDAP	lipid droplet-associated proteins
LPA	lysophosphatidic acid

Abbreviations

M	molar
mdg	midgut
mdy	*midway*
mg	milligramme
mm	millimeter
MNC	median neurosecretory cells
mRNA	messenger RNA
miRNA	micro RNA
mt	malpighian tubules
µg	microgramme
µl	microliter
µm	micrometer
µM	micromolar
ng	nanogramme
nm	nanometer
ORF	Open Reading Frame
ORO	Oil Red O
PA	phosphatidic acid
PBS	phosphate buffered saline
PC	phosphatidylcholine
PCR	polymerase chain reaction
PE	phosphatidylethanolamine
Pect	Phosphoethanolamine cytidylyltransferase
Pka	Protein kinase A
Plin1	Perilipin1
PLM	phospholipid monolayer
POE	phosphoethanolamine
pv	proventriculus
qRT-PCR	quantitative reverse transcription polymerase chain reaction
rel.	relative
RFC	relative FC changes
RNA	ribonucleic acid
RNAi	RNA interference
RpL32	*Ribosomal protein L32*
rpm	revolutions per minute
rpr	*reaper*
RU486	mifepristone
SDS	sodium dodecyl sulfate polyacrylamide
SDS-PAGE	SDS-gel electrophoresis
sec	seconds
siRNA	small interfering RNA
sNPF	*short neuropeptide F*
SOCE	store-operated calcium entry
SREBP	Sterol regulatory element-binding protein
Stim	Stromal interaction molecule

Abbreviations

TA	transcriptional activator
TAG	triacylglycerol
TAL	Transkriptionsanalyselabor
TARGET	temporal and regional gene expression targeting
TLC	thin layer chromatography
to	*takeout*
Tub	Tubulin
GAL80ts	temperature sensitive GAL80
U	unit
UAS	upstream activating sequence
upd2	*unpaired 2*
VDRC	Vienna *Drosophila* RNAi Center
w	*white*
WHO	world health organization
wun2	*wunen-2*
w/v	weight per volume
y	*yellow*

1 Introduction

Health care is and will be one of the biggest challenges for humanity in the future. This includes the characterization of complex biological networks in order to develop novel therapeutic treatments. One of the biggest and most increasing problems in health care is obesity, which has doubled worldwide since 1980. Obesity is defined by excess body fat accumulation to an extent that it may have a negative effect on health. In addition, obesity is defined by a BMI (body mass index = kg/m^2) ≥30, whereby the prestage "overweight" is defined by a BMI ≥25<30. In fact, more than 1.4 billion adults of the age twenty and older were overweight and more than 500 million were obese (World Health Organization [WHO], 2008). Even more alarming is that more than 40 million children under the age of five were overweight in 2011. Beside the social consequences obesity can have, more worrisome are the effects on health. Obesity favors the development of major diseases like diabetes, musculoskeletal disorders, osteoarthritis, some kinds of cancer and cardiovascular diseases (mainly heart disease and stroke), which were the leading cause of death in 2008 (WHO, Fact sheet N°311, March 2013). These facts support the importance to understand the underlying causes for this disease. Since obesity is due to a disturbed energy homeostasis, the search for central regulators of this process is a promising way to understand the genetic basis for obesity. Actually, only few genes were shown to lead to obesity due to a direct mutation, *e.g.* mutants of the *Adipose triglyceride lipase* (ATGL) gene (Zimmermann *et al.*, 2004). Since energy homeostasis requires a very well defined tuning to adapt the energy needs of an organism even in periods of starvation or in response to rapidly increased energy consumption, various organs need to be regulated *via* intra-cellular signals or other signaling pathways. This leads to the assumption that obesity is caused by a disturbed modulation of several genes in a time- and tissue-dependent manner and thereby a disruption of energy homeostasis. Therefore, it is even more important to use a suitable and highly accessible model system, which allows the time- and tissue-targeted modulation of genes, in order to identify novel regulators of energy homeostasis.

1.1 Energy homeostasis and obesity

Energy homeostasis is an essential process for all animal organisms to adapt and survive under changing environmental and nutritional conditions. It consists of a finely tuned regulatory network of energy uptake, energy storage and the energy expenditure, which keeps the energy balance of a whole organism intact (Fig. 1).

Fig. 1 Network of energy homeostasis. The energy homeostasis depends on energy uptake, energy storage and energy expenditure. Energy uptake depends on the quality of the food and the food intake, whereby the food intake depends on the availability. Energy expenditure consists of the activity, the dietary thermogenesis and the metabolic rate. The energy storage serves as a "buffer" between energy uptake and expenditure to keep the organismal and cellular energy levels balanced. The main energy storage form is the neutral lipid triacylglycerol.
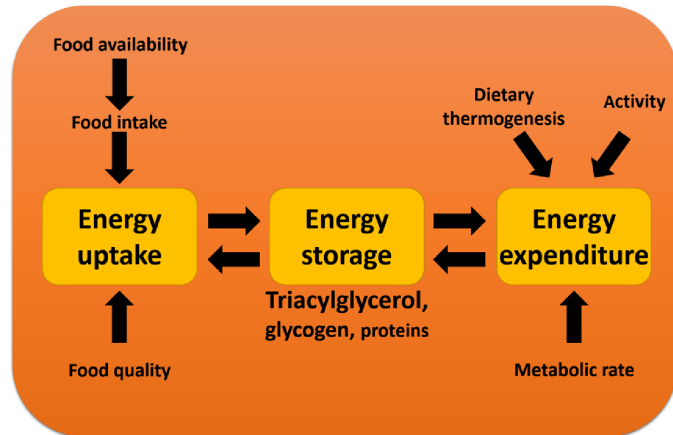
In this network, the energy expenditure depends on metabolic rate, activity and the thermogenic effects of feeding (Friedman, 2004; Guyenet and Schwartz, 2012). One major effort of energy homeostasis is to balance the total energy expenditure to the energy uptake. In higher animals, the energy uptake is mainly determined by the food intake. Most adult animals exhibit a discontinuous feeding behavior, whereas the expenditure is a dynamic but continuous process. This rises the need to store energy in order to buffer this imbalance.

But how are the cells of higher organisms able to keep the energy level relatively constant? To ensure that the internal energy level of the whole organism is balanced, complex regulations are necessary and the stored energy must be able to respond to periods of starvation or rapid energy consumption. Adenosine-5-triphosphate (ATP) is the energy currency of all organisms but its pool is tightly regulated and limited. For instance, locusts can fly for several hours, whereby the ATP pool in the locust flight muscle theoretically lasts for only a few seconds (Arrese and Soulages, 2010; Canavoso *et al.*, 2001). To maintain ATP levels,

energy storages from carbohydrates, proteins or triacylglycerol (TAG) are mobilized (Flatt, 1995). An example from an adult man with a body weight of 70 kg shows that 420.000 kJ (100.000 kcal) of the energy is stored in TAGs, 100.000 kJ (24.000 kcal) in proteins (mainly in muscles), 2.500 kJ (600 kcal) in glycogen and 170 kJ (40 kcal) in glucose (Stryer *et al.*, 2012). These facts highlight that the dominant energy storage form consists of neutral lipids (mainly TAGs), whereby TAGs are uncharged esters of fatty acids with a glycerol backbone and the fatty acids serve as the major fuel molecules. When fatty acids are mobilized from TAGs, they will be further oxidized by the β-oxidation to produce ATP (Stryer *et al.*, 2012). The reason why TAG and not glycogen was prefered during evolution is quiet simple. Glycogen has to be saved in a hydrated form, while TAGs are non-polar and stored in a nearly anhydrous form. Hence, to save the same amount of energy, glycogen storage would result in a higher mass than TAG. In addition, the complete oxidation of carbohydrates and proteins results in only 17 kJ/g (4 kcal/g), while oxidation of fatty acids results in 38 kJ/g (9 kcal/g). Conclusively, a normal 70 kg man would increase his total body weight by 64 kg, if he would store his energy completely in the form of glycogen (Stryer *et al.*, 2012). Therefore, most of the glycogen storage is limited to the muscles, where it can provide the energy much faster than stored TAGs. In general, all cells of an organism can synthesize and temporarily store lipids (Murphy, 2001) but the largest amount of lipids are stored in specialized tissues, *e.g.* liver and adipose tissue in vertebrates or the fat body in insects. The storage lipids can be either generated from dietary lipids or by *de novo* synthesis from other biochemical compounds like carbohydrates (Canavoso *et al.*, 2001). A chronic imbalance of energy homeostasis, for instance by increased food intake or reduced energy expenditure, could also affect the energy storage. This can result in a massive accumulation of energy in the form of storage lipids like TAG (Friedman, 2009; Guyenet and Schwartz, 2012; Speakman, 2004).

Since the energy storage is a central process in energy homeostasis, it is not surprising that cellular lipid storage regulators are conserved from yeast (Czabany *et al.*, 2007) over flies (Kühnlein, 2011) to mammals (Zechner *et al.*, 2012). Body

fat accumulation and obesity are to the current view mainly caused by environmental factors, like overeating and physical inactivity, but also genetic predispositions have a prominent role in the development of obesity. Since the occurrence of obesity in humans and therefore the prevalence of dangerous secondary diseases increased, several studies were performed to identify obesity-associated single nucleotide polymorphisms with the final aim to unvover the genetic basis for obesity. Based on these studies, severeal models were proposed, which can not completely explain the underlying mechanisms of obesity (reviewed in Speakman (2013)), which is likely due to its polygenic characteristics (Choquet and Meyre, 2011). At least some genetically obese or lean individuals have been identified in different animal species like nematodes (Ashrafi *et al.*, 2003), insects (Pospisilik *et al.*, 2010), mice (Haemmerle *et al.*, 2006) and man (Montague *et al.*, 1997). Conclusively, the identification of novel conserved energy homeostasis regulators is of high importance for the revealing of physiological and molecular mechanisms, which participate in obesity.

1.2 Body fat storage control

TAG is the most represented energy storage form in animal organisms and is stored in the adipose tissue, respectively called adipocytes in mammals and fat body in insects (Ahmadian *et al.*, 2010; Arrese and Soulages, 2010). Considerable, TAGs are not soluble in water, wherefore they need to be packed in a soluble container, the lipid droplets (LD) (reviewed in: Murphy (2012) and Stryer *et al.* (2012)). The fully differentiated adipocyte of mammals contains only a large (~100µm) single LD (Brasaemle *et al.*, 2004), while the LDs of the insect fat body vary in size (0.5-10µm) (Beller *et al.*, 2006). The LD consists of a phospholipid monolayer (PLM), which surrounds a core of neutral lipids, mainly TAG. LD-associated proteins (LDAP) are embedded in the PLM (Fig. 2; (Murphy, 2012)) and were shown to be involved in the regulation of TAG storage (Beller *et al.*, 2010).
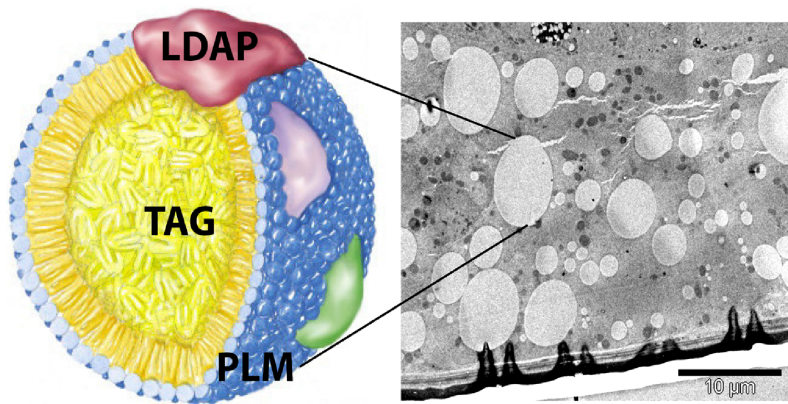
Fig. 2 Electron microscopy (EM) view and schematic composition of a lipid droplet (LD). Shown are LDs of the adult *Drosophila melanogaster* fat body, imaged by EM (scale is 10 µm). Blue: Phospholipid monolayer (PLM) unique for lipid droplets. Yellow: Stored lipids, mainly triacylglycerol (TAG). Red, green and purple: LD-associated proteins (LDAP). The schematic LD view (right) is modified after Kühnlein (2011).

Therefore LDs are highly metabolically active organelles (Liu *et al.*, 2004), which are important in lipid uptake and its transport (Murphy, 2012) besides the regulation of other cellular processes (Wu *et al.*, 2000). LDs are believed to be synthesized at the endoplasmic reticulum (ER), where the PLM is derived from the cytoplasm-oriented membrane leaflet of the ER (Hapala *et al.*, 2011). During the biogenesis of the LDs, neutral lipids like TAG, diacylglycerol (DAG) or sterol esters are incorporated into the inter-membrane space of the ER, whereupon filling the outer leaflet separates from the inner layer causing the budding of the LD.

To preserve the organismal energy homeostasis, complex physiological systems regulate the inter-organ communication between the adipose tissue, the central nervous system, the intestine, the liver, muscles and the pancreas, e. g. in mammals (reviewed in Guyenet and Schwartz (2012)). The communication between these organs is largely mediated *via* hormones like insulin, glucagon, leptin or cholecystokinin to provide short-term and long-term adaptions. While cholecystokinin is secreted by the digestive tract and leptin is secreted by adipose tissue, they both cause a feeling of satiety in the brain, which conclusively leads to less energy intake (reviewed in Guyenet and Schwartz (2012)). From the physiological site, both hormones are important, since leptin reports on the status of the triacylglycerol stores as a long-term control (Halaas *et al.*, 1995) and cholecystokinin relay satiety signals to the brain while eating is in progress as a short-term control (Moran and McHugh, 1982). Further long-term signals besides

leptin are the hormones insulin and glucagon. In contrast to leptin, insulin is secreted by the β-cells of the pancreas and reports the status of blood glucose (carbohydrates) to the brain (Stryer *et al.*, 2012). Also insulin was reported to regulate the orexigenic neuropeptide Y (NPY) in the brain (White *et al.*, 1990), which can cause the lack of proper food intake control and hyperphagia. The fact that insect short neuropeptide F (sNPF) is a functional homolog of mammalian NPY (Nässel and Wegener, 2011) supports an evolutionary conservation of this regulation. The antagonist of insulin is glucagon, which is also secreted by the pancreas. While insulin signals the fed state and stimulates the formation of glycogen and TAG, glucagon signals a low blood-glucose level (starvation state) and stimulates glycogen breakdown, gluconeogenesis by the liver and triacylglycerol hydrolysis by the adipose tissue. In agreement with this, insulin levels fall on starvation and rise with feeding and obesity, whereas glucagon shows an antagonistic regulation (Fig. 3 and Stryer *et al.* (2012)). Thus, inter-organ communication is central for energy homeostasis and body fat storage and an interference can cause obesity, which is shown in *e.g.* obese leptin receptor mutant *db/db* mice and *fa/fa* rats (Chua *et al.*, 1996).

Fig. 3 Energy homeostasis and body fat storage control by inter-organ communication. Eating behavior is controlled by the brain, whereby the energy from the diet is absorbed in the intestine and transported by the blood to either the storage organs (fat, adipose tissue; glycogen, liver) or directly to the energy consuming organs (*e.g.* muscles). The release and uptake of energy storage forms in mammals can be regulated by the hormones insulin (storage of glucose) and glucagon (release of glucose), whereby this regulation is connected to body fat storage/mobilization. The release of these hormones is regulated by the pancreas. The eating behavior in the brain can be controlled by either endocrine signals released by the digestive tract, like cholecystokinin, or the hormone leptin, which acts as a lipostatic signal. The release of leptin is controlled by the adipose tissue in proportion to the stored fat content. Both, leptin and cholecystokinin cause a feeling of satiety in the brain and consequently less eating. Scheme modified after Stryer *et al.* (2012).
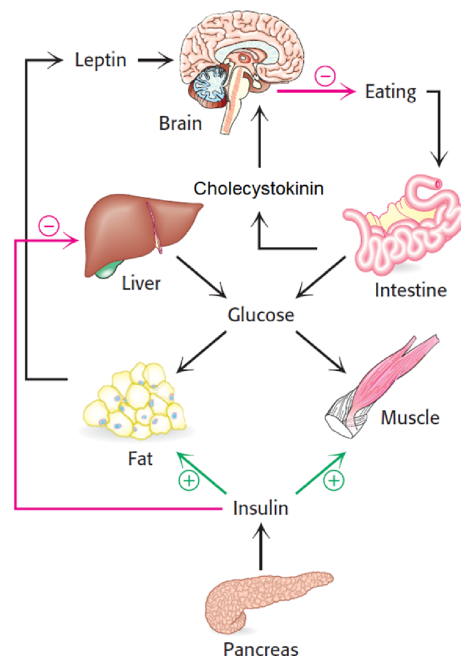
Introduction

Beside the importance of inter-organ communication in maintaining energy homeostasis, also cell-autonomous regulators are important. In the adipose tissue, regulators of lipogenesis and lipolysis play a critical role in adapting the energy stores to the acute energy needs of an organism. Conclusively, a chronic interference of lipogenesis or lipolysis in the adipose tissue affects the whole body fat storage and can cause obesity (Guyenet and Schwartz, 2012). The LD-associated protein Perilipin1 (Plin1) is a key regulator of TAG lipolysis in the adipocytes of mammals (Greenberg *et al.*, 1991) but also in fat body of the fruit fly *Drosophila melanogaster* (Beller *et al.*, 2006, 2010). It was shown that insect Plin1 can be phosphorylated by an Adipokinetic hormone (Akh)-mediated activation of Protein kinase A (Pka, (Patel *et al.*, 2005)), which causes an increased lipolytic activity in the insect fat body (Arrese and Wells, 1994). A similar mechanism also exists in mammals, whereby glucagon or adrenalin mediates the activation of PKA and the phosphorylation of PLIN1 (Londos *et al.*, 2005) followed by recruitment of ATGL (Lass *et al.*, 2006). ATGL was shown to be an important regulator in lipid storage mobilization (Zimmermann *et al.*, 2004) and catalyzes the hydrolysis of TAGs into DAGs. In *Drosophila*, the evolutionary conserved ATGL homolog Brummer (Bmm/*Dm*ATGL) was identified as a regulator of body fat control, whereby *bmm* knockout-mutant leads to obese flies (Grönke *et al.*, 2005) comparable to *plin1*-mutants. In both mutants lipolytic activity is reduced or delayed but still remains (Beller *et al.*, 2010), whereby a double-mutant causes a complete inhibition of lipolysis in *Drosophila* (Grönke *et al.*, 2007). On the other hand, an important regulator in lipogenesis is the Diacylglycerol acyltransferase 1 (Dgat1), which catalyzes synthesis of TAG from DAG and acetyl-CoA (Chen *et al.*, 2002). The fact that mice deficient for *Dgat1* (Smith *et al.*, 2000) or flies deficient for the fly homolog *midway* (*mdy/DmDGAT1*) are lean (Beller *et al.*, 2010) adds further support for an evolutionary conserved role of cell-autonomous regulators in energy homeostasis and body fat control of the whole organism. Due to the conservation of central lipid metabolism regulators, *Drosophila* can serve as a powerful model system to get a better understanding in the complex nature of obesity in humans.

1.3 *Drosophila melanogaster* as a model for fat storage research

The fruit fly *Drosophila melanogaster* is one of best described animal model organism due to the availability of a large number of tools. The whole genome of *Drosophila* is published (Adams *et al.*, 2000) and public databases like FlyBase (www.flybase.org) and FlyAtlas (www.flyatlas.org) even offer the option to check for expression patterns. The genome of *Drosophila* has a relatively small size of ~ 139.5 million base-pairs with 15662 genes on only four chromosomes (NCBI, http://www.ncbi.nlm.nih.gov/genome/47). The option to easily generate transgenic flies (Spradling and Rubin, 1982) was widely used to generate whole genome fly libraries. Constructs of these libraries can be designed to specifically target single gene activities by making use of the GAL4/UAS-system (UAS: Upstream Activating Sequence; (Brand and Perrimon, 1993)). Sequence analysis against the human genome also showed a high conservation for disease-related genes. In detail, 714 out of 929 distinct human disease genes searched, showed a homology to 548 unique *Drosophila* sequences (77%) (Reiter *et al.*, 2001). As mentioned under chapter 1.2, genes involved in lipid storage also show a homology to mammals, which makes *Drosophila* an even more attractive model organism in lipid research. Furthermore, *Drosophila*`s lifestyle contains most aspects of energy homeostasis (Fig. 1) with a short generation time (ten days at 25 °C), which offers the possibility to generate high fly numbers in a short period.

Drosophila`s lifestyle depends highly on its life cycle, which can be divided into four different stages. From embryogenesis over larval stages and pupae to adult flies it takes ten days of development (on 25 °C; Fig. 4 and Flagg (1988)). The development begins with the egg laying followed by the embryogenesis, which takes ~ 1 day. Since the *Drosophila* embryo is a not able to undergo energy intake (=food intake), most of the energy necessary for the development is provided by maternal contributions, *e.g.* by TAG loading to the egg. These TAGs are mainly stored in lipid droplets, which are spread throughout the whole embryo (Welte *et al.*, 1998). The importance of the maternal TAG contribution is demonstrated by embryos, which die if the contributed TAG amounts are too low to fulfill the organismal energy demands for development (Buszczak *et al.*, 2002).

Furthermore, during late embryonic development a specialized organ is differentiated from the mesoderm, the so-called fat body (Hartenstein, 1993), which is the major fat storage organ with liver-like functions (Canavoso *et al.*, 2001; Gilbert and Chino, 1974). When the embryos develop into larval stages they become continuous feeders (Zinke *et al.*, 2002). The high amount of energy is stored in the newly formed fat body as TAGs, to prepare the larvae for the next developing step. After approximately four days, the larvae stored enough energy in the fat body to undergo pupation and finally metamorphosis into the adult fly. The freshly hatched "immature" adult fly still contain remains from the larval fat body, which dissociated into ~780 adipocytes (Bodenstein, 1950; Demerec, 1994). The adipocytes vanish after approximately four days and the adult fat body replace them. These flies are called "mature" adult flies, since the fat body is now fully developed for the rest of the fly's life.
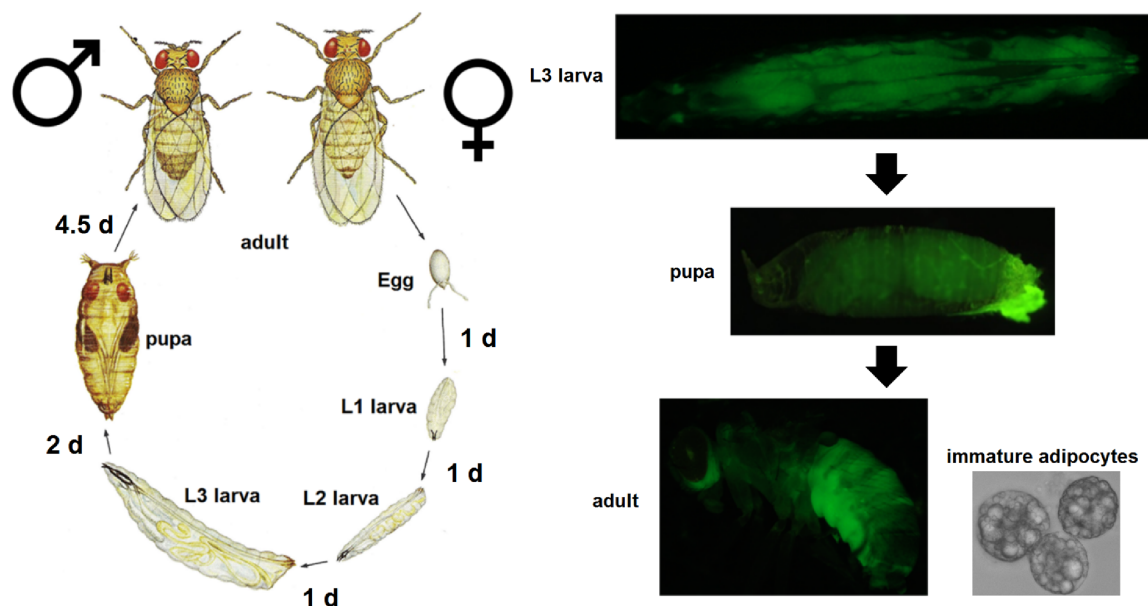
Fig. 4: Life cycle and fat storage tissues of *Drosophila*. Left Panel: At 25 °C, the L1 larva will hatch from the fertilized eggs in ~1 day. There are three larval instars, L1, L2 and L3 that last for 1 day, 1 day and 2 days, respectively. These larval instars are continuously feeding for 110 hours after egg laying (AEL) and the pupation occurs at 120 hours AEL. The period from pupation to the eclosion of the immature fly is approximately 4.5 days ((Ashburner, 1989); scheme modified after Carolina Biological Supply Company (2006)). Right panel: Shown is the fat body of the L3 larva, which is still intact in the pupa. After pupal stage and during the development of the immature to the mature adult fly, the larval fat body, which is still present in the form of adipocytes (lower right panel), dissociates and the adult fat body is finally formed. Fat bodies are marked by genetically encoded GFP (green) under the control of a chronic fat body driver (FB-Gal4).

Introduction

Like mammals, *Drosophila* regulates energy homeostasis adapted to the environment through nutrient-sensing pathways, *e.g. via* the insulin/IGF (insulin-like growth factors) signaling (IIS) pathway, which plays a key role in growth, metabolism, stress resistance, reproduction and longevity (Broughton and Partridge, 2009; Edgar, 2006). *Drosophila* encodes seven *Drosophila* insulin-like peptides (Dilps) with a characteristic spatio-temporal expression pattern, whereby only Dilp2, 3 and 5 could be detected in median neurosecretory cells (MNCs) of the adult fly brain (Broughton *et al.*, 2005; Grönke *et al.*, 2010). The ablation of the MNCs in early or late larval stages causes increased hemolymph carbohydrate levels, increased storage of lipids, elevated resistance to starvation/oxidative stress and an increased lifespan (Broughton *et al.*, 2005; Rulifson *et al.*, 2002). Under normal conditions, the Dilps bind to the Insulin receptor (InR), which transmits the signal *via* its substrate encoded by the gene *chico* to the central regulator Akt1 (Fig. 5). Due to activation of the InR, Akt1 gets phosphorylated (=activated) and inhibits the *Drosophila* Forkhead box O transcription factor (dFOXO) by excluding it from the nucleus (Edgar, 2006; Puig *et al.*, 2003). A mutation of either *InR* or *chico* can cause a massive body fat accumulation (Böhni *et al.*, 1999; Brogiolo *et al.*, 2001; Tatar *et al.*, 2001). Furthermore, overexpression of dFOXO in fat body was sufficient to enhance *bmm* gene expression and to promote lipid depletion (Wang *et al.*, 2011). Since *bmm* was shown to be a regulator of lipid mobilization (Grönke *et al.*, 2005), the observed effects of insulin signaling on lipid metabolism are likely mediated by dFOXO-dependent activation of *bmm* gene expression (Fig. 5).
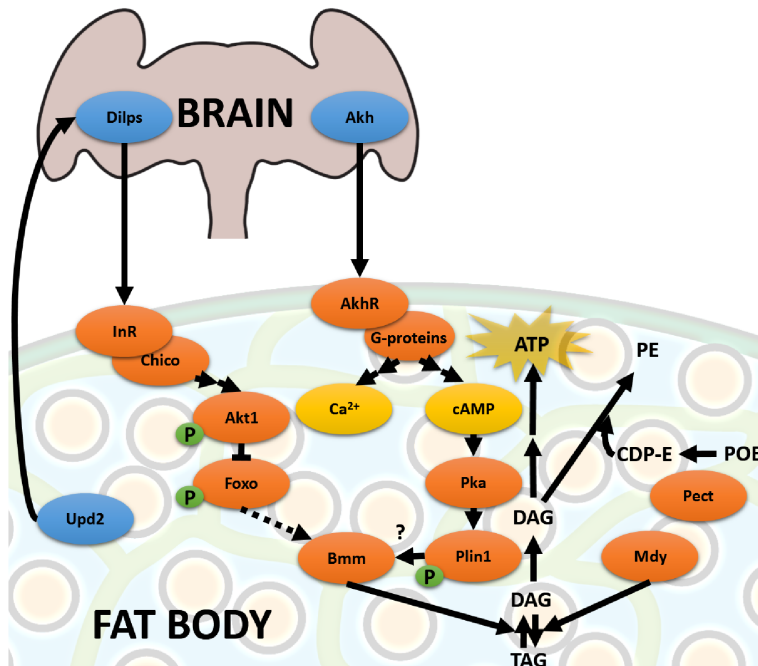
Fig. 5 Body fat storage regulation in *Drosophila*. The leptin homolog Unpaired 2 (Upd2) is secreted from the fat body and causes secretion of *Drosophila* insulin like peptides (Dilps) from the insulin pro-ducing cells (IPC) at the brain. Dilps act systemically and bind at target tissues like the fat body to the insulin receptor (InR), whereby the signal is trans-mitted over Chico to the central insulin signaling regulator Akt1. Akt1 becomes phosphorylated (=active) and in turn phospho-rylates the *Drosophila* forkhead box O transcription factor (dFOXO), which prevents dFOXOs transcriptional act-ivator activity and therefore transcription of the *brummer* (*bmm*) gene. The Adipokinetic hormone (Akh) is also secreted from the corpora cardiaca cells of the brain and acts systemically by binding to the Akh receptor (AkhR), mainly at the fat body. The signal is now transmitted over G-proteins and the second messengers Ca^{2+} and cAMP, whereby cAMP activates the Protein kinase A (Pka). Pka phosphorylates Perilipin 1 (Plin1), which in turn causes a lipolytic activity in the fat body. The Brummer lipase was also shown to consists of a lipolytic activity by converting the main storage fat triacylglycerol (TAG) to the transport form diacylglycerol (DAG). DAG can be further used to produce energy in the form of ATP or for the synthesis of membrane lipids like phosphatidylethanolamine (PE) by conversion with CDP-ethanolamine (CDP-E). CDP-E is provided by conversion from phosphoethanolamine (POE), which is catalyzed by the Phosphoethanolamine cytidylyltransferase (Pect). On the other hand DAG can also be converted back to TAG by the activity of Midway (Mdy). Proteins: orange; second-messenger molecules: yellow; secreted peptides: blue; phosphorylation signals: green.

Vice versa Drosophila lipid mobilization is regulated by the Akh-signaling pathway (Grönke *et al.*, 2007; Patel *et al.*, 2005). Akh is a short neuropeptide that interacts specifically with the Akh receptor (AkhR) to initiate lipid mobilization (Arrese and Wells, 1994; Lee and Park, 2004) and to inhibit protein (Orchard *et al.*, 1982), RNA (Lee and Goldsworthy, 1995) and lipid synthesis (Kodrík *et al.*, 2000) in a variety of insects. Akh was first described in *Locusta migratoria* (Stone *et al.*, 1976) and is phylogenetically related to vertebrate gonadotropin-releasing hormones (GRHR; (Lindemans *et al.*, 2011)), *e.g.* mammalian glucagon (Van der Horst *et al.*, 2001; Lee and Park, 2004). Accordingly, Akh is also involved in carbohydrate mobilization and in locomotion control and is therefore a central regulator of energy homeostasis in insects (Lorenz and Gäde, 2009). The Akh signaling is controlled

by the release from the corpora cardiaca (cc) cells of the ring gland, the major endocrine organ of insects (Noyes *et al.*, 1995; Stone *et al.*, 1976), where Akh is synthesized. The release of Akh in *Drosophila* is under control of the extracellular trehalose concentrations (Kim and Rulifson, 2004). Conclusively, the cc cells release Akh into the hemolymph in response to starvation or energy demanding activities, *e.g.* insect flight (Gäde and Auerswald, 2003; Van der Horst *et al.*, 2001). When Akh is released to the hemolymph it can bind to AkhR in target tissues like the fat body, where it initiates a G-protein-coupled receptor (GPCR) signaling (Staubli *et al.*, 2002; Ziegler *et al.*, 1995). As a consequence, a complex response is triggered by the second messenger cAMP and intracellular Ca^{2+} (iCa^{2+}; (Arrese *et al.*, 1999; Vroemen *et al.*, 1995), which results in Akh-dependent storage lipid mobilization (Fig. 5). This can be observed in diverse insect species like *Gryllus bimaculatus* (Anand and Lorenz, 2008)), *Manduca sexta* (Arrese *et al.*, 1996), but also *Drosophila melanogaster* (Grönke *et al.*, 2007). These findings support the importance of Akh-signaling in energy homeostasis, whereby the fat body responds in a context-dependent manner, which varies between different species- and developmental stages, likely to adapt to the different energy demands.

As in mammals, *Drosophila* also reckons up informations on nutrition, metabolism and systemic growth (Britton and Edgar, 1998) from the energy storing cells, mainly the fat body, back to the brain, whereby the fat body also serves as an nutrient sensing organ (Colombani *et al.*, 2003; Géminard *et al.*, 2009). While leptin is signaling the fed state in mammals, the fat body expressed cytokine Unpaired 2 (Upd2) is signaling to the central nervous system of *Drosophila* followed by a remote controlled release of Dilps from the insulin producing cells (IPCs) in the brain. This was shown by transgenic flies, which were subjected to an *upd2* knockdown in the fat body. These flies accumulate Dilp2 protein in the IPCs and are normophagic, hyperglycemic and lean likely due to reduced systemic insulin signalling (Rajan and Perrimon, 2012). Another regulator in the flies brain was shown to regulate the energy uptake (=food intake). A brain-specific up-regulation of *sNPF* can be induced by starvation (Hong *et al.*, 2012), which consequently causes an increased food intake. Conversely, a *sNPF* neuron-specific *sNPF*

interference reduces food intake (Lee *et al.*, 2004) and increases starvation sensitivity (Kahsai *et al.*, 2010).

Besides global regulators of energy homeostasis and body fat storage, *Drosophila* metabolism also includes cell-autonomous regulators. As mentioned in chapter 1.2, Plin1 (Beller *et al.*, 2006, 2010) and Bmm (Grönke *et al.*, 2010) are central regulators in lipid mobilization, whereby a double mutant of both regulators causes a complete loss of lipid mobilization on energy demanding conditions, *e.g.* starvation (Grönke *et al.*, 2007). Bmm was identified as a lipase (Grönke *et al.*, 2005) and converts the storage lipids TAG to DAG, which can be further mobilized by other enzymes to produce free energy in the form of ATP or for synthesis of new membrane lipids, *e.g.* phosphatidylethanolamine (PE), the main membrane lipid in flies (Fast, 1966). On the other hand, the regulator Plin1 is known to be phosphorylated by an Akh-mediated activation of Pka (Patel *et al.*, 2005), which causes an increased lipolytic activity (Arrese and Wells, 1994). Since an Akh overexpression in a *bmm*-mutant background still causes a massive storage lipid mobilization (Grönke *et al.*, 2007), Plin1 and Akh seems to be part of the activation, which involves another so far unknown lipase in *Drosophila* (Fig. 5). The fact that a *bmm*-mutant causes obesity and *bmm* can be induced by starvation, which can be mimicked by an overexpression of the gene resulting in lean animals (Grönke *et al.*, 2005), gives further support for the importance of this regulator. The antagonistic pathway to the lipid mobilization is the synthesis of new storage lipids. A key regulator of this pathway in flies is Mdy, which converts DAG to the lipid storage form TAG by adding acetyl-CoA. An overexpression of *mdy* causes obese and a knockdown causes lean flies (Beller *et al.*, 2010; Buszczak *et al.*, 2002). In a direct connection to lipogenesis/lipolysis is the generation of PE from DAG and CDP-ethanolamine. While DAG is a main intermediate in lipolysis/lipogenesis, CDP-ethanolamine is produced by the Phosphoethanolamine cytidylyltransferase (Pect), which is the rate-limiting step in the CDP-ethanolamine pathway of PE synthesis (Fullerton *et al.*, 2009) (Fig. 5 and 13A). The fact that a global *Pect* knockdown causes lipotoxic cardiomyopathy and obesity in flies (Lim *et al.*, 2011) adds further support for the link between the phospholipid and the glycerolipid

metabolism. Furthermore, a *Pect* knockdown causes the procession of the transcriptional activator Sterol regulatory element-binding protein (SREBP; also known as Helix loop helix protein 106 [HLH106]), which results in a lipogenic reponse by up-regulation of the *Acetyl-CoA carboxylase* (*ACC*) and *Fatty acid synthase* (*Fas*) genes (Dobrosotskaya *et al.*, 2002; Lim *et al.*, 2011).

Conclusively, it was shown that the metabolism of the fruit fly *Drosophila melanogaster* consists of energy homeostasis and body fat storage regulators on different levels, *e.g.* hormones, enzymatic actvities and second messengers. A finely tuned network of regulators and inter-organ communication is necessary to balance the energy intake, storage and expenditure of *Drosophila* to its energy demands, whereby a misregulation can cause obesity or leannes in flies.

1.4 The search for new fat storage regulators

As mentioned in chapter 1.1, the pandemic outspread of obesity catches scientific interest, which yields to genome-wide association studies. Furthermore, the approaches involved genome-wide scans in different ethnic populations to unveil chromosomal regions, which show linkage with obesity in large collections of families (Clement *et al.*, 2002) or the usage of single-gene mutant and genetically modified animal model organisms, which leads to the identification of genes and pathways that can regulate body fat storage (Brockmann and Bevova, 2002). Unfortunately, most of the regulator genes, which can cause obesity due to an interference, remain unknown in humans (Flier, 2004). Therefore, genetic screens in more accessible model systems like yeast (Daum *et al.*, 1999; Natter *et al.*, 2005), nematodes (Ashrafi *et al.*, 2003) or flies (Pospisilik *et al.*, 2010) were done. By these efforts, the limitations of mammalian model systems were bypassed and multiple evolutionary conserved obesity/anti-obesity genes were identified. Nevertheless, many regulators remain unknown, which consequently rises the need for further screening under different conditions.

As described in chapter 1.3, *Drosophila* offers several advantages as a model organism. This also includes the temperature-controlled *in vivo* TARGET system

(McGuire *et al.*, 2003), an enhancement of the GAL4/UAS-system, which allows to perform an *in vivo* modulation of gene activity in a time- and tissue-dependent manner (Fig. 6A; see chapter 4.1.1 for details). Thus, it is possible to induce the gene modulation in the desired tissue and developmental stage, which allows to exclude developmental effects by an adult-specific induction of the system. Alternatively, the so-called Gene Switch system acts very similar (Fig. 6B; (Roman *et al.*, 2001)), whereby the TARGET system is induced by a temperature shift and the Gene Switch system by addition of a drug called mifepristone (RU486) to the food of the flies.
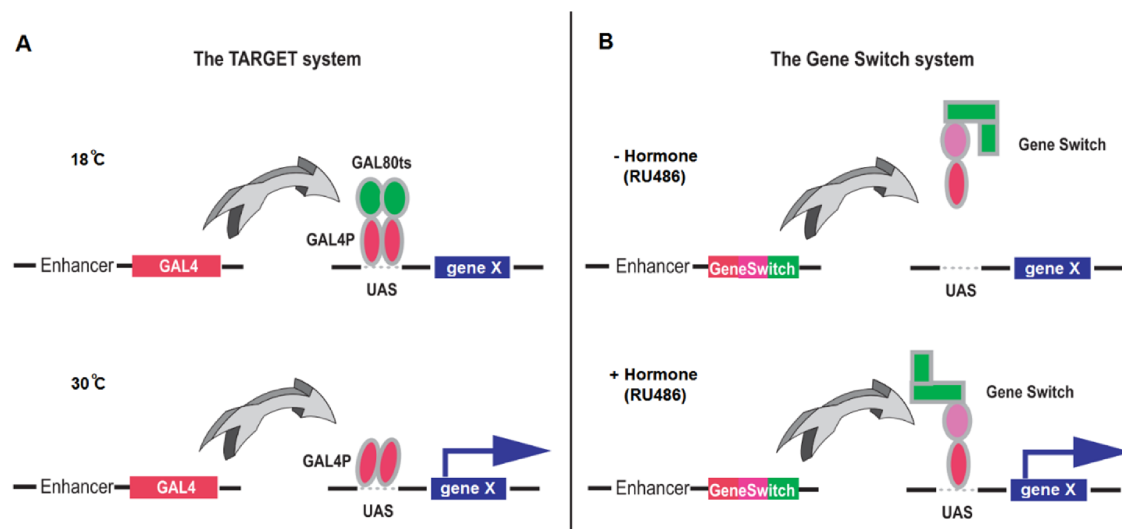
Fig. 6 Principle of the TARGET and the Gene Switch systems. The expression of a gene (gene X) or other constructs depends on the activation of its promotor UAS-element. Only if an activator binds to the UAS-element, the expression is activated. (**A**) In the TARGET system, a GAL4 can bind to an UAS-element directly, which can cause the expression of gene X. Under low temperature (18 °C) a temperature sensitive GAL80 (GAL80ts) binds to the GAL4, which prevents the expression of gene X. Due to a shift to higher temperature (30 °C) the GAL80ts is degraded and GAL4 can now activate the expression of gene X. (**B**) In the Gene Switch system this activator is a module, which is expressed under the control of an enhancer element. Also the module is in a conformational state, where it can not bind to the UAS-element. When the hormone mifepristone (RU486) is added, it binds to the Gene Switch module, causing conformational changes. Therefore the Gene Switch can bind the UAS-element followed by expression of the gene X. Scheme is after McGuire *et al.* (2004).

Another elegant tool to inhibit gene activity *via* the TARGET- or Gene Switch-systems is the usage of RNA interference (RNAi). The potent and specific genetic interference by doublestranded RNA was first described in *C. elegans* (Fire *et al.*, 1998) and was also sucessfully used in *Drosophila* (Piccin *et al.*, 2001). The

mechanism to interfere and regulate a specific mRNA by doublestranded RNA is also conserved in mammals (Elbashir *et al.*, 2001). As a part of the gene regulation in most eukaryotes, a non-coding guide miRNA can bind to so-called Argonaute-proteins. The resulting Argonaute–miRNA complexe then binds to complementary mRNAs, which results in the cleavage of the targeted mRNA. RNAi is a very similar process, whereby double-stranded RNAs, *e.g.* hairpin RNAs (hpRNA), are cleaved into 21-nucleotide fragments by Dicer proteins. This small interfering RNAs (siRNAs) are bound by the Argonaute proteins to form a RISC complex that finally cleaves complementary mRNAs resulting in a decreased gene activity. (Fig. (Meister and Tuschl, 2004)). By combination of the GAL4/UAS-system with the expression of inverted repeats, the tissue-specific expression of a specific hpRNA is possible, which consequently results in RNAi of the target gene (Fig. 7). Fortunately, UAS-RNAi libraries exist (Dietzl *et al.*, 2007), which allows large-scale *in vivo* gene knockdowns (KD) of most *Drosophila* genes.
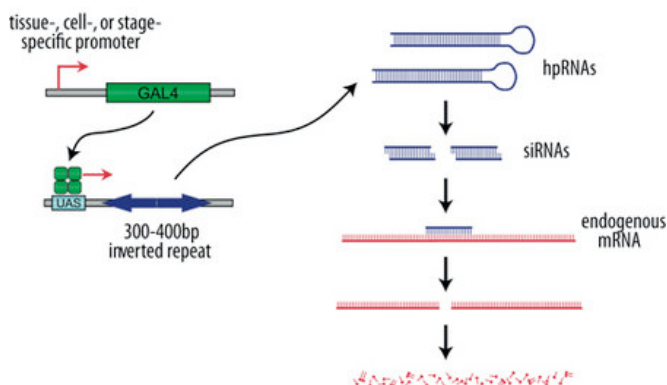
Fig. 7 GAL4/UAS-controlled RNAi in *Drosophila melanogaster*. The tissue-specific GAL4/UAS-system is used to drive the expression of a double-stranded hairpin RNA (hpRNA). The hpRNAs are processed into small interfering RNAs (siRNAs), which causes a sequence-specific degradation of the endogenous target mRNA. Scheme after http://stockcenter.vdrc.at/.

2 Results

2.1 Identification of novel body fat regulators by an *in vivo* fat storage-restricted RNAi knockdown screen in *Drosophila* adults

In order to identify new body fat storage regulators, a conditional large-scale fat storage-restricted *in vivo* gene knockdown screen in *Drosophila melanogaster* was performed. To identify the fat storage depots, *w*-control flies were fed on standard food at 25 °C for 6 days after hatching and the body fat storage depots were identified by doing cryosections and Oil Red O (ORO) staining of male flies. This staining showed a localization of body fat storage depots in the head fat body, the abdominal fat body and also parts of the midgut (Fig. 8 A+B I). Next, a conditional temperature-sensitive fat storage driver line (ts-FB-Gal4) was tested for its time- and tissue-dependent specificity and therefore its suitability for the screen by making use of the TARGET system (McGuire *et al.*, 2003). The ts-FB-Gal4 driver-line was crossed with flies expressing a nuclear ß-Galactosidase:eGFP (lacZ:eGFP) reporter. By splitting the progeny of this cross, which contains the ts-FB-Gal4 driver and the nuclear lacZ:eGFP reporter, to 30 °C (active-condition) and 18 °C (repressed-condition), I was able to switch on the reporter expression in a time- and tissue-dependent manner. This is shown by a blue nuclear lacZ-staining, specifically in the fat storage organs of the adult fly, *i.e.* the head/abdominal fat bodies and parts of the midgut (Fig. 8 A+B III), which implicates the tissue-specificity. The activity is also time-specific due the inhibitory effect of the GAL80ts on repressed-conditions (Fig. 8 A+B II) and the release of the effect on active-conditions (Fig. 8 A+B III). Therefore, the suitability of this expression system for a fat storage-restricted screen was demonstrated.
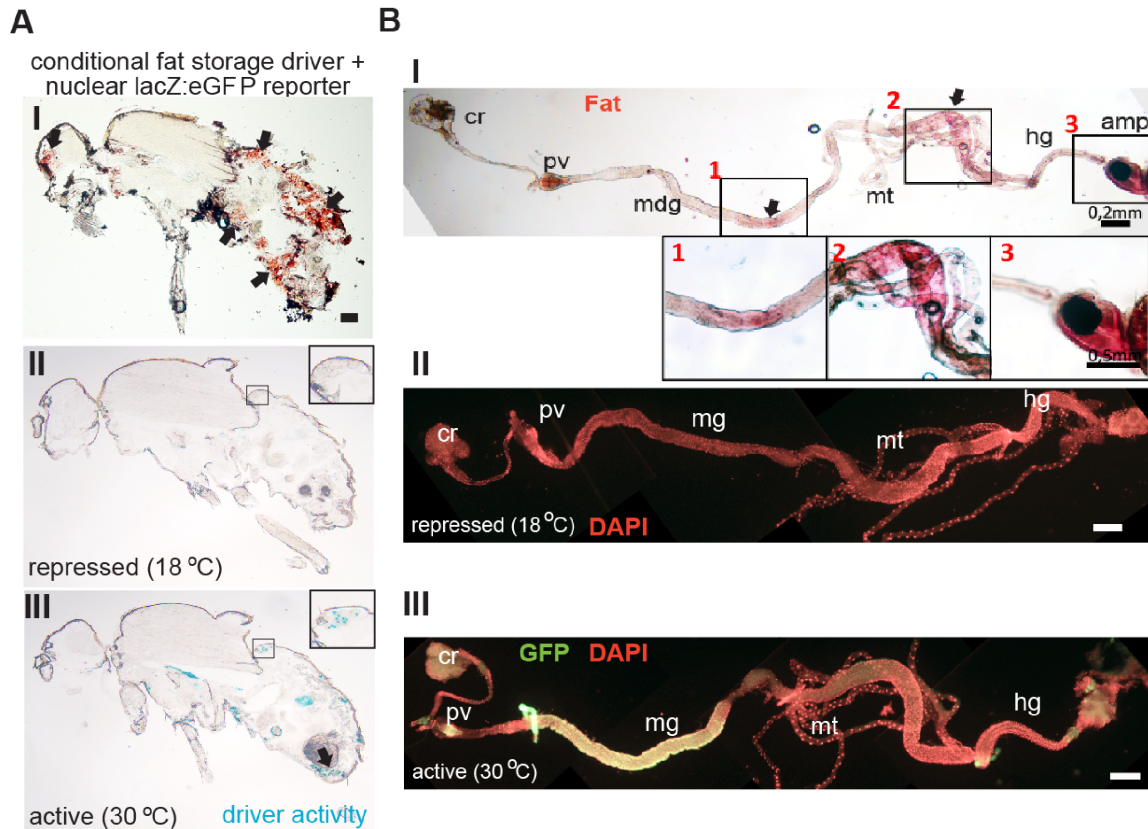
Fig. 8 Storage fat distribution in *w*-control flies stained with ORO (**A+B** I, marked by arrowheads and magnified, 1-3) **and conditional tissue-specific ts-FB-Gal4 driver activity** (**A+B** II+III, in blue). The progeny of a cross between the conditional ts-FB-Gal4 and the nuclear lacZ:eGFP reporter was analyzed (**A+B** II repressed condition; III active condition). By shifting the flies to active-conditions it was shown that the nuclear driver activity (blue in **A** II+III; green [GFP] in **B** II+III) is specific for the fat storage tissues of the abdominal fat body (arrows in **A**) or the midgut (**B**) of adult male flies (scale bar = 200μm; Abbreviations: cr: crop, pv: proventriculus, mg: midgut, mt: Malpighian tubules, hg: hindgut, amp: ampulla). Figure modified after Baumbach *et al.* (2014).

By making use of the TARGET system (see chapter 1.4 or 4.1.1 for details), the conditional ts-FB-Gal4 driver was crossed in a large-scale against transgenic UAS-RNAi effector fly lines (Dietzl *et al.*, 2007). In summary, the progeny was raised under repressed conditions until hatching of flies to prevent pre-adult gene knockdown activity. Flies were then shifted on active-conditions to induce RNAi-mediated gene knockdown for 6 days prior to body fat analysis (Fig. 9A). By this approach, early embryonic/larval/pupal lethality can be prevented and additional candidate genes can be identified, which would otherwise escaped the screening process.

Results
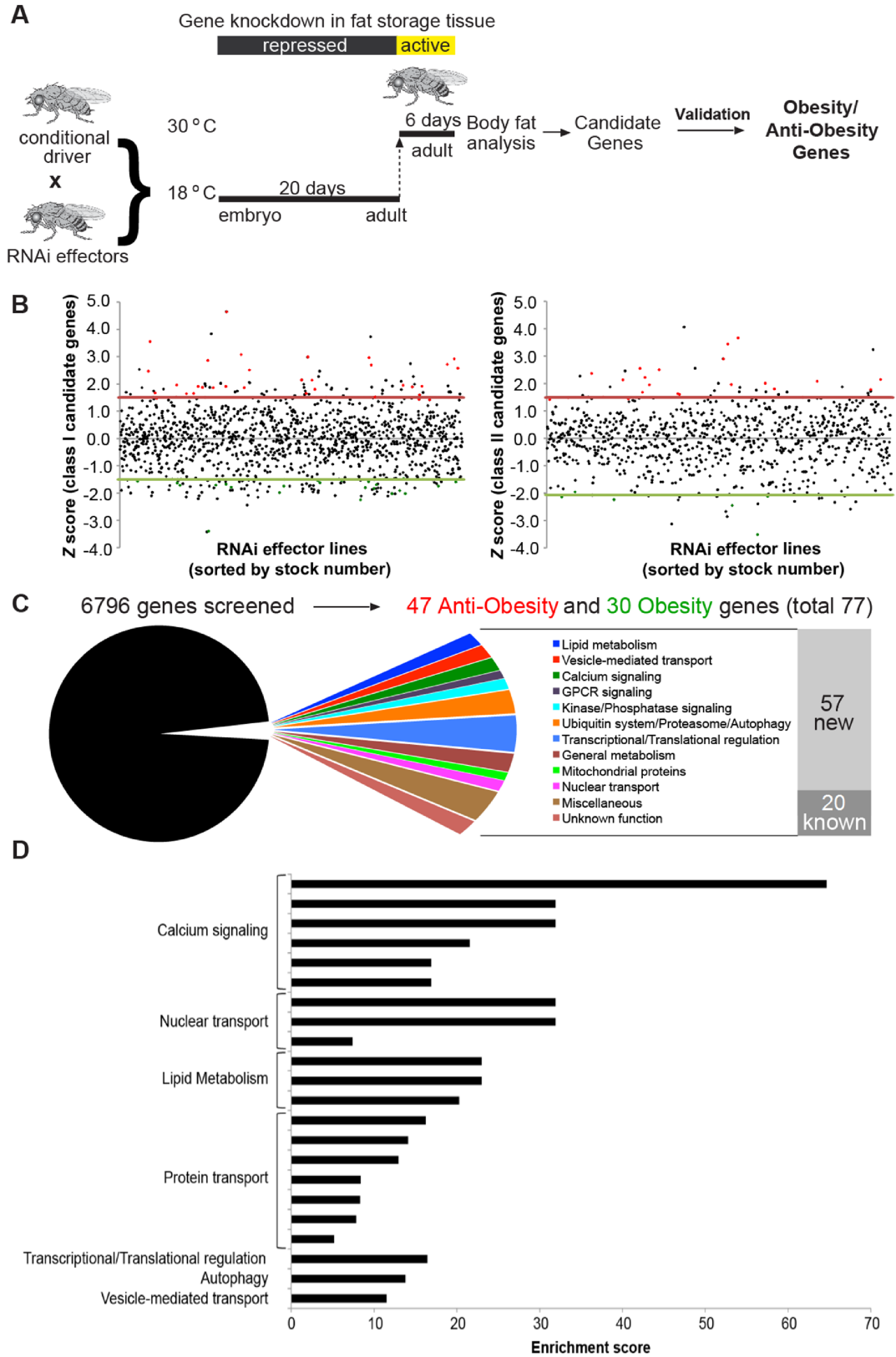
Results

Fig. 9 A conditional fat storage-restricted *in vivo* RNAi knockdown screen in *Drosophila* identified 77 obesity/anti-obesity genes involved in different pathways. (**A**) Schematic workflow of the fly obesity/anti-obesity gene identification. Progeny of the conditional ts-FB-Gal4 and RNAi effectors were raised under repressed conditions until hatching and shifted to active-conditions for 6 d prior to body fat analysis. Candidate genes were identified after two rounds of screening (primary and secondary). Obesity and anti-obesity genes were selected among the candidate genes by a restrictive *in silico* and experimental validation scheme. (**B**) Graphical representation of the final candidate gene identification based on body fat changes relative to all primary screen candidates (class I; left) or to individual controls (class II; right). Shown are plots of *Z* scores for all primary candidate fly lines subjected to class I or class II selection criteria with the thresholds for obese (red lines) and lean (green lines) candidate genes, respectively. Fly lines, which represent validated anti-obesity (red) and obesity (green) genes are highlighted by colored dots. (**C**) Numeric representation of the large-scale conditional gene knockdown screen results. In total, 6796 genes were analyzed in the screen, which identified 77 obesity/anti-obesity genes (1.1 %), whereof 57 (74%) were previously unknown body fat storage regulators. Functional classification (in colors) of all obesity/anti-obesity genes based on manually edited gene ontology term assignments. (**D**) A Gene Ontology (GO) analysis unveiled enriched (predicted) biological functions among the obesity/anti-obesity genes identified in the genetic screen (Filter criteria: $p<0.01$; enrichment factor >3; for details see Table S3). The enrichment factor represents the over-representation of genes associated with a particular GO term relative to all genes with the same GO term among the 6796 genes covered by the knockdown screen. Terms connected to "Calcium signaling" showed the highest enrichment. For an overview of all candidates identified in this screen, see Fig. 10 and Table S2. Gene Onotology analysis in (**D**) was done by Petra Hummel. The genetic screen was done by J. Baumbach, I. Bickmeyer, K.M. Kowalczyk, M. Frank, K.Knorr and R. P. Kühnlein (Baumbach *et al.*, 2014). Figure modified after Baumbach *et al.* (2014).

By analyzing the body fat content of these flies, the *in vivo* gene knockdown screen examined the effects of a functional impairment on the fly body fat storage. Gene knockdowns that caused flies with very low or high body fat content in comparison to the average of the cohorts (see Materials & Methods 4.1.2.1 for more details) were re-tested in a second round of screening to confirm a possible function as body fat storage regulators (Fig. 9A). For the secondary screens, either the average body fat content of the primary screen candidates (class I; Fig. 9B left) or control flies with the individual RNAi insertions but without the driver transgene (class II; Fig. 9B right) served as a reference regarding the body fat content. Furthermore, candidate fly RNAi-lines with a low target specificity were excluded to minimize false positive identifications and an experimental validation was done by using different adult fat body driver lines (*to*-Gal4 for autosomal lines; *yolk*-Gal4 for x-chromossomal lines) and/or alternative RNAi effector lines with unchanged target genes. Depending on the reproducibility of the primary screen results, a

validation score was assessed for the validation of candidate genes (see chapter 4.1.2.2 for more details, Table S2).

In total, the effects of 7524 RNAi effector strains targeting 6796 individual genes corresponding to 49% of all protein coding *Drosophila* genes were screened (see digital supplement Table S4 for a list of all tested genes/fly lines, modified after Baumbach *et al.* (2014)). After re-testing and validation, 77 (1.1%) genes were identified (Fig. 10), whereof the majority of them (57 genes, 74%) has not been previously associated with body fat control in the fly (Table S2). Among these, 47 gene knockdowns caused obese flies (called anti-obesity genes in the following) and 30 gene knockdowns caused lean flies (called obesity genes in the following). Also an *in silico* analysis with InParanoid reveals that the majority of the 77 obesity/anti-obesity genes (64; 83%) possess a human ortholog (Table S2 and Fig. 10). Interestingly, a pre-adult knockdown of the 77 obesity/anti-obesity genes, achieved by raising individuals on active-conditions over the whole development, resulted in pre-adult lethality of almost half of the identified genes (35; 45%, Table S2). This implicates essential functions for the newly identified obesity/anti-obesity genes in the developing fly. Since the corresponding individuals never developed into adult flies, these newly identified obesity/anti-obesity genes would have escaped the identification as body fat regulators by conventional mutant analysis. For further characterization and prioritization of the identified fly obesity and anti-obesity genes (Fig. 10 and Table S2), they were subjected to an *in silico* analysis by Gene Ontology (GO). For 55 (71%) obesity and anti-obesity genes at least one GO-term for "biological process" could be assigned. By a functional annotation of these GO-terms, diverse molecular and cellular processes including lipid metabolism, vesicle-mediated transport, and calcium signaling could be assessed (Fig. 9 C+D and Table S3). Therefore, the prioritization approach revealed these processes as important regulators of body fat storage and energy homeostasis.

In summary, a body fat-based large-scale *in vivo* RNAi screen (Baumbach *et al.*, 2014), which targets the fat storage tissues in a time- and tissue-dependent manner, identified 77 fly obesity and anti-obesity genes, including 57 novel ones.

Results

In addition, this screened revealed cellular processes beside the lipid metabolism to have an effect on body fat storage. In fact, the GO-terms for calcium signaling (regulation of ion transport) were highly enriched, which prefers this process for further analysis in the context of this work.

Functional class   *Anti-Obesity gene/short name* **or** *Obesity gene/short name* **(human ortholog)**

■ **Lipid metabolism**

Adipokinetic hormone receptor/AkhR (GNRHR), *brummer/bmm* (ATGL), *Phosphoethanolamine cytidylyltransferase/Pect* (PCYT2)

midway/mdy (DGAT1), *CG14512*

■ **Vesicle-mediated transport**

ADP ribosylation factor 79F/Arf79F (ARF1), *sec71* (ARFGEF1/2), *stenosis/sten* (SEC24C), *CG5484* (YIF1B), *Ykt6*

■ **Calcium signaling**

Calmodulin/Cam (CALM), *purity of essence/poe* (UBR4), *Stromal interaction molecule/Stim* (STIM1)

Calcium ATPase at 60A/Ca-P60A (ATP2A2), *olf186-F* (ORAI3)

■ **GPCR signaling**

G protein α49B/Ga49B (GNAQ), *G protein γ 1/Gγ1* (GNG12), *Leucine-rich repeat-containing G protein-coupled receptor 1/Lgr1* (LHCGR)

■ **Kinase/Phosphatase signaling**

CG9238 (PPP1R3C)

multiple ankyrin repeats single KH domain/mask (ANKHD1), *punt/put* (ACVR2), *CG16903* (CCNL1)

■ **Ubiquitin system/Proteasome/Autophagy**

COP9 complex homolog subunit 4/CSN4 (COPS4), *Aut1* (ATG3), *Ecdysone-induced protein 74EF/Eip74EF*

Proteasome α5 subunit/Prosα5 (PSMA5), *Proteasome β3 subunit/Prosβ3* (PSMB3), *Regulatory particle non-ATPase 6/Rpn6* (PSMD11), *Regulatory particle non-ATPase 7/Rpn7* (PSMD6), *Regulatory particle non-ATPase 8/Rpn8* (PSMD7), *Fbw5* (FBXW5)

■ **Transcriptional/Translational regulation**

bip2 (TAF3), *Retinal Homeobox/Rx, Rpd3* (HDAC2), *split ends/spen* (SPEN), *Br140* (BRD1), *CG6272* (CEBPG), *CG6937* (MKI67IP)

Es2 (DGCR14), *held out wings/how* (QKI), *ftz transcription factor 1/ftz-f1* (NR5A2), *Eukaryotic initiation factor 1A/eIF-1A* (EIF1AX), *Suppressor of variegation 3-9/Su(var)3-9* (SUV39H2), *Ribosomal protein L26/RpL26* (RPL26L1), *lethal (2) NC136/l(2)NC136* (CNOT3)

■ **General metabolism**

antdh (DHRS11), *Carbonic anhydrase 2/CAH2, Tyramine β hydroxylase/Tbh* (DBH), *CG10166* (DPM1), *CG15890, CG31915* (COLGALT2), *CG9940* (NADSYN1)

■ **Mitochondrial proteins**

tamas/tam (POLG), *CG4743* (SLC25A26), *CG3214* (NDUFA12)

■ **Nuclear transport**

Cullin-4/Cul-4 (CUL4B)

CAS/CSE1 segregation protein/Cas (CSE1L), *Megator/Mtor* (TPR), *Nuclear transport factor-2/Ntf-2* (NUTF2)

■ **Miscellaneous**

Na,K-ATPase Interacting/NKAIN, Related to the N terminus of tre oncogene/RN-tre (TBC1D3), *Vacuolar H+ ATPase M8.9 accessory subunit/VhaM8.9* (ATP6AP2), *Vacuolar H+ ATPase subunit 16-1/Vha16-1* (ATP6V0C), *CG7379* (ING2), *CG7770* (PFDN6), *unc-45* (UNC45B), *CG6750* (EMC3), *CG14210*

Lasp, pecanex/pcx (PCNXL), *pollux/plx*

■ **Unknown function**

CG15142, lethal (2) 05714/l(2)05714

lethal (3) 05822/l(3)05822, CG14270 (C19orf52), *CG3500* (TEX261), *CG15618* (THADA)

(Fig. 10 legend on next page)

26

Fig. 10 A conditional body fat based *in vivo* RNAi screen identified 77 fly obesity and anti-obesity genes. Shown are the full and short names of all identified *Drosophila* anti-obesity (red) or obesity (green) genes, their respective human orthologs (black) and the functional classification (in colors) based on manually edited Gene Ontology term assignment. For more details see Table S2 and S3. The genetic screen was done by J. Baumbach, I. Bickmeyer, K.M. Kowalczyk, M. Frank, K.Knorr and R. P. Kühnlein (Baumbach *et al.*, 2014). Figure modified after Baumbach *et al.* (2014).

2.2 Characterization of anti-obesity/obesity genes involved in lipid metabolism

In order to confirm the validity of the novel screening approach for the identified obesity and anti-obesity regulators, previously known obesity/anti-obesity genes, which were also identified by the screen, were further analyzed by independent methods for their body fat content. The *Drosophila* diacylglycerol O-acyltransferase (*Dm*DGAT1) encoded by the *midway (mdy)* gene (Beller *et al.*, 2010; Buszczak *et al.*, 2002) and the triacylglycerol (TAG) lipase encoded by *brummer* (*bmm/DmATGL*) (Grönke *et al.*, 2005) are previously described body fat storage regulators, where *mdy* is central for lipogenesis and *bmm* is central for lipolysis. Since both genes were among the 77 identified obesity/anti-obesity genes, they were chosen to validate the novel screening approach (Table S2 and Fig. 11).

The central regulator of lipogenesis *mdy* was identified as an obesity gene. In agreement with this result, a fat storage-restricted RNAi KD of *mdy* phenocopied the effects of a *mdy*^{QX25}-mutant and leads to lean flies. This is shown by determination of body fat levels using a coupled colorimetric assay (CCA, Fig. 11A; 40% total body fat reduction in RNAi ON and 70% in *mdy*^{QX25} flies) and quantification of separated lipid classes by thin layer chromatography (TLC, Fig. 11B), which directly shows the depletion of the main storage lipid TAG. Moreover, a lipid depletion could be observed in the subcutaneous abdominal fat body in response to the *mdy* knockdown (Fig. 11C) that confirmed the tissue-specific response of the body fat modulation.

A

B

C
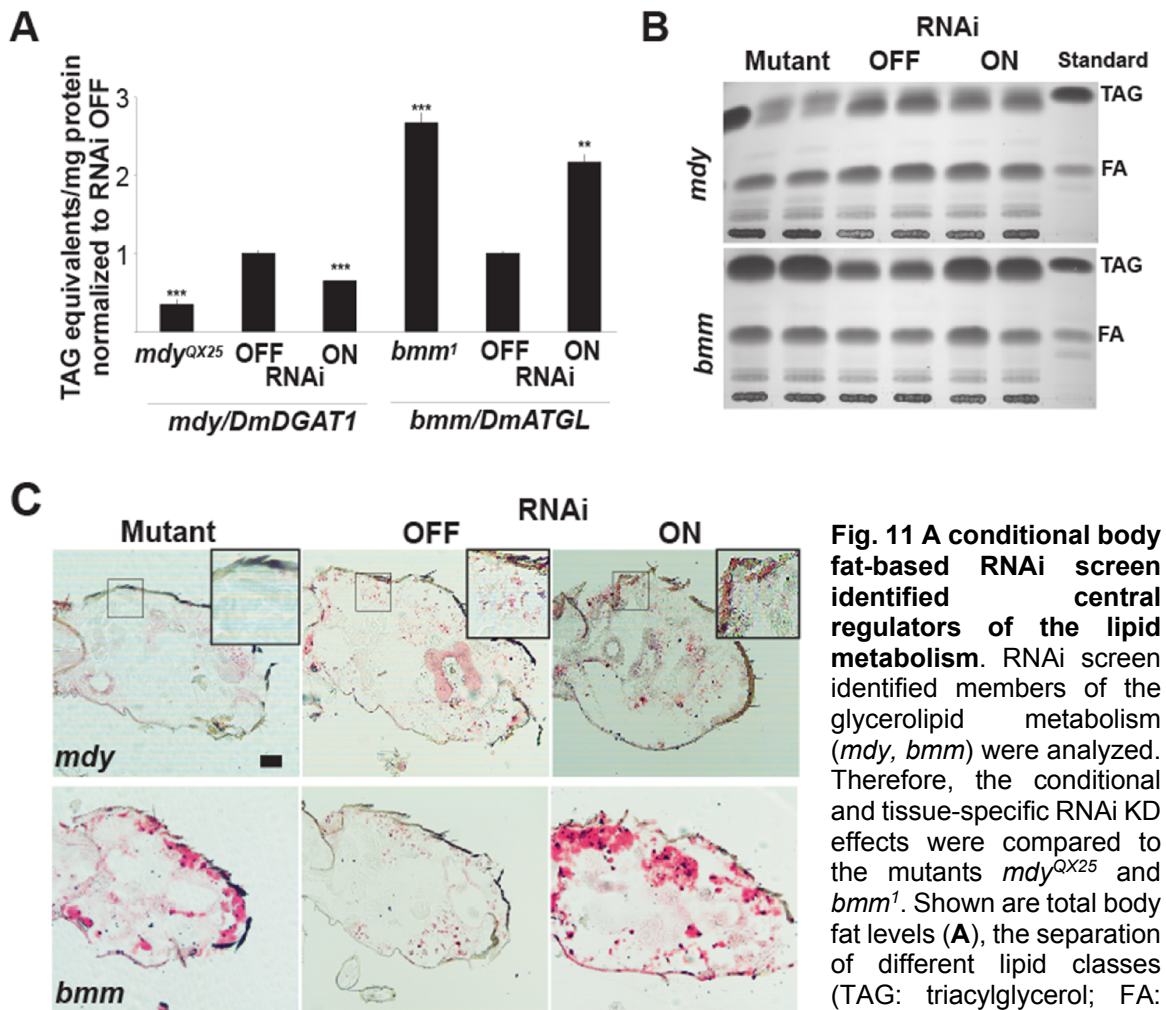
Fig. 11 A conditional body fat-based RNAi screen identified central regulators of the lipid metabolism. RNAi screen identified members of the glycerolipid metabolism (*mdy, bmm*) were analyzed. Therefore, the conditional and tissue-specific RNAi KD effects were compared to the mutants *mdy*^{QX25} and *bmm*^{1}. Shown are total body fat levels (**A**), the separation of different lipid classes (TAG: triacylglycerol; FA: fatty acids) by thin layer chromatography (**B**), and ORO staining on sagittal cryosections of adult male fly abdomen (**C**). TLC in (**B**) was done by Anja Hildebrand (Baumbach *et al.*, 2014). **p≤0.01 and ***p≤0.001 for all comparisons to RNAi OFF. Scale bar represents 100µm. Figure after Baumbach *et al.* (2014).

To show that also anti-obesity genes could be identified by the screening approach, the well-characterized lipid mobilization regulator *bmm* (Grönke *et al.*, 2005) was analyzed by the above described methods. A fat storage-restricted RNAi KD as well as a *bmm*^{1}-mutant caused a dramatic accumulation of total body fat (Fig. 11A; +90% total body fat accumulation in RNAi ON and +130% in *bmm*^{1} flies) and TAG (Fig. 11B). Furthermore, these effects were specific to the fat body, which is shown by ORO-stained cryosections (Fig. 11C).

In summary, it could be shown that obesity and anti-obesity genes identified by our screening approach can be evaluated by a CCA, TLC and ORO staining of cryosections. In addition, it could be exposed that the observed global body fat changes, primarily determined by a CCA, are due to changed levels of the main storage lipid TAG, which is predominantly stored in the subcutaneous abdominal fat body.

2.2.1 Interference of phospholipid metabolism causes massive body fat accumulation

In addition to the in chapter 2.1 described genes in the glycerolipid metabolism, a central regulator of the phospholipid biosynthesis was identified as a critical anti-obesity gene in the adult fly. The *Pect/DmPCYT2* gene encodes a phosphoethanolamine (PE) cytidylyltransferase, which is the fly homolog of mammalian PCYT2. Since this enzyme catalyzes the rate-limiting step "phosphoethanolamine to CDP-ethanolamine" in the CDP-ethanolamine pathway of PE synthesis (Fullerton *et al.*, 2009), it is a central regulator of the phospholipid synthesis. The synthesized CDP-ethanolamine is further combined with diacylglycerol (DAG) to generate PE. DAG is a common precursor for the PE pathway as well as for the Kennedy pathway of TAG biosynthesis. Therefore, phospholipid and glycerolipid metabolisms are interconnected *via* the need for DAG as a substrate/intermediate (Fig. 12A).

A fat storage tissue-specific KD of *Pect* mediated by two independent RNAi effector lines caused an up to 190% increase in fly body fat content (Fig. 12B) and an increase in TAG storage (Fig. 12C), which can also be observed as enhanced ORO staining in the subcutaneous abdominal fat body of sagittal cryosections (Fig. 12D). Additionally, the TLC was quantified for the relative DAG amount compared to RNAi OFF controls, which revealed a doubled body DAG content (Fig. 12B). Furthermore, a possible influence to lipogenesis on the transcriptional level was analyzed by a quantitative reverse transcription polymerase chain reaction (qRT-PCR) on the *Fas*, *ACC*, *Acetyl Coenzyme A synthase (ACS)* and *mdy* gene

expression. In agreement with the observed TAG and DAG accumulation, these lipogenesis genes are significantly up-regulated (Fig. 12E), which is consistent with the nodal role of *Pect* in PE and TAG biosynthesis.
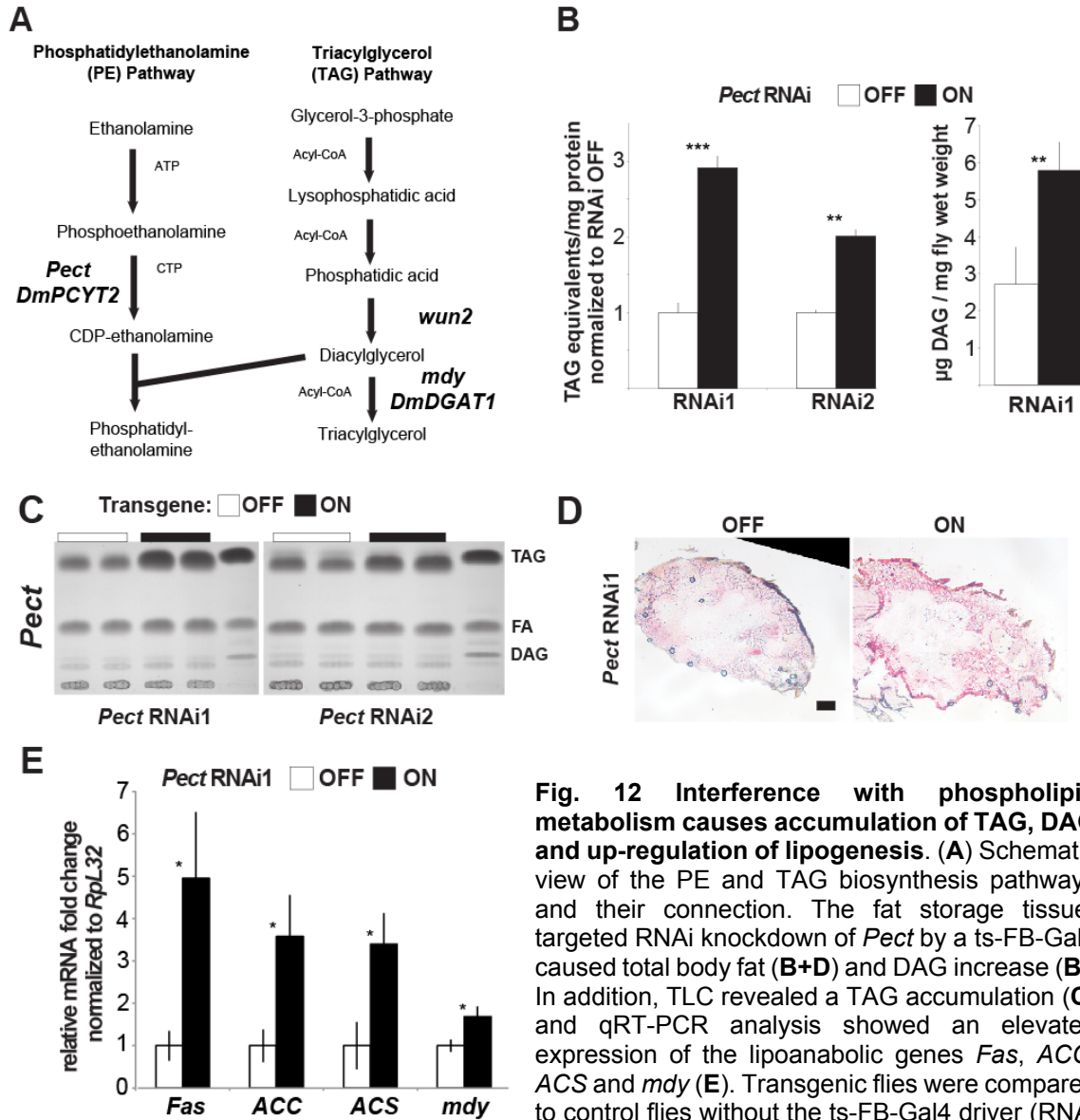
Fig. 12 Interference with phospholipid metabolism causes accumulation of TAG, DAG and up-regulation of lipogenesis. (**A**) Schematic view of the PE and TAG biosynthesis pathways and their connection. The fat storage tissue-targeted RNAi knockdown of *Pect* by a ts-FB-Gal4 caused total body fat (**B+D**) and DAG increase (**B**). In addition, TLC revealed a TAG accumulation (**C**) and qRT-PCR analysis showed an elevated expression of the lipoanabolic genes *Fas*, *ACC*, *ACS* and *mdy* (**E**). Transgenic flies were compared to control flies without the ts-FB-Gal4 driver (RNAi OFF). TLC in (**C**) was done by Anja Hildebrand (Baumbach *et al.*, 2014). *p ≤ 0.05, **p≤0.01 and ***p≤0.001 for all comparisons to RNAi OFF. Scale bar represents 100 µm. Figure modified after Baumbach *et al.* (2014).

In summary, a conditional fat storage tissue-specific KD of the central PE synthesis gene *Pect* causes a body fat and DAG/TAG accumulation, which is mediated by an activation of the lipogenesis genes *Fas, ACC, ACS* and *mdy*.

2.2.2 Knockdown of the glycerolipid regulator *wunen-2* causes leanness in adult male flies

In the context of the *in vivo* RNAi screen, the lipid metabolism gene *wunen-2 (wun2)* was identified as a candidate gene and was further analyzed by a CCA, by TLC and by ORO staining of sagittal cryosections. The *wun2* gene encodes a lipid phosphate phosphatase, which was shown to dephosphorylate lysophosphatidic acid (LPA) and phosphatidic acid (PA) to DAG *in vitro* (Fig. 12A) (Renault *et al.*, 2004). An adult fat storage-restricted knockdown of *wun2* caused lean flies with a substantial reduction in global body fat by 59% (Fig. 13A). Furthermore, the total TAG content and the subcutaneous fat storage was decreased (Fig. 13B, C).

Accordingly with the lean phenotype and its substrate specificity for LPA and PA, which are both intermediates in the TAG biosynthesis (Fig. 12A), *wun2* seems to be an important fat storage regulator in the TAG biosynthesis pathway.
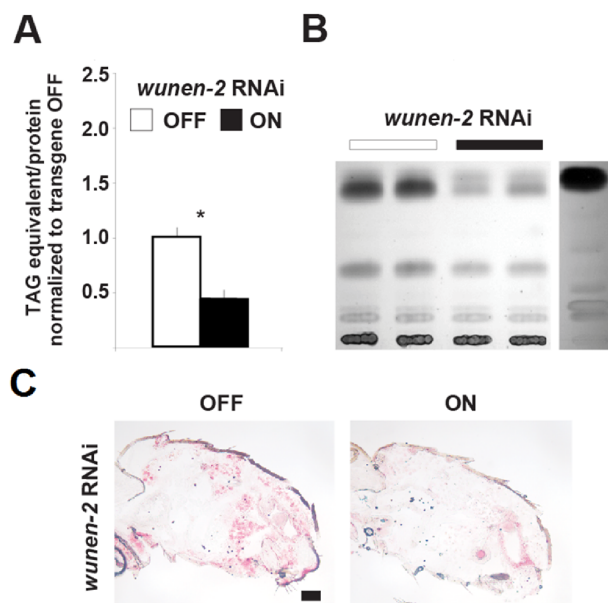
Fig. 13 The fat storage tissue-targeted RNAi KD of the glycerolipid regulator *wunen-2* causes leanness in adult male flies. Progeny of ts-FB-Gal4 crossed with *wunen-2* RNAi flies was analyzed by CCA (**A**), TLC (**B**), and ORO staining on sagittal cryosections of adult male fly abdomen (**C**). Transgenic flies were compared to control flies without the ts-FB-Gal4 driver (RNAi OFF). TLC in (**B**) was done by Anja Hildebrand (Baumbach *et al.*, 2014). *p ≤ 0.05*, for all comparisons to RNAi OFF. Scale bar represents 100 µm.

2.3 Intracellular vesicle-mediated transport factors act as anti-obesity genes

The *in silico* Gene Ontology analysis of the 77 identified obesity-/anti-obesity genes showed an enrichment of genes from the vesicle-mediated transport (Fig. 9C, D). In order to test a potential role of vesicle trafficking in the body fat storage regulation of adult flies, genes with this term were further characterized. The screen identified the *ADP ribosylation factor at 79F (Arf79F/DmARF1)* and *sec71/DmARFGEF1/2* as anti-obesity genes (Table S2) but also *gartenzwerg (garz/DmGBF1)* as a candidate gene, which did not pass the validation scheme, because no alternative RNAi lines were available. The small GTPase Arf79F is the fly ortholog of mammalian ARF1, a central regulator of COPI-mediated retrograde transport between Golgi and ER (Fig. 14) and a critical factor for Golgi integrity. In *Drosophila* tissue culture cells, it has been previously shown that a knockdown of *Arf79F* strongly increases the lipid stores (Beller *et al.*, 2008; Guo *et al*., 2008). The *Drosophila* ortholog of *GBF1* is encoded by *garz* (Wang *et al.*, 2012) and *sec71* is the fly homolog of mammalian *ARFGEF1/2*. While *garz* and *Arf79F* are important for the retrograde transport of vesicle trafficking, *sec71* is important in the trans-Golgi transport (Fig. 14; reviewed in Kirchhausen (2000)).
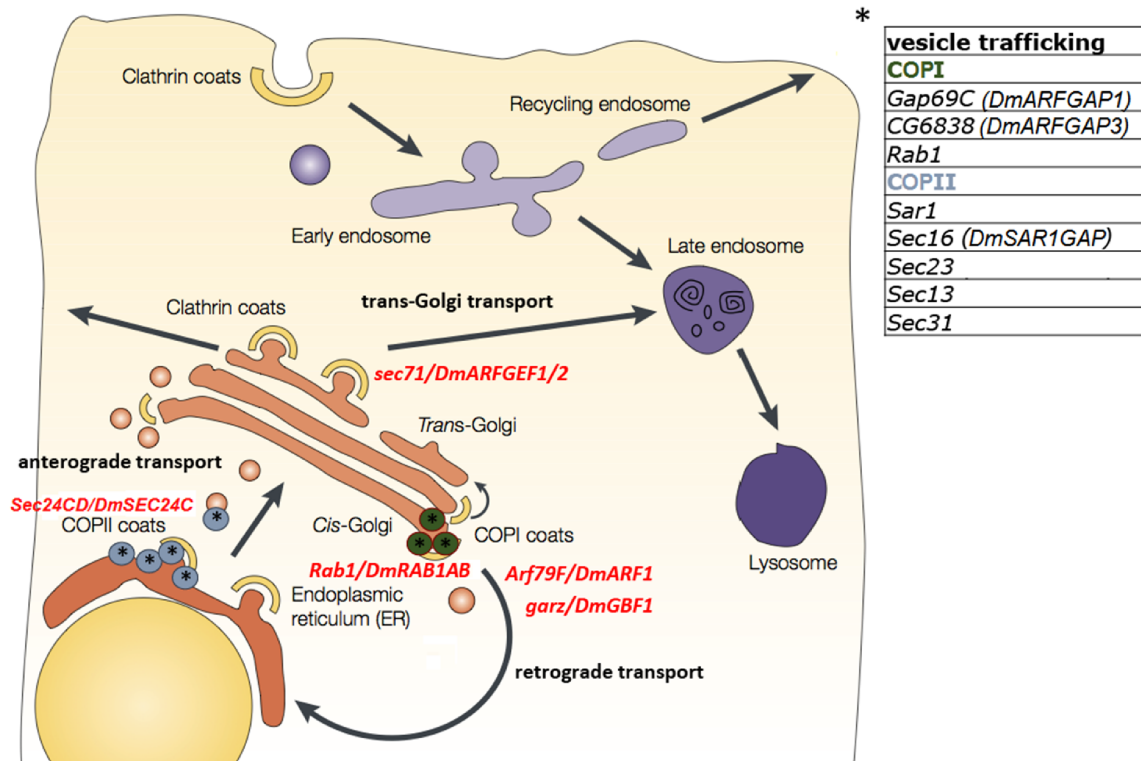
Fig. 14 Schematic overview of the intracellular vesicle-mediated transport. Genes causing body fat accumulation due to RNAi KD are highlighted in red. Three pathways are known to transport vesicles and their cargo: The trans-Golgi transport is important for Golgi to plasma membrane transport, the retrograde COPI mediated pathway is crucial for Golgi to ER transport and the anterograde COPII mediated pathway is essential for the ER to Golgi transport. The evolutionarily conserved small GTPase gene *Arf79F/DmARF1*, the guanine nucleotide exchange factor genes *sec71/DmARFGEF1/2* and *garz/DmGBF1*, and the *Sec24CD/DmSEC24C* gene, coding for a COPII coat protein, were identified in the RNAi screen as anti-obesity or candidate genes. Further screening of selected vesicle trafficking genes (*, shown in the right panel) also identified another conserved small GTPase *Rab1/DmRAB1AB as an anti-obesity gene*. Scheme was modified after Kirchhausen (2000).

A fat storage-restricted RNAi knockdown of any of the three fly genes caused an up to 120% total body fat accumulation (Fig. 15A). In addition, TAG is accumulated in the fat storage tissue shown by TLC (Fig. 15B) and by visualization of lipid accumulation in the adult subcutaneous fat storage tissue (Fig. 15C).
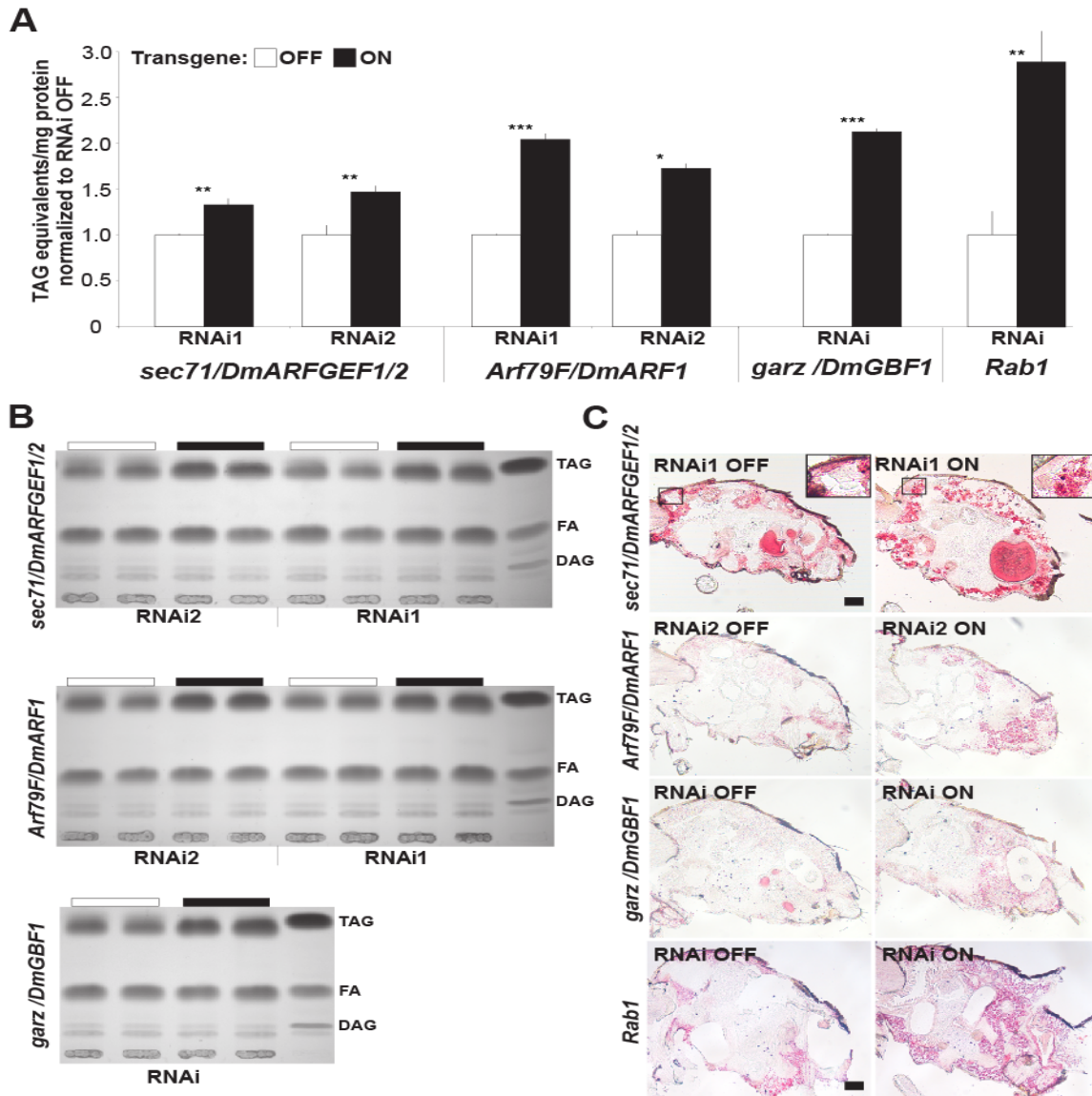
Fig. 15 Vesicle-mediated transport factors act as anti-obesity genes. Body fat increase in adult male flies upon adipose tissue knockdown of evolutionarily conserved small GTPase genes *Arf79F/DmARF1*, *Rab1* and guanine nucleotide exchange factor genes *sec71/DmARFGEF1/2*, *garz/DmGBF1* involved in the ER-Golgi vesicle transport. Shown are elevated body fat levels (**A**), an elevated TAG content (by TLC in **B**) and subcutaneous lipid accumulation (by ORO staining in **C**) compared to RNAi OFF control flies. TLC in (**B**) was done by Anja Hildebrand (Baumbach *et al.*, 2014). Scale bar in (**C**) represents 100 µm. *p≤0.05, **p≤0.01 and ***p≤0.001. Figure modified after Baumbach *et al.* (2014).

In order to identify additional body fat regulators in the vesicle trafficking pathway, eight additional genes were tested by determination of total body fat after fat

storage-restricted RNAi in adult flies (Fig. 14, *upper right panel). Next to *Arf79F*, a second small GTPase encoded by the *Rab1/DmRAB1AB* gene was identified by this effort as an anti-obesity gene in adult flies. An *Rab1* knockdown in the adult fat storage tissue causes a 190% increase of the total body fat content (Fig. 15A) and a massive accumulation of lipids in the subcutaneous fat storage tissue of adult flies (Fig. 15C).

Collectively, these findings demonstrates the importance of the vesicle-mediated transport for the *in vivo* regulation of body fat storage in the adult fly. This is also supported by the RNAi-screen identification of the anti-obesity gene *Sec24CD/DmSEC24C* a component of the COPII-dependent anterograde transport (Table S2, Fig. 14).

2.4 Characterization of the *Stromal interaction molecule* in body fat control

2.4.1 Body fat control by the store-operated calcium entry

The *in silico* Gene Ontology analysis of RNAi screen-identified obesity/anti-obesity genes unveiled several highly enriched GO terms (Fig. 9D). The highest enriched terms were associated to calcium signaling. The anti-obesity genes *Stromal interaction molecule* (*Stim/DmSTIM1)* and *olf186-F/DmORAI1* were directly linked to this term and were described as core components of a process called store-operated calcium entry (SOCE; (Roos *et al.*, 2005; Vig *et al.*, 2006; Zhang *et al.*, 2006)). In addition, the RNAi screen identified other genes linked to this process. The coding genes for the Inositol-1,4,5,-tris-phosphate (IP3) receptor (Itp-r83A/*Dm*ITPR), the calcium pump Ca-P60A/*Dm*SERCA and the high intracellular Ca^{2+} (iCa^{2+}) triggered downstream effector Calmodulin (Cam) were either directly identified or *via* additional screening and validation. In summary, all genes that

encode for the core components of the SOCE were identified as body fat storage regulators.

In order to unveil the potential role of the SOCE in body fat storage regulation, I characterized the effects of a single gene KD or gain of function (gof) by determination of the body fat content. A fat storage-restricted KD of *Ca-P60A* or the overexpression of either *olf186-F* or *Stim* should cause high intracellular Ca^{2+} (iCa^{2+}) levels according to the current view on SOCE (reviewed in Soboloff *et al.* (2012)). Interestingly, these genetic manipulations of the SOCE core genes resulted in lean flies and depleted the body fat stores by up to 85% (Fig. 16A). By TLC and ORO staining, it could also be shown that this depletion is paralleled by a strong reduction in TAG levels and subcutaneous abdominal lipid stores (Fig. 16B, C). On the other hand, manipulation of SOCE genes, which should result in lower iCa^{2+} levels, like a knockdown of *Itp-r83A* or *Stim*, or the overexpression of a dominant-negative (DN) form of *Itp-r83A,* caused an increase in body fat by up to 250%, accompanied by the elevation of TAG levels and an accumulation of subcutaneous body fat in male flies (Fig. 16A, B, C). The hypothesis that *Cam* is a potential downstream target of SOCE (Chin and Means, 2000) and can transmit SOCE-dependent body fat regulation is in agreement with the observed body fat and TAG accumulation (175%) due to a fat storage-restricted knockdown.

Furthermore, I showed by a western blot analysis of the Stim protein that the genetic manipulations by RNAi or gof are resulting in lower protein levels due to a KD and higher levels in a *Stim* gof (Fig. 16A, lower panel). Consequently, these changes in the protein amount are causing the observed changes in body fat storage.

In summary, a fat storage-restricted manipulation of SOCE gene activities causes changes in body fat storage according to the proposed change in iCa^{2+}. This was shown by analyzing the total body fat storage *via* CCA, the determination of TAG by TLC and the imaging of ORO-stained subcutaneous abdominal cryosections.
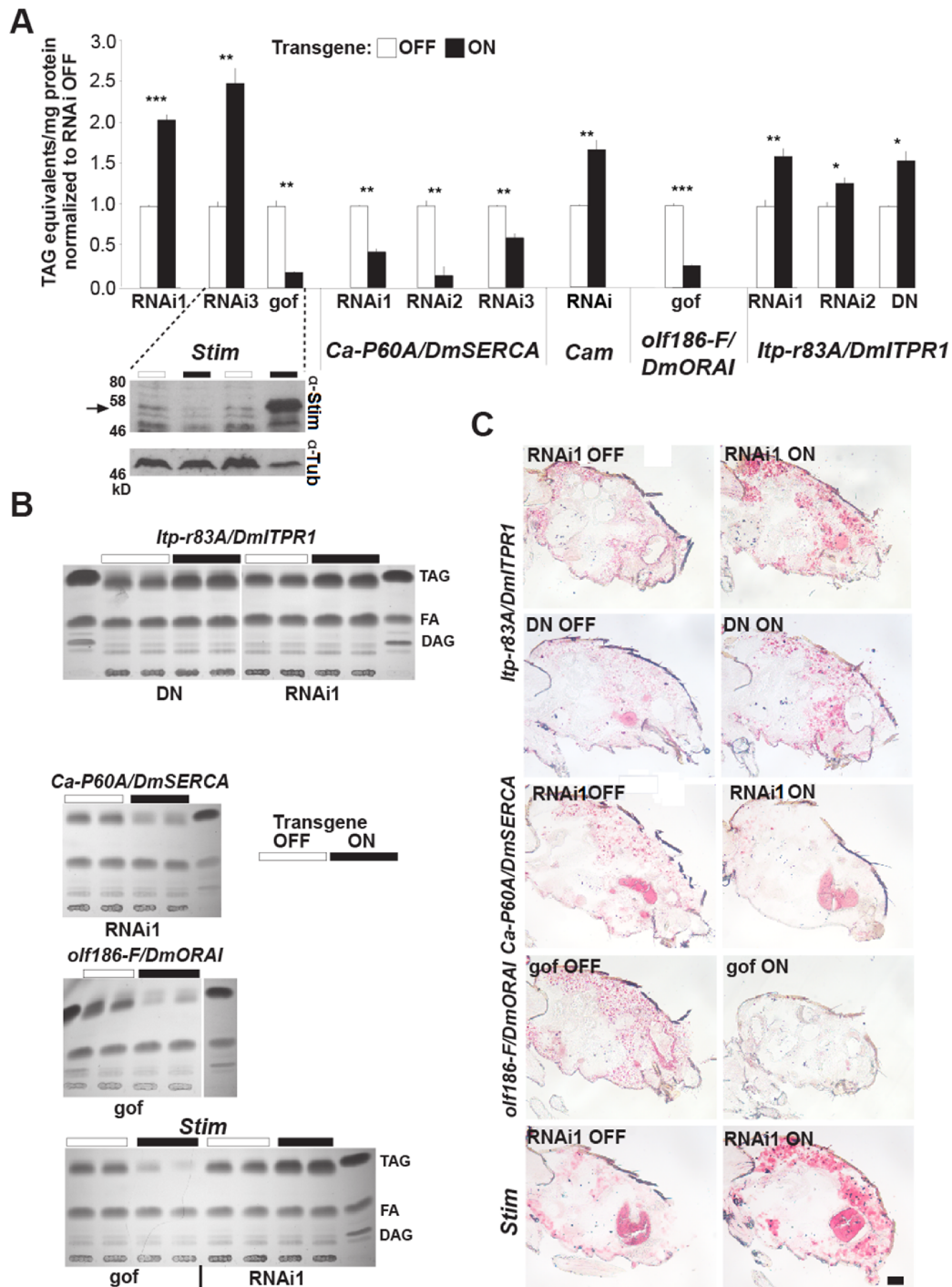
Fig. 16 The modulation of SOCE-related genes *Itp-r83A/DmITPR*, *Ca-P60A/DmSERCA*, *olf186-F/DmORAI*, *Stim/DmSTIM1* and of *Cam* in the adult male fly fat storage tissue causes changes in body fat content. Six days induced males were assayed by total body fat analysis (**A**), TLC (**B**) and ORO staining on sagittal cryosections of adult male fly abdomen (**C,** scale bar: 100 µm). In addition, Stim protein abundance in total fly abdomen homogenates were analyzed by a western blot for *Stim* RNAi3 and gof flies. TLC in (**B**) was done by Anja Hildebrand (Baumbach *et al.*, 2014). Statistical significance: *p≤0.05, **p≤0.01 and ***p≤0.001. Figure modified after Baumbach *et al.* (2014).

2.4.2 A fat storage-restricted *Stim* KD causes obesity *via* iCa^{2+} down-regulation in the abdominal fat body

In order to examine the molecular and cellular effects of SOCE manipulation in the body fat storage regulation in more detail, I concentrated on the characterization of the *Stim* function. As shown in Fig. 16A-C, a conditional fat storage-restricted knockdown of *Stim* (*Stim* KD) results in reduced Stim protein levels, body fat accumulation and TAG increase. To confirm, that the *Stim* KD causes the expected decrease in iCa^{2+} directly in fat body cells, which mediates further responses *via* iCa^{2+} sensors like Cam, I used the genetically encoded CaLexA system (Masuyama *et al.*, 2012). This system contains of a plasma membrane-targeted GFP-reporter, which is translated in response to the iCa^{2+} concentrations *via* the Ca^{2+}-dependent nuclear import of a synthetic transcription factor. By inducing a chronic fat storage-restricted *Stim* KD in combination with the CaLexA system, I was able to show that a *Stim* KD caused the expected decrease in iCa^{2+} concentrations. This is shown by the reduced GFP in adult female fat body cells, which were imaged by confocal microscopy (Fig. 17A). Also confocal microscopy of 6 days induced *Stim* KD female fat bodies showed a massive increase in the cellular lipid content and cell size (Fig. 17B), which was quantified and turned out to be significant (Fig. 17C). Consistently, electron microscopy images of these flies showed enlarged lipid droplets in the fat body (Fig. 17D). Quantification of lipid droplets >8 µm also showed this trend to be significant (Fig. 17E). These findings could also be validated by subjecting male *Stim* KD flies to paraffin sectioning and Eosin-Hematoxylin staining of sagittal sections. While in the control flies (RNAi1 OFF) LDs are hardly visible, in *Stim* KD flies LDs can be easily shown as white dots directly in the subcutaneous abdominal fat body (Fig.17F).

In summary, these findings indicate that *Stim* KD-mediated obesity is characterized by massive TAG accumulation and an increase in LD and cell size directly in the fat body tissue likely as a consequence of a decreased iCa^{2+}.
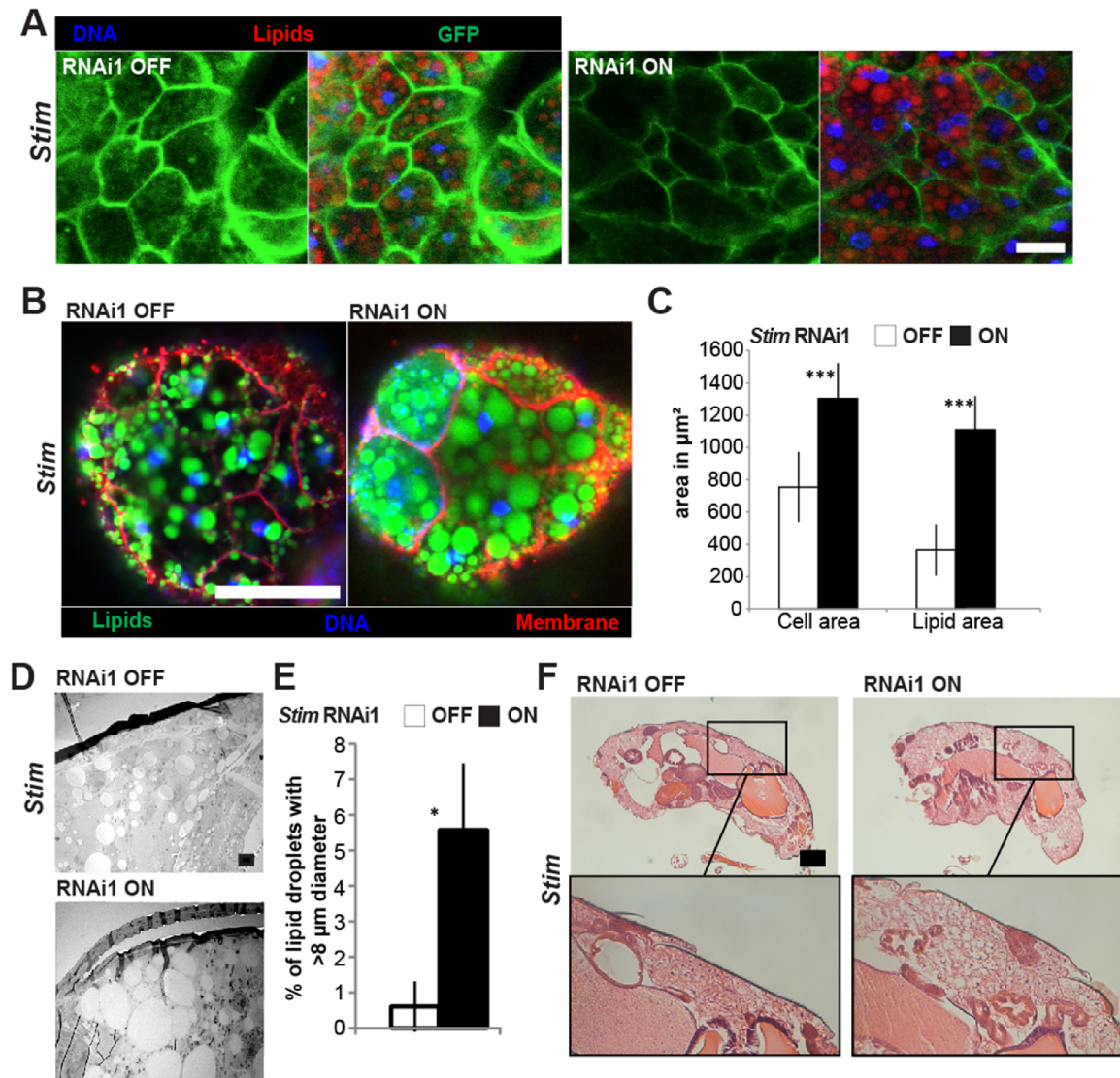
Fig. 17 A fat storage-restricted *Stim* KD causes decreased iCa^{2+} and lipid accumulation in the abdominal fat body. The CaLexA system (based on the Ca^{2+}-dependent transcription of membrane-targeted GFP reporter protein) was used to measure low iCa^{2+} concentration in adult fly fat body upon a *Stim* KD (**A**; left panel: GFP [=iCa^{2+}]; right panel: overlay with LD and DNA stainings). The increase in LD size (**E,** in percentage of LD >8 µm) and total lipid and cell area (**C**) in adult male fat body cells subjected to *in vivo Stim* gene knockdown were assayed by electron microscopy (**D**) and confocal microscopy (**B;** green: lipids; blue: DNA; red: membranes). In addition, the accumulation of LD is shown by white dots directly in the fat body in paraffin sections stained with Eosin-Hematoxylin (**F**). Preparation of fly samples and EM images in (**D**) were done by Dr. Dietmar Riedel (Baumbach *et al.*, 2014). Statistical significance: *p≤0.05 ***p≤0.001; Scale bar represents 20 µm in **A,** 50 µm in **B,** 4 µm in **D** and 100 µm in **F**. Figure modified after Baumbach *et al.* (2014).

2.4.3 The *Stim* KD-mediated obesity is restricted to adult flies

In order to examine *Stim* KD-mediated obesity in different development stages, I analyzed the effects of a *Stim* KD on the body fat content in migratory L3 larvae and freshly hatched immature adult flies. As shown in the previous chapter, a chronic or acute *Stim* KD in the mature male adult fat storage tissue causes massive body fat accumulation. By using a chronic fat storage-restricted driver (FB-Gal4), the *Stim* KD was induced from the beginning of egg development and results in up to 51%-reduced Stim protein levels in L3 larvae, immature and mature adult male flies, shown by quantitative western blot analysis (Fig. 18A). Interestingly, no significant differences in the body fat content could be detected between *Stim* KD and control L3 larvae/immature adults (Fig. 18B). On the other hand, 6 days old mature adult males showed a more than doubled body fat content, when compared to OFF-controls without the FB-Gal4 driver.
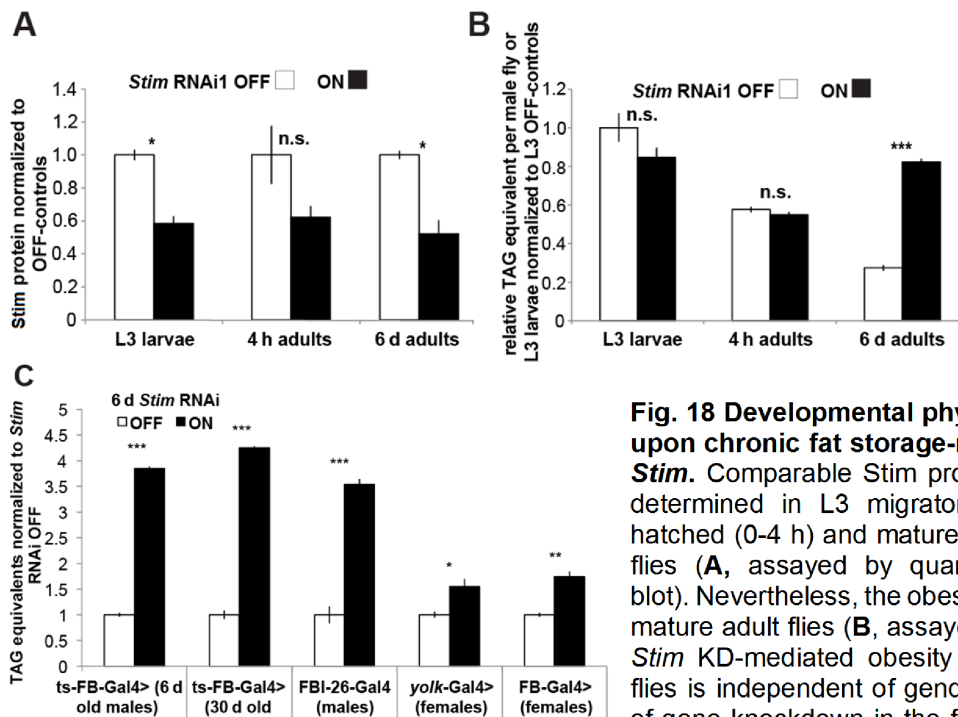
Fig. 18 Developmental physiology of flies upon chronic fat storage-restricted KD of *Stim*. Comparable Stim protein levels were determined in L3 migratory larva, freshly hatched (0-4 h) and mature adult (6 d) male flies (**A,** assayed by quantitative western blot). Nevertheless, the obesity only occurs in mature adult flies (**B**, assayed by CCA). The *Stim* KD-mediated obesity in mature adult flies is independent of gender, age or mode of gene knockdown in the fat storage tissue (**C,** assayed by CCA). In detail, male flies of different age were subjected to a TARGET-system-mediated conditional *Stim* KD (ts-FB-Gal4) or to a Gene Switch system-mediated conditional *Stim* KD (FBI-26-Gal4). Adult female flies were subjected to either conditional TARGET-dependent (ts-FB-Gal4)/–independent (*yolk*-Gal4) *Stim* KD or a KD throughout the whole development (FB-Gal4). In all cases, the *Stim* KDs were restricted to the fat storage tissues. Statistical significance: n.s.: p>0.05, *p≤0.05, **p≤0.01 and ***p≤0.001. Figure modified after Baumbach *et al.* (2014).

By inducing the fat storage-restricted knockdown of the *Stim* gene in adult flies of different gender, age, by different independent *Stim* RNAi transgenes and by different targeting expression systems, including a temperature-independent switchable fat body driver (FBI-26-Gal4), the *Stim* KD-mediated obesity could be triggered (Fig. 18C).

Conclusively, the *Stim* KD-mediated obesity is restricted to mature adult flies independent from the age or gender, which emphasizes the hypothesis that Stim executes the regulation of the energy uptake/consumption directly in the adult fat storage tissues. The restriction of this phenotype to the mature adult fat storage tissues might be explained by the different feeding behaviours of larvae and adult flies.

2.4.4 A transient short-term interference of *Stim* leads to massive body fat accumulation and a gain in body weight

In order to examine whether the *Stim* KD-dependent obesity is reversible with respect to the total body fat, I analyzed the body fat content of *Stim* KD males, which were induced only transiently for a short duration and subsequently incubated at repressed conditions. Therefore, I used 6 days old mature adult male *Stim* KD and control flies and induced them transiently for 34 h (short-term) on active-conditions. By determination of the *Stim* transcript *via* qRT-PCR and the Stim protein *via* quantitative western blots, I were able to show that both are significantly reduced upon a long-term (6 days) and short-term *Stim* KD (34 h, Fig. 16A and Fig. 19A). In addition, a slight increase in the body fat content could be observed directly after the short-term induction (+29%). Interestingly, further incubation of these flies at repressed-conditions for 5 days attenuated the Stim protein and *Stim* transcript levels back to normal but did not cause a "recovery" of the body fat content back to normal (Fig. 19A). Unexpectedly, further incubation of *Stim* KD flies for 10 days, 20 days and 30 days at repressed-conditions caused a dynamic and massive increase in the total body fat content by up to 840% compared to controls. This effect could also be achieved by using 18 days old male

flies with a short-term *Stim* KD induction or 6 days old flies on even shorter induction times (14 h), where the body fat content increases by up to 390% 10 days after the induction (Fig. 19B). By using bright-field imaging and body weight determination, I also observed an increase in the abdomen size (Fig. 19C) and the body weight (Fig. 19D) in short-term *Stim* KD induced flies after 30 days incubation at repressed-conditions.

AkhR and *bmm* are known regulators in lipid metabolism. While AkhR acts as an receptor for Akh and can mediate lipolytic signals *via* cAMP and Ca^{2+} signaling (Arrese *et al.*, 1999), *bmm* is directly involved in the mobilization of stored lipids upon starvation (Grönke *et al.*, 2005). To unveil if the observed short-term *Stim* KD effects are due to a general short-term interference of lipid metabolism, the known regulators *AkhR* and *bmm* were transiently impaired by a short-term RNAi induction (34 h) followed by a 10 days incubation at repressed-conditions. While the initial body fat accumulation in a *bmm* KD (+65%) could be recovered to normal levels after 10 days, the *AkhR* and *Stim* KD-mediated obesity increased by up to 250% (Fig. 19E).

In summary, a short-term interference of SOCE, which is represented by a transient fat storage-restricted *Stim* KD, results in a "programmed" obesity and a gain in body weight. This "programmed" obesity seems not to be due to a general impairment of body fat levels, since a short-term impairment of the well-known body fat regulators *bmm* and *AkhR* causes individual effects. Since *AkhR* and *Stim* KDs show similar effects, these results adds evidence for the hypothesis that AkhR-signaling acts *via* SOCE and Stim to regulate iCa^{2+} and lipid mobilization, which will be examined later on in this work.
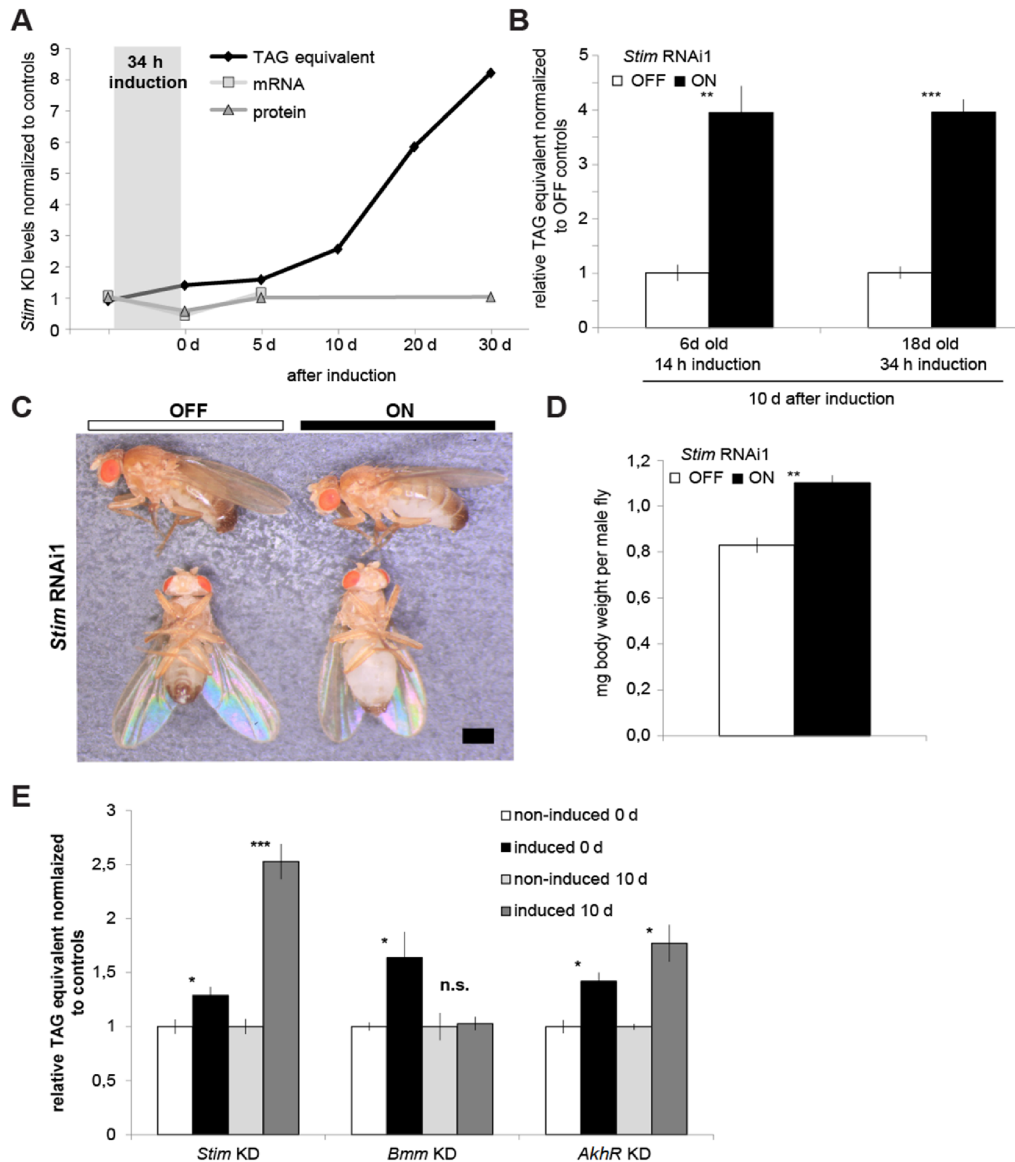
Fig. 19: A transient fat storage-restricted KD of *Stim* causes a "programmed" obesity in mature adult male flies. Six days old adult male *Stim* KD flies were transiently incubated (34 h) on repressed- or active-conditions using the ts-FB-Gal4 driver. Afterwards flies were kept for up to 30 days at repressed-conditions. While protein (measured by quantitative western blots) and transcript levels (measured by qRT-PCR) are back to normal 5 d after induction, the body fat (measured by CCA) is steadily increasing (**A**). This phenotype could also be observed with shorter induction times (14 h) or in older flies (18 d old upon induction start) measured by CCA (**B**). A clear difference in the abdominal size between induced (ON) and non-induced (OFF) flies could be observed 30 d after induction (**C**), which also causes a gain in body weight (**D**). A transient (34 h) KD of *Stim* and known fat storage regulators *bmm* and *AkhR* showed an increase in body fat directly after induction (0 d) compared to non-induced controls. *Stim* and *AkhR* KDs are causing further body fat accumulation 10 days after the transient induction, while the *bmm* KD-mediated body fat accumulation completely recovered (**E,** quantified by CCA). Scale bar in (**C**) represents 300 µm. Statistical significance: n.s.: $p > 0.05$, *$p \leq 0.05$, **$p \leq 0.01$ and ***$p \leq 0.001$.

2.4.5 A fat storage-restricted *Stim* KD causes an increased mitotic cell division activity

The control of body fat storage is a finely tuned network dependent on different factors such as lipogenesis, lipolysis, food intake and dietary composition. Since a fat storage-restricted *Stim* KD causes hypertrophy of the fat body tissue and massive accumulation of body fat (Fig. 17), I wanted to know whether the cell number is changed due to a fat storage-restricted *Stim* KD. So far it was not directly shown that the mature adult fat body can undergo cell divisions, whereby indirect approaches revealed a gain in fat mass and fat cell number due to overexpression of a *InR* DN construct (DiAngelo and Birnbaum, 2009). Therefore, I analyzed the cell division upon a *Stim* KD directly in the mature adult fat body of female flies. By using a heat shock (hs) induced system, which consists of hs-FLP (flippase), an UAS-GFP and an *Act*-cd2-Gal4 driver, I was able to induce GFP-marked single cell clones with normal or interfered *Stim* function, 3 days after the initial heat shock (Fig. 20). Interestingly, the size of the single cell clones (shown by GFP) increased in non-interfered single cell clones from a 1-cell-state (3 days after hs) over a 2-cell-state (5 days after hs) to a 4-cell-state (8 days after hs). When the single cell clones were interfered with a *Stim* KD, I was not able to distinguish between the single cell clones anymore, since 5 days after the initial hs their increased size seems to cause a fusion with neighbouring single cell clones. Therefore, the mature *Drosophila* fat body seems to undergo cell divisions and a *Stim* KD in this tissue causes a higher cell division compared to controls.

Results
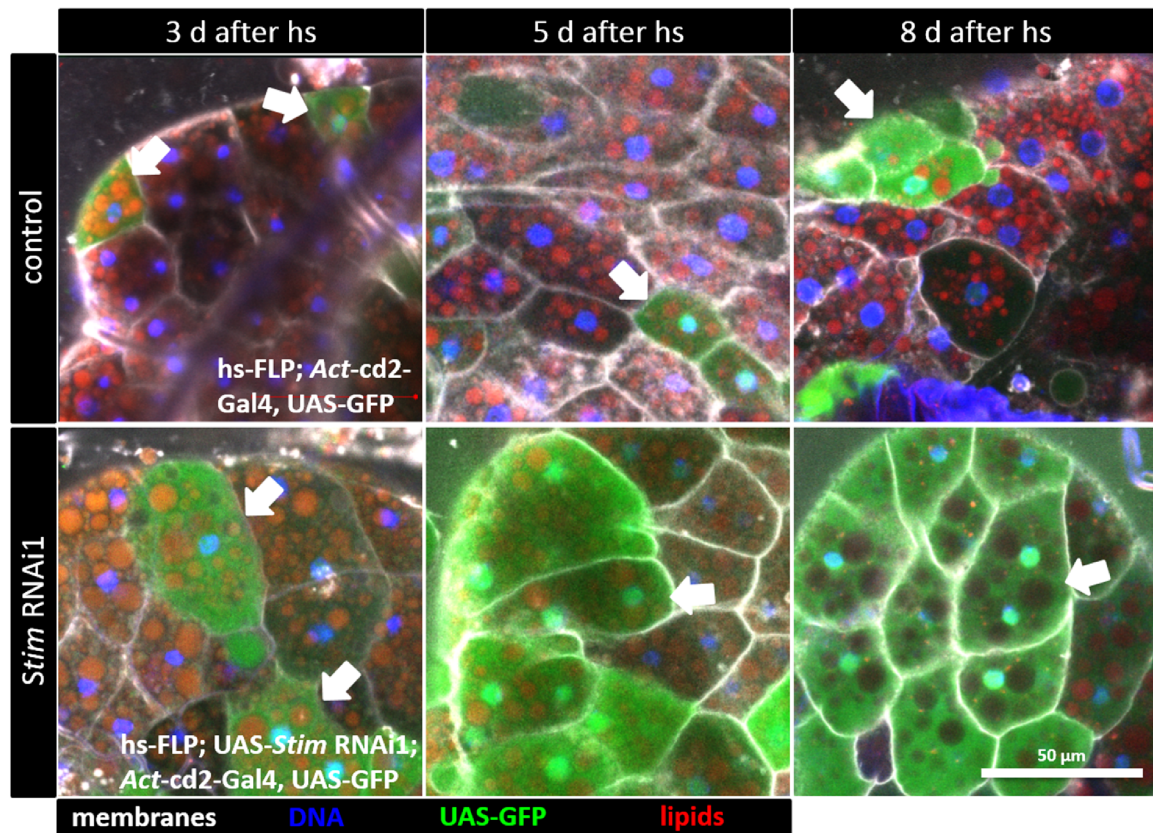
Fig. 20: A single cell clone analysis in the adult female fat body revealed a basal cell division in control and an increased cell division in *Stim* KD flies. Single cell clones were marked (GFP: green; white arrows) by a single heat shock (hs) in 5 d old adult female flies inducing an hs-FLP, which activates an *Act*-cd2-Gal4, UAS-GFP driver. In parallel, single *Stim* KD cell clones were induced by using UAS-*Stim* RNAi. DNA was labeled by DAPI (blue), lipid droplets by LD540 (red) and cell membranes by Cell Mask (white). Single cell clone size increased in control and even more in *Stim* KD flies after the initial hs, revealed by comparison of different observation time points (3 d, 5 d and 8 d). The Scale bar represents 50 µm.

In order to unveil if the observed change in the cell division of *Stim* KD induced single cell clones is due to a change in the mitotic activity of the cells, I decided to use the mitotic marker pHis3S10, which stains specifically the nucleus of mitotically active cells (Gurley *et al.*, 1974). Fat bodies of mature female *Stim* KD flies were subjected to an immunohistochemistry with a pHis3S10 antibody. Subsequently, the fat bodies were imaged by confocal microscopy, which revealed lipid accumulation and bigger/more intense nuclear pHis3S10-signals in the *Stim* KD fat body tissue compared to controls (Fig. 21). In control fat bodies, a weak nuclear pHis3S10-signal could be detected, which is in agreement with Fig. 20 and implicates a basal cell division in non-interfered fat body cells.

45
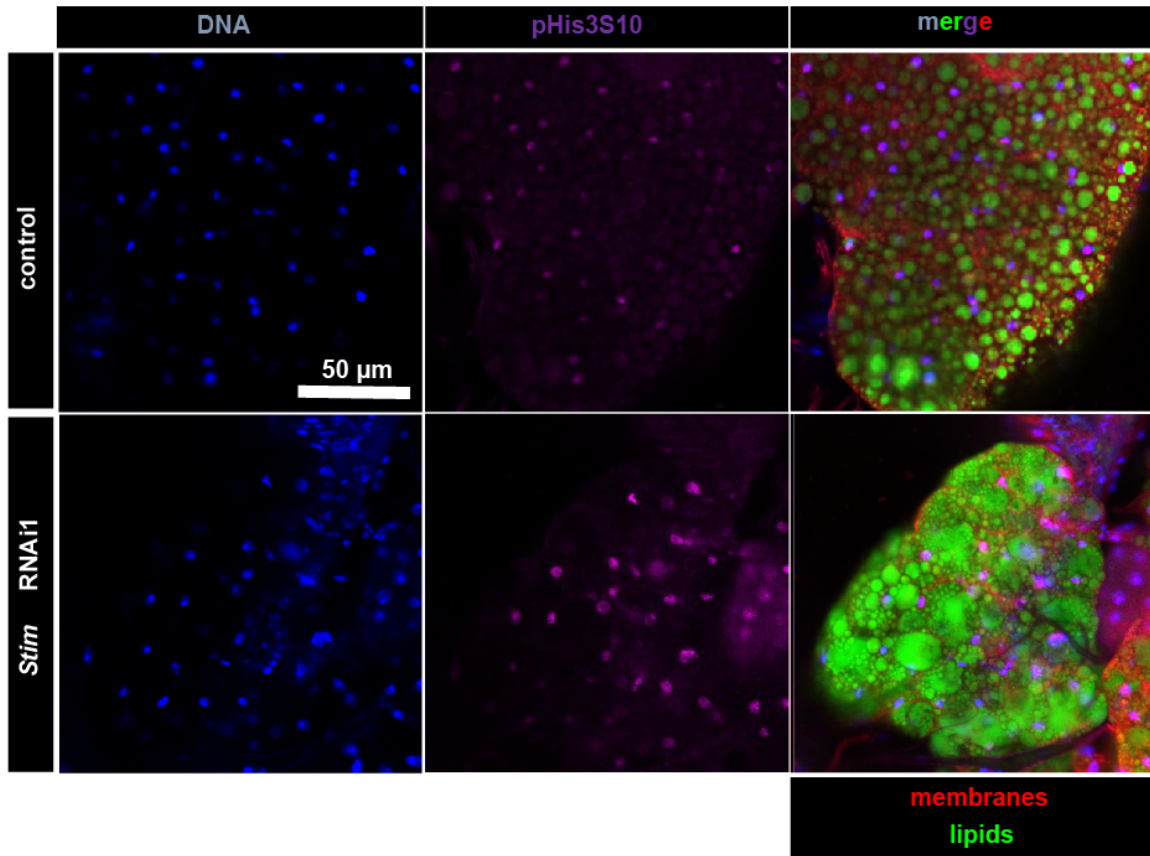
Fig. 21: A fat storage-restricted *Stim* KD causes an increase in mitotic activity. Mature female *Stim* RNAi1 and control flies were induced for 6 d and fat body enriched carcass were prepared. Carcass were subjected to an immunohistochemistry with the mitotic marker pHis3S10 (middle panel, in violet), which revealed more intense signals (=cells in mitotic state) in *Stim* RNAi1 fat bodies compared to controls. Other stains were DAPI for DNA (blue, left panel), CellMask for membranes (red, right panel) and BODIPY for lipid droplets (green, right panel). The Scale bar represents 50 µm.

In Summary, the adult mature fat body of flies is able to undergo cell divisions. Therefore, a finely tuned balance seems necessary to control the fat body cell number to store the appropriate amounts of body fat. In a fat storage-restricted *Stim* KD, this balance is interfered since a higher cell division and mitotic activity could be observed, which seems to cause hyperplasia of the fat body tissue.

2.4.6 A fat storage-restricted *Stim* gof causes lean flies by triggering apoptotic cell death

Since a fat storage-restricted *Stim* KD results in massive body fat accumulation, which seems to be at least partially mediated by hypertrophy and hyperplasia, I analyzed if a *Stim* gof is causing antagonistic effects related to the body fat content and the control of cell number.

For this purpose, a fat storage-restricted *Stim* gof was induced in 6 d old mature adult male flies. Determination of the body fat content by CCA showed a quick loss of body fat after one day, which is decreasing even more on longer induction times (5 days) down to 4% of the control body fat level (Fig. 22A). A 4 days *Stim* gof induction also seems to cause a loss of fat body tissue, shown by imaging of male flies with a GFP-marked fat body (Fig. 22B), whereby the GFP-signal is nearly lost compared to controls. This is further supported by electron microscopy pictures of 6 days induced *Stim* gof flies, where LD containing fat body cells are hard to identify (Fig. 22C) and remaining fat body cells show a degradation of their mitochondria (Fig. 22D). Interestingly, the body fat effects can be recovered by shifting 6 days induced *Stim* gof flies to repressed-conditions for a longer period. After 20 days, a complete recovery of the body fat storage could be observed (Fig. 22E), which is consistent with the hypothesis that the fat body can undergo cell divisions and is therefore able to recover the *Stim* gof-mediated loss of fat body tissue.
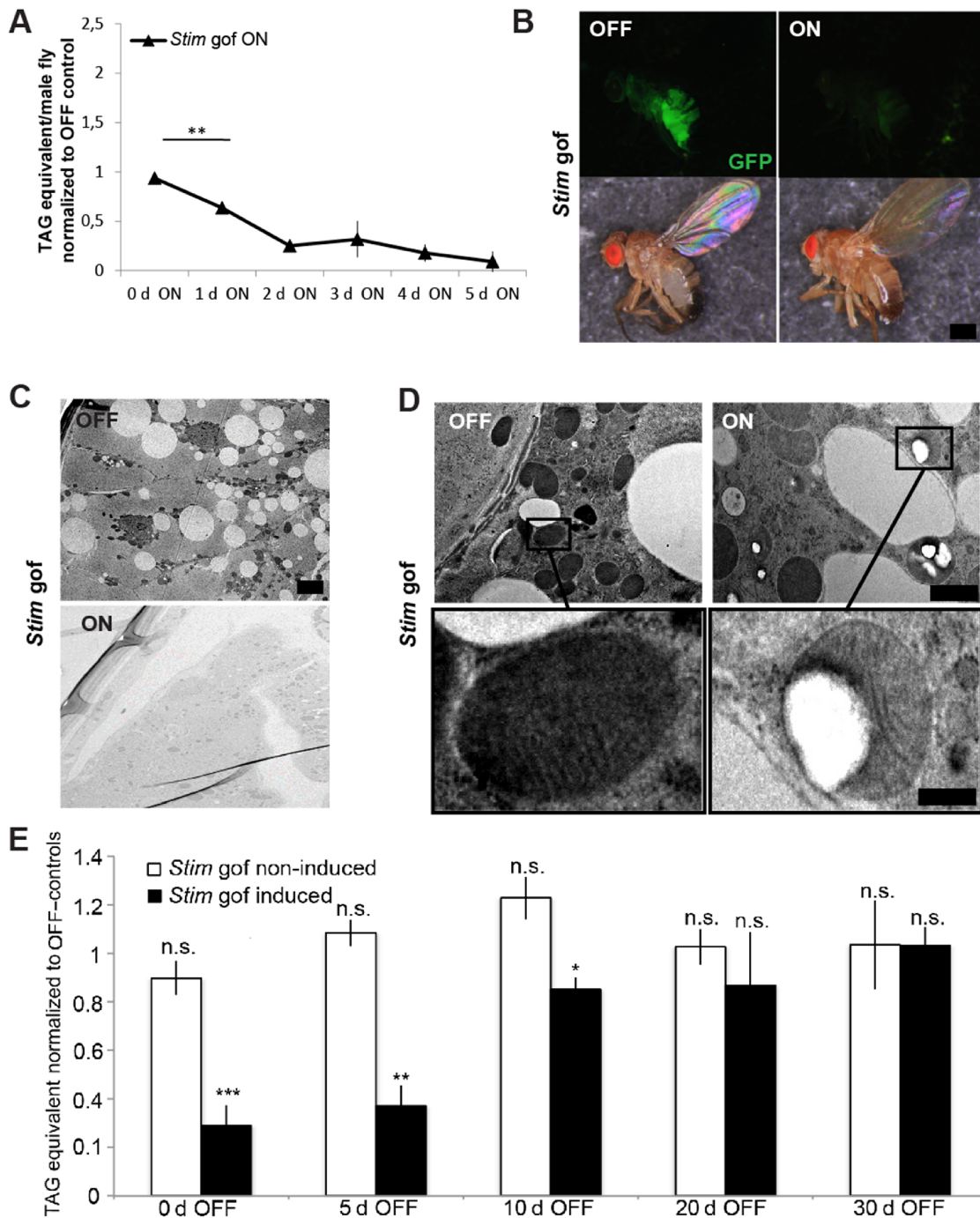
Fig. 22: An overexpression of *Stim* causes a loss of fat storage tissue. A fat storage-restricted (ts-FB-Gal4) overexpression of *Stim* (*Stim* gof) results in a quick and dynamic loss of body fat shown by CCA for 0-5 d of induction (**A**). After 4 d induction, the fat storage tissue (marked by GFP [green]) was strongly reduced (**B**). A 6 d induction resulted in a loss of LD-containing fat body cells (**C**) and a decay of their mitochondria (**D**). Shifting 6 d induced flies back to repressed-conditions causes a complete recovery of global body fat levels after 20 d, shown by CCA (**E**). CCA values were normalized against OFF-controls (without driver). Scale bars represents 300 µm (**B**), 4 µm (**C**) and 1 µm (200 nm for magnifications) (**D**). Preparation of fly samples and EM images in (**D**) and (**E**) were acquired by Dr. Dietmar Riedel (Baumbach *et al.*, 2014). Statistical significance: n.s.: p>0.05, *p≤0.05, **p≤0.01 and ***p≤0.001.

Results

Since these results also support the hypothesis that a *Stim* gof can control the cell number by triggering cell death, I wanted to show a rescue for the *Stim* gof mediated cell death in the eye. The *Drosophila* eye is widely used as a model system for changes in cell number by proliferation and cell death (Hay *et al.*, 1994; Leevers *et al.*, 1996). It is known that high iCa^{2+}, which I propose for a *Stim* gof, can induce apoptotic cell death (Giorgi *et al.*, 2012). Therefore, I tried to rescue the *Stim* gof mediated effects by co-expression with the apoptotic cell death inhibitor p35 (Hay *et al.*, 1994). To determine the cell death effects, the chronic *eyeless*-Gal4 driver (*ey*-Gal4) was used for different eye-specific overexpressions and the eye sizes of were analyzed. Overexpression of *Stim* resulted in significant smaller eyes even when co-expressed with a Stinger GFP (Fig. 23A, B). In addition, a direct induction of apoptosis in the eye by overexpression of the pro-apoptotic gene *reaper* (*rpr*) causes similar eye size reductions. Both eye size reductions could be completely rescued by co-expression with the apoptotic cell death inhibitor p35.
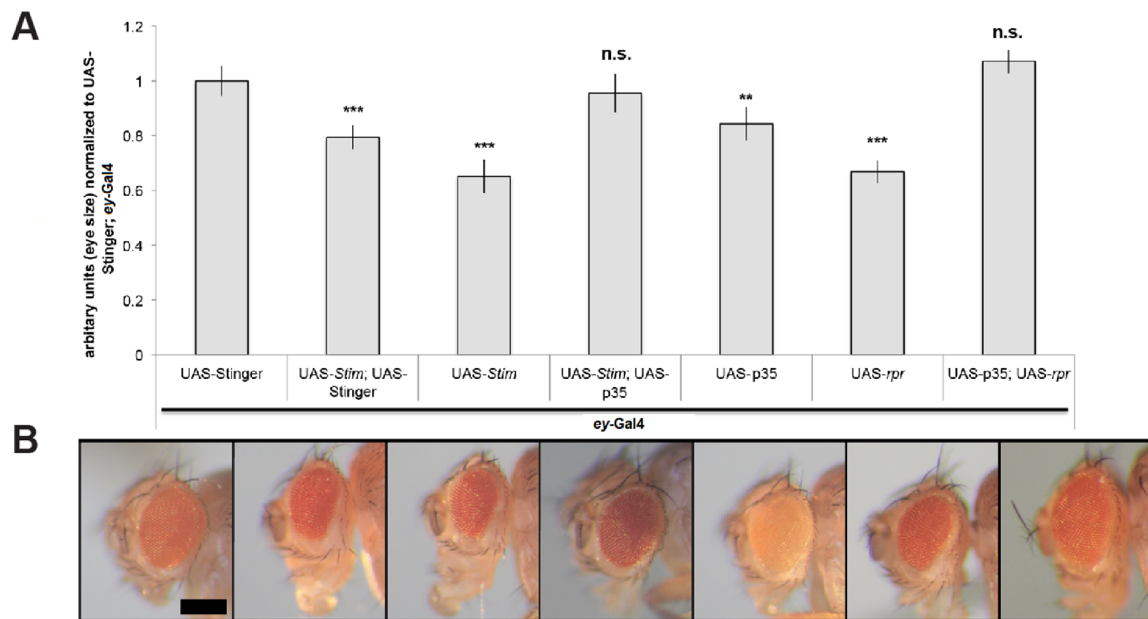
Fig. 23: An overexpression of *Stim* can cause cell death by triggering apoptosis. An *ey*-Gal4 driver was used to specifically overexpress *Stim* or a Stinger GFP control (UAS-Stinger) in the adult male eye. The overexpression of *Stim* resulted in smaller eye size (**A**) with a rough structure (**B**) comparable to the effects caused by the apoptosis inducer *rpr*. Co-expression with the anti-apoptotic protein *p35* coding gene from baculovirus rescues apoptotic effects and eye size for *rpr* and *Stim* overexpressions. Scale bar represents 200 μm. Statistical significance: n.s.: p>0.05, **p≤0.01 and ***p≤0.001.

In summary, a fat storage-restricted overexpression of *Stim* causes a decrease in body fat, which is at least partially mediated by the apoptotic cell death pathway. This is supported by a *Stim* gof mediated degradation of mitochondria and the fact that *Stim* gof effects on the eye size could be completely rescued by co-expression with the apoptotic cell death inhibitor p35.

2.4.7 A fat storage-restricted *Stim* KD has no effect on carbohydrate circulation and storage

In order to examine, whether other energy storage pathways are also impaired in a fat storage-restricted *Stim* KD, I analyzed the levels of different carbohydrates and the body-fat response to dietary sugars. Monitoring of hemolymph trehalose/glucose levels, the main circulating sugars, on different dietary sugar concentrations revealed no differences between obese *Stim* KD flies and controls with a normal body fat content (Fig. 24A). Both, the fat storage-restricted *Stim* KD as well as control flies showed no change in hemolymph sugar levels in response to different dietary sugar concentrations, indicating a functional hemolymph sugar regulation. The examination of glycogen, the main carbohydrate storage form, under fed and starvation-induced glycogen mobilization, also revealed no significant differences between *Stim* KD and control flies (Fig. 24B). Furthermore, the response to different dietary sugar concentration on the body fat content of *Stim* KD compared to control flies seems to be unaffected (Fig. 24C), since both accumulate similar high amounts of body fat in response to higher dietary sugar concentrations, which is in line with published results for control flies (Skorupa *et al.*, 2008).

Fig. 24: A *Stim* KD-mediated obesity causes a dysregulation in lipid but not carbohydrate metabolism. (**A**) Determination of circulating hemolymph sugar levels in *Stim* KD and control flies, fed on different dietary sugar concentrations, showed euglycemic conditions. In addition, the glycogen storage/mobilization (**B**) and the body fat response to dietary sugar, shown by a CCA of whole flies (**C**), are comparable to controls. For the determination of total body glycogen content and mobilization in (**B**), adult male flies were starved on a water-only diet until median starvation time (~36 h for controls; ~54 h for *Stim* KD). Statistical significances: *p≤0.05, **p≤0.01 and ***p≤0.001. Figure modified after Baumbach *et al.* (2014).

Taken together, carbohydrates are not affected by the fat storage-restricted *Stim* KD, which is in contrast to lipids. No differences could be detected in the hemolymph sugar concentrations and the body fat response to different dietary sugars. Furthermore, glycogen and its starvation-induced normalization are unaffected. Consequently, the energy homeostasis imbalance in *Stim* KD-mediated obesity is specifically based on varying body fat stores, which suggest the involvement of central lipid metabolism regulators.

2.4.8 The *Stim* KD-dependent obesity is partially mediated by the central lipid metabolism regulators *mdy* and *bmm*

Since previous results in a fat storage-restricted *Stim* KD indicate an influence on central lipid metabolism regulators, I initially analyzed the effect of a *Stim* KD on the lipid mobilization. A water-only starvation revealed a starvation resistance of *Stim* KD flies (Fig. 24B and 25A). While the median starvation time of control flies was relatively short (~27 h), *Stim* KD flies survived for a longer period (~49 h). Interestingly, the starvation-induced lipid mobilization of *Stim* KD flies seems to be delayed compared to controls (Fig. 25B), since no lipid mobilization could be observed after 24 h in *Stim* KD flies, whereas control fat stores are completely depleted. In addition to this, *Stim* KD flies could not mobilize the complete body fat stores even when starved to death, which is in contrast to controls (Fig. 25B, C, D). Conclusively, an interference of lipid mobilization at least partially contributes to the body fat accumulation of obese *Stim* KD flies.

To further address this, I analyzed the effects of a chronic fat storage-restricted *Stim* KD in a *bmm*[1]-mutant background, since *bmm* is known to regulate lipid mobilization (Beller *et al.*, 2010). A knockout of *bmm* in flies causes similar obesity (Fig. 11 and Fig. 25C) and lipid mobilization defects as a fat storage-restricted *Stim* KD (Fig. 25C). Interestingly, a *bmm*[1]-mutant caused body fat accumulation (>2 fold), while a *Stim* KD in this background further elevated the body fat level (>4 fold). This indicates that *Stim*-dependent obesity also involves additional effectors in the fly fat storage tissue. Therefore, I tested the *Stim* KD effect on the body fat accumulation in a genetic background, where lipid mobilization is completely inhibited. It is known that *bmm plin1* double mutant flies are completely blocked in storage lipid mobilization (Beller *et al.*, 2010), which results in body fat accumulation (>2.5 fold). A *Stim* KD in this background caused additional body fat accumulation (>5 fold), indicating that other mechanisms and regulators independent from the lipid mobilization must be involved, too (Fig. 25D).
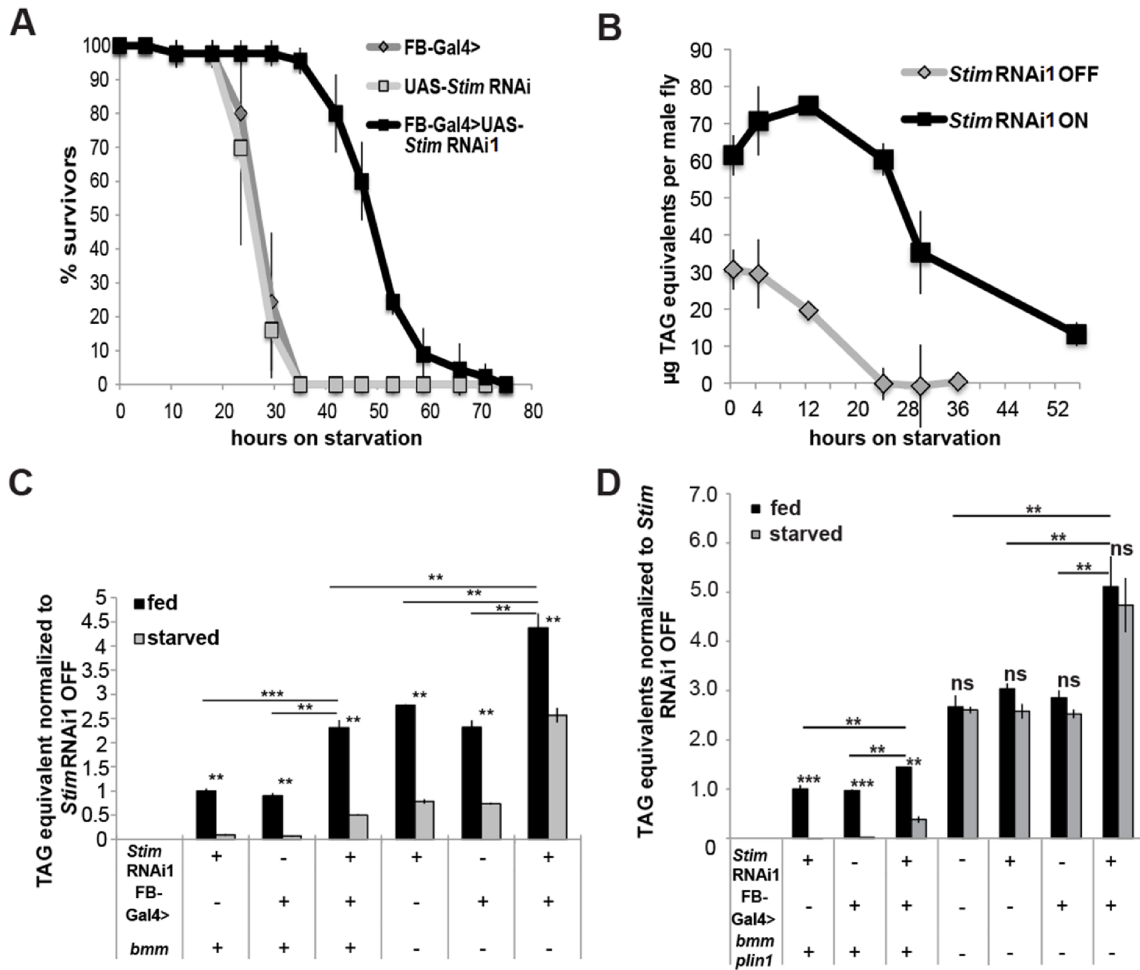
Fig. 25: *Stim* KD-mediated obesity is partially mediated by lipid mobilization defects. A water-only starvation assay revealed a starvation resistance for *Stim* KD flies compared to controls (**A**). In addition, a delayed and incomplete storage fat mobilization could be observed on a water-only diet, determined by CCA (**B**). Genetic interaction between *Stim* and the lipolytic *bmm/DmATGL* revealed an additional body fat accumulation due to a chronic fat storage-restricted *Stim* KD in a *bmm*[1]-mutant background (**C**, black bars) and also an even more incomplete lipid mobilization on starvation (grey bars), compared to *bmm*[1]-mutants. Comparison of body fat levels (measured by CCA) between water-only starved flies (grey, *post mortem*) and flies fed on a standard diet (black) revealed additional body fat accumulation in already obese *bmm*[1] *plin1*[1]-mutant male flies in response to a chronic fat storage-restricted *Stim* knockdown (**D**). Statistical significances: n.s.: $p > 0.05$, **$p \leq 0.01$ and ***$p \leq 0.001$. Figure modified after Baumbach *et al.* (2014).

Since other processes beside the lipid mobilization seem to contribute to the *Stim* KD-dependent obesity, I addressed a potential obesogenic transcriptional response at the onset of body fat accumulation. An acute 34 h short-term induction of *Stim* KD flies revealed that obesity starts quickly and progresses rapidly. By qRT-PCR and CCA, I was able to show that *Stim* mRNA was reduced by >40 % (Fig. 19A and Fig. 26A) and body fat was increased by up to 39 % after a 34 h induction (Fig. 19A and Fig. 26B). Therefore, this condition seems to be representative for the onset of *Stim* KD-mediated obesity. Subsequently, I analyzed the mRNA levels of the lipoanabolic *mdy*, a previously known obesity gene that was also identified in our study, and the lipocatabolic *bmm* gene, since both are central regulators in lipid metabolism of the fly (Beller *et al.*, 2010; Grönke *et al.*, 2005). Remarkably, the *mdy* gene is 2.8-fold up-regulated after 34h *Stim* KD induction, whereas *bmm* is down-regulated by 83% at the same time (Fig. 26C). These observations raise the question, how *Stim*-mediated iCa^{2+} depletion is connected to *mdy* and *bmm* gene regulation. Two potential regulators, which might transmit the iCa^{2+} changes to the obesogenic transcription profile, are Cam and the cyclic-AMP response element binding protein B (CrebB/*Dm*CREB). Cam is a known to sense iCa^{2+} (Soboloff *et al.*, 2012) and CrebB is regulated by cAMP but also Ca^{2+} *via* the CREB-regulated transcription coactivator (Crtc/*Dm*TORC2) (Bittinger *et al.*, 2004; Iijima *et al.*, 2009). Interestingly, a fat storage-restricted knockdown of *Cam* and the impairment of the *CrebB* by a DN overexpression, also causes a similar body fat accumulation after 50 h induction (Fig. 26B), compared to a 34h *Stim* KD. Notably, the physiological body fat increase and the obesogenic transcriptional profiles of *mdy* and *bmm* largely match to the *Stim* KD-mediated profile (Fig. 26B, C).
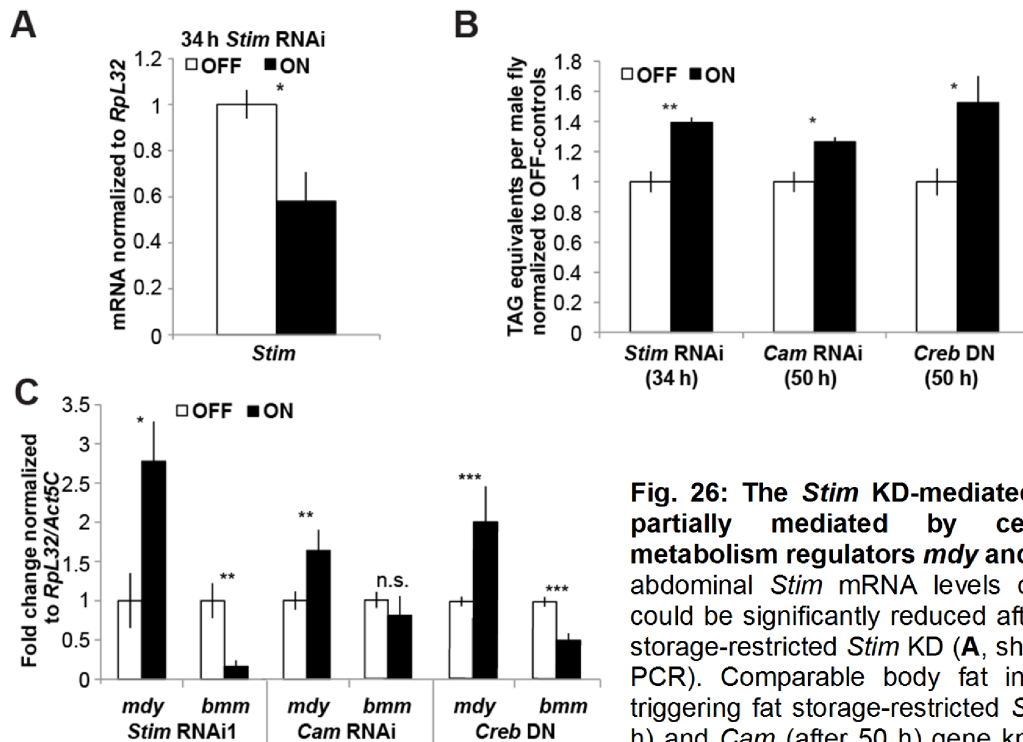
Fig. 26: The *Stim* KD-mediated obesity is partially mediated by central lipid metabolism regulators *mdy* and *bmm*. Total abdominal *Stim* mRNA levels of male flies could be significantly reduced after a 34 h fat storage-restricted *Stim* KD (**A**, shown by qRT-PCR). Comparable body fat increase after triggering fat storage-restricted *Stim* (after 34 h) and *Cam* (after 50 h) gene knockdown, or *Creb* DN overexpression (after 50h), quantified by CCA (**B**). At this physiological body fat state (27-53% increase) similarity in lipogenic and lipolytic gene expression patterns of *mdy* and *bmm* could be shown for *Stim* or *Cam* knockdown, and *Creb* DN overexpression (**C**). Statistical significances: n.s.: p>0.05, *p≤0.05, **p≤0.01 and ***p≤0.001. Figure modified after Baumbach *et al.* (2014).

Conclusively, these data supports Cam and CrebB as possible candidate factors for the transcriptional readout of *Stim* KD-mediated iCa^{2+} modulation, which in turn controls body fat storage by modulating the expression of the central lipid metabolism regulators *bmm* and *mdy*.

2.4.9 *Stim*-dependent obesity is driven by *sNPF*-mediated hyperphagia and subsequent regulations of lipogenesis and lipolysis

A chronically positive energy balance by either up-regulated energy intake or metabolic disorders can cause obesity progression. The observed up-regulation of lipogenesis shown by *mdy* and the down-regulation of lipolysis by *bmm* in adult fly abdomen are insufficient to explain the underlying *Stim*-dependent obesity, since a pre-adult *Stim* knockdown does not affect the body fat content of L3 larvae (Fig.

18B). Therefore, it is more likely that *Stim*-dependent obesity depends on the lifestyle of mature adult flies by dysregulation of energy uptake/consumption and might involve inter-organ communication, since the energy intake is mainly controlled in the brain.

To resolve whether energy expenditure is affected or the main cause of obesity progression in adult *Stim* KD flies, I determined the metabolic rate and the cumulative locomotor activity. As analyzed by measurements of CO_2 production, the metabolic rate of obese *Stim* KD flies showed only minor differences at the beginning (+0 Zeitgeber time) or in the mid (+5 Zeitgeber time) of the light cycle compared to genetically matched controls (Fig. 27A). In average, a significant difference between *Stim* KD and control flies could not be observed with respect to the metabolic rate (Fig. 27B). In addition, the cumulative locomotor activity of *Stim* KD flies was indistinguishable from control flies (Fig. 27C), while in the same timeframe the body fat content increased at the first day of *Stim* RNAi induction and continues to increase until day six, whereby the body fat content was more than doubled (Fig. 27C). Conclusively, the activity-dependent energy expenditure is unaffected in *Stim* KD-mediated obesity progression and does not contribute to the body fat accumulation. While the energy expenditure is not affected in *Stim* KD flies, the energy intake correlates well with body fat accumulation. A conditional fat storage-restricted *Stim* KD caused hyperphagic flies within two days after RNAi induction and the *ad libitum* food intake was more than doubled from day four onwards, when compared to controls without the driver transgene (Fig. 27D). Interestingly, when the food intake of *Stim* KD flies was adapted to the level of normophagic control flies (pair fed), the body fat accumulation observed under *ad libitum*-conditions is nearly gone (Fig. 27E). Under pair fed-conditions, *Stim* KD flies accumulated only 31% of the body fat gain observed under *ad libitum* feeding and stored only slightly more body fat as compared to the normophagic controls. Conclusively, these results implicate a *Stim* KD-mediated hyperphagia causing body fat accumulation *via* the elevated energy intake.
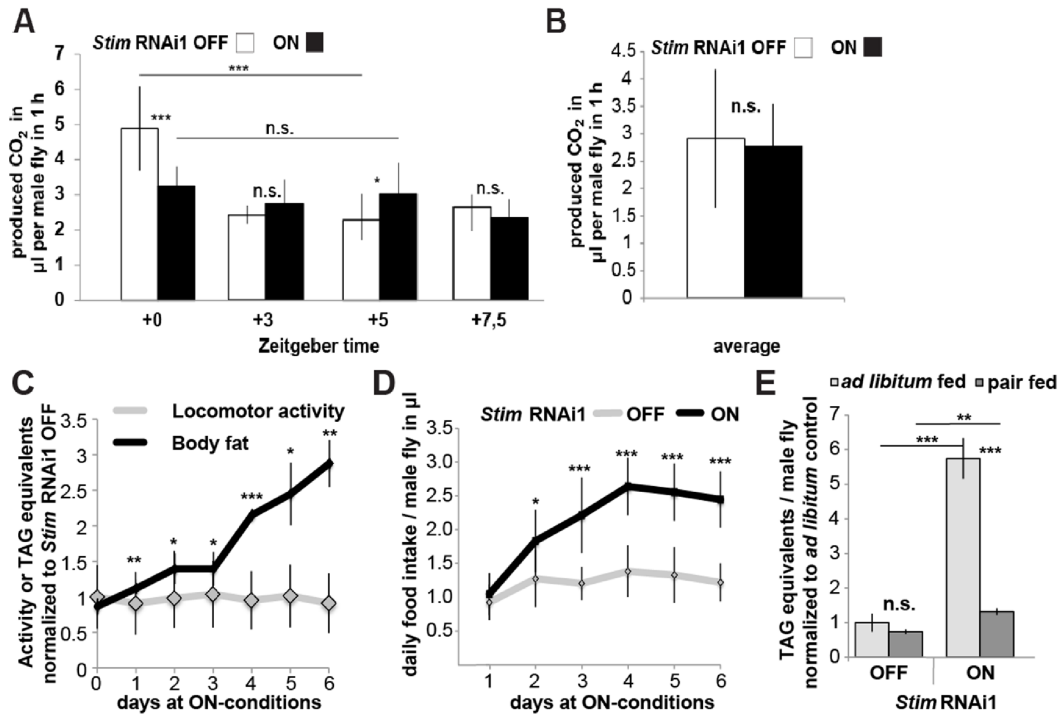
Fig. 27 The *Stim* KD-mediated obesity is related to higher energy intake and has no effect on the energy consumption. The estimation of the metabolic rate in 6 d induced *Stim* KD males compared to controls was done by determination of the CO_2-production/hour. This was done for different "Zeitgeber times" (time after lights ON in a 12 h dark/12 h light-cycle), which revealed slightly differences at +0 and +5 (**A**) but shows no effect in average (**B**). In addition, a fat storage-restricted *Stim* KD causes a dynamic body fat accumulation with no change in the spontaneous locomotor activity (**C**). Measurement of the daily food intake in male flies during the first six days of *Stim* KD induction with a CAFE assay showed an increase in food intake (**D**) and body fat content (**E**), whereby the *Stim* KD-mediated obesity can be suppressed by pair fed (offered food was adapted to control levels). Statistical significance: n.s.: $p > 0.05$, *$p \leq 0.05$, **$p \leq 0.01$, ***$p \leq 0.001$. Figure modified after Baumbach *et al.* (2014).

Since a fat storage-restricted *Stim* KD causes hyperphagia, the proper food intake control by the central nervous system might be affected. Therefore, central neuropeptides were analyzed to reveal their possible role in the obesity-progression of fat storage-restricted *Stim* KD flies. Food intake is known to be regulated by the expression of the orexigenic short neuropeptide F (sNPF) in the nervous system under starvation (Hong *et al.*, 2012). Interestingly, *sNPF* gene expression in the brain was significantly up-regulated (by 37%; Fig. 28A), when I impaired *Stim* specifically in the fat storage tissue of adult flies for 6 days. Since brain *Stim* expression was unaffected under these conditions, it is very likely that a so far unknown factor is signaling from the fat body to the brain. A potential factor to fill this gap is Unpaired 2 (Upd2), which has been described as the fly homolog

of the mammalian anorexigenic leptin peptide. A knockdown of *upd2* in the fat body causes leanness in flies and prevents the secretion of Dilp2 from the insulin producing cells (IPCs) of the brain (Rajan and Perrimon, 2012). Therefore, I analyzed the brain-expression of the *Dilp2* and *Dilp5* genes in addition to *upd2*, in fat storage-restricted *Stim* KD flies. While *Dilp2* and *Dilp5* are not transcriptionally regulated, *upd2* is significantly down-regulated by 49% (Fig. 28A) and 39% less Dilp2 is stored in the IPCs, implicating a higher Dilp2 release (Fig. 28B, C). Since this is in contrast to published results, which showed that reduced *upd2* levels in the fat body resulted in lean flies and inhibited Dilp2 release, a so far unknown factor must be involved in addition to *upd2* in the fat body-brain communication.
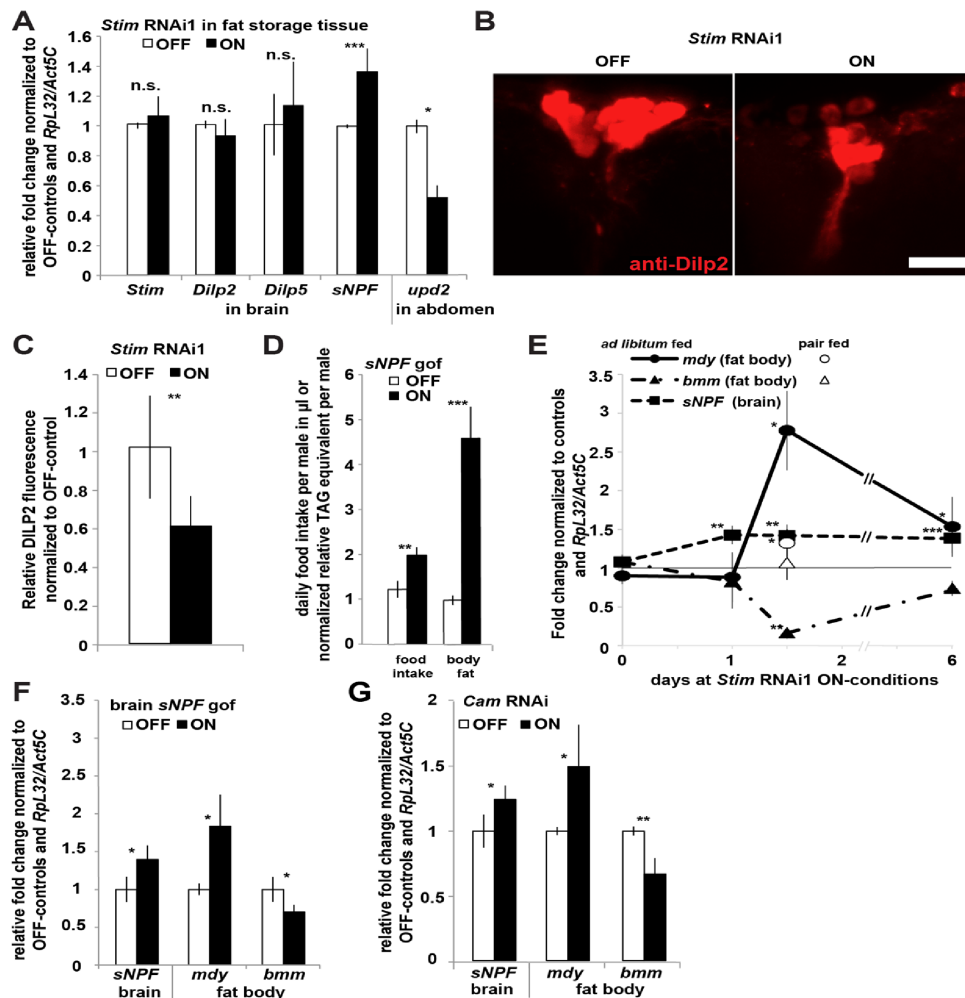
(Fig. 28 legend on next page)

Fig. 28 The *Stim* KD-dependent obesogenic gene expression and the subsequent obesity is driven by brain *sNPF*-mediated hyperphagia. (**A**) A fat storage-restricted *Stim* KD results in an up-regulation of orexigenic *sNPF* but not *Dilp2*, *Dilp5* and *Stim* in the brain, measured by qRT-PCR of total brain mRNA. In addition, an abdominal down-regulation of *upd2* could be observed. (**B**) In contrast to the transcriptional levels, a fat storage-restricted *Stim* KD causes decreased Dilp2 protein levels in brain IPCs, shown by maximum intensity projections of anti-Dilp2 immunohistochemistry. (**C**) Quantification of the fluorescence validated this observation. Scale bar represents 20 μm. (**D**) An overexpression of *sNPF* restricted to the *sNPF*-positive neurons of the brain (*sNPF*-Gal4) leads to hyperphagia, measured by a CAFE assay and body fat accumulation, measured by a CCA. (**E**) A fat storage-restricted impairment of *Stim* results in the up-regulation of brain *sNPF* prior to the up- or down-regulation of lipogenic *mdy* and lipolytic *bmm* genes. The obesogenic regulation of *mdy* and *bmm* can be largely suppressed by pair feeding. Shown are relative qRT-PCR quantifications of total head mRNA (for *sNPF*) and total abdomen mRNA (for *mdy/bmm*) normalized to controls without a driver transgene and *RpL32/Act5C* gene expressions. (**F**) An overexpression (gof) of brain *sNPF* is able to mimic the obesogenic *mdy* and *bmm* gene regulation observed in a fat storage-restricted impairment of *Stim*. (**G**) A fat storage-restricted *Cam* knockdown causes a similar *mdy/bmm/sNPF*-gene expression profile compared to a *Stim* KD, implicating an involvement of *Cam* in the inter-organ communication of body fat control. Statistical significance: n.s.: $p > 0.05$, $*p \leq 0.05$, $**p \leq 0.01$ and $***p \leq 0.001$. Figure modified after Baumbach *et al.* (2014).

Since the role of *upd2* seems to be controversial and complex, while the *sNPF* up-regulation correlates well with the higher food intake in obese *Stim* KD flies, I characterized the role of *sNPF* in more detail. An overexpression of *sNPF* in the *sNPF*-expressing neurons, which mimics the *Stim* KD-mediated *sNPF* up-regulation in the brain, caused hyperphagia and body fat accumulation in flies (Fig. 28D). In order to figure out the chronological order of *Stim* KD-mediated obesity progression, I analyzed the transcriptional profile of the lipid metabolism effectors *mdy* and *bmm* in fat storage tissue and *sNPF* in the brain in a time-dependent manner. Prior to the fat storage-restricted *Stim* KD induction, the expression levels of *sNPF, mdy* and *bmm* were unchanged compared to controls (Fig. 28E). However, a fat storage-restricted *Stim* KD induction for 24 h caused *sNPF* up-regulation in the brain (+42%), while *mdy* and *bmm* expression levels in the abdomen were still unchanged. After 34 h fat storage-restricted *Stim* KD induction, brain *sNPF* was still up-regulated and this trend continued until day six, while the fat storage tissue started to show an obesogenic transcriptional response by up-regulation of *mdy* (+178%) and down-regulation of *bmm* (-84%). During progression of obesity until day six, the *Stim* KD-dependent effect on *mdy* and *bmm* expression attenuated but still showed the same trends as observed after 34

h of induction. The observed time-dependent expression profiles of *mdy*, *bmm* and *sNPF* implicates that a fat storage-restricted *Stim* KD reults in *sNPF* up-regulation in the brain, which in turn causes hyperphagia resulting in an obesogenic transcriptional response of the fat body. This is supported by the observation that an overexpression of *sNPF* in the brain caused a similar *mdy/bmm*-expression profile as *Stim* KD flies showed (Fig. 28F). Furthermore, pair feeding of *Stim* KD flies nearly blunted the obesogenic transcriptional response in the fat body (Fig. 28F) and those flies accumulated only slightly more body fat compared to controls (Fig. 27E). In those flies, the *bmm* gene expression was unaffected and *mdy* was only weakly up-regulated (Fig. 28F, pair fed). Taken together, these results suggest that a fat storage-restricted *Stim* KD leads to up-regulation of brain *sNPF*, which triggers hyperphagia and causes an obesogenic response of *mdy* and *bmm* back in the fat body. Interestingly, a fat storage tissue targeted *Cam* KD also altered the *sNPF*, *mdy* and *bmm* expression as observed with *Stim* KD flies (Fig. 28G), which implicates that *Cam* is involved in the inter-organ feedback control *via* *sNPF* signaling.

To further address the role of the *sNPF*, *mdy* and *bmm* gene regulations in a *Stim* KD-mediated obesity progression, these genes were co-expressed by overexpression or repressed by RNAi to antagonize the *Stim* KD-mediated regulations. The overexpression of *sNPF* in the brain (Fig. 28D), *mdy* in the fat body (Fig. 29B) or the *bmm* knockdown in the fat body (Fig. 11A) caused body fat accumulations similar to *Stim* KD flies. Conversely, an RNAi knockdown of *sNPF* in the *sNPF*-expressing neurons (*sNPF*-Gal4), a fat storage-restricted knockdown of *mdy* and a fat storage-restricted overexpression of *bmm* caused lean flies (Fig. 29A, B, C). To analyze if the *Stim* KD-mediated obesity is actually mediated by *sNPF*-regulations in the brain, brain *sNPF* was directly impaired by RNAi and *Stim* was impaired in the fat storage tissue at the same time. These flies showed a reduction in the body fat content, compared to single *Stim* KD flies (Fig. 29A). Similar experiments were done to suppress the *Stim* KD-mediated *mdy* up-regulation in the fat storage tissue by co-expression with *mdy* RNAi, which caused a strong suppression of the *Stim* KD-mediated body fat accumulation (Fig. 29B).

Furthermore, a *bmm* gof in the fat storage tissue of *Stim* KD flies counteracted the *Stim* KD-mediated down-regulation of *bmm* and consistently reduced the *Stim* KD-mediated body fat accumulation at the onset of obesity (Fig. 29C).
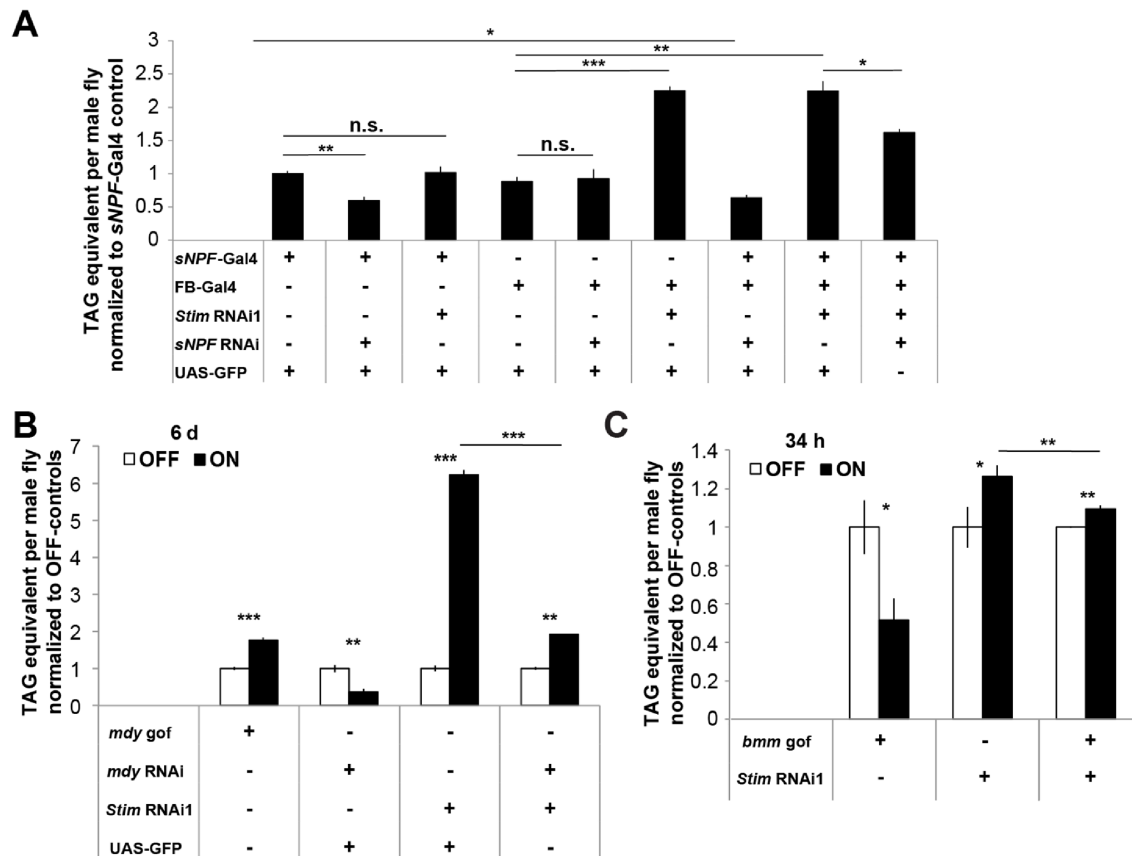

Fig. 29 The *Stim* KD-mediated obesity can be partially suppressed by transgenic correction of *sNPF*, *mdy* and *bmm* gene dysregulations. (A) The *Stim* KD-mediated body fat accumulation can be partially suppressed by simultaneous *sNPF* knockdown in the *sNPF*-positive neurons. A *sNPF*-positive neuron-specific (sNPF-Gal4) *sNPF* RNAi caused decreased body fat levels, while a *Stim* knockdown in the *sNPF*-positive neurons or a chronic *sNPF* knockdown in the fat storage tissue (FB-Gal4) had no effect. **(B)** The *Stim* KD-mediated obesity can be largely suppressed by simultaneous *mdy* RNAi in the fat storage tissue. Single gene modulations caused body fat accumulation due to fat storage tissue targeted *mdy* overexpression or *Stim* RNAi, but also a body fat decrease by an *mdy* RNAi. **(C)** The onset of *Stim* KD-mediated obesity can be partially suppressed by simultaneous *bmm* gene overexpression (gof) in the fat storage tissue. On the other hand, the single *bmm* gene overexpression causes a body fat decrease. Note: The male fly body fat content was quantified by a CCA after a constitutive (**A**), a long conditional (6 d, **B**) or a short-term conditional knockdown (34 h, **C**) of the respective genes. Note that an UAS-GFP was used to match the number of effector transgenes (**A, B**). *$p \leq 0.05$, **$p \leq 0.01$ and ***$p \leq 0.001$ n.s. not significant. Figure modified after Baumbach *et al.* (2014).

Collectively, these results indicate that *sNPF* activity in the brain is needed for the *Stim* KD-dependent regulation of *mdy* and *bmm* expression in fat storage tissue. This also implicates a tissue non-autonomous body fat storage control in the *Stim* KD-mediated obesity progression (Fig. 29A). Therefore, one can propose a model in which the fat storage-restricted impairment of *Stim* initiates *sNPF* up-regulation in the central nervous system *via* an unknown factor, which might be activated by Cam in response to iCa^{2+} changes in the fat body tissue. Subsequently, the *sNPF* up-regulation in the central nervous system causes hyperphagia, which triggers an obesogenic program in the fat storage tissue by adapted regulation of lipogenesis *via mdy* and lipolysis *via bmm*.

2.5 Identification and characterization of *Gαq, Gγ1* and *Plc21C* as new body fat regulators

Since with *Cam*, *sNPF*, *bmm* and *mdy* potential downstream body fat regulators of *Stim* and SOCE were found, I further characterized, which factors act upstream of *Stim* and SOCE in body fat control. It is known that SOCE is activated due to the binding of an IP3 to Itp-r83A, which causes a depletion of ER Ca^{2+} stores (reviewed in Soboloff *et al.* (2012)). The IP3 signaling molecule can be synthesized by a Phospholipase C, whereof the activity is under the control of a G-protein coupled receptor (GPCR). The RNAi-screen and additional body fat-based validations revealed the well-known GPCR AkhR (Bharucha *et al.*, 2008; Grönke *et al.*, 2007)*,* the G-proteins Gαq/*Dm*GNAQ and Gγ1 as well as the Phospholipase Plc21C/*Dm*PLCB1 as body fat storage regulators (Table S2). To address a specific role of *Gαq, Gγ1* and *Plc21C* in lipid metabolism control *via* modulation of SOCE, the gene activities were modulated *via* RNAi and gof by using the TARGET system (McGuire *et al.*, 2003) and the conditional fat storage driver (ts-FB-Gal4). Furthermore, different techniques were used to visualize the lipid accumulation and the iCa^{2+} changes directly in the fat body.

2.5.1 *Drosophila* body fat storage control by *Gαq*, *Gγ1* and *Plc21C*

Consistently to previous results, a 6 days induced fat storage tissue-specific *Stim* knockdown caused massive body fat accumulation (up to 180% more body fat; Fig. 30A). When *Gαq, Gγ1* and *Plc21C* genes were impaired under the same conditions, the body fat content exceeded 200% of accumulation compared to controls (Fig. 30A). The accumulation could also be observed in *AkhR* gene knockdown flies (+143% body fat) or in *AkhR* deletion mutants (+172% body fat; Fig. 30A). The Akh neuropeptide is synthesized in the neuroendocrine cc and binds the AkhR of target tissues to mediate lipolytic signals *via* cAMP and Ca^{2+} signaling (Arrese *et al.*, 1999). Therefore, a cc-specfic RNAi-mediated reduction of the Akh peptide was done in adult flies that caused nearly a duplication of the body fat content (Fig. 30A). Accordingly, Akh or AkhR overexpression (gof) in the fat body led to antagonistic effects and caused a body fat reduction by 70% (Fig. 30A). These effects could also be mimicked by overexpression of *Gαq* (-77% body fat) or *Stim* (-93% body fat; Fig. 30A). Constantly, TLC and ORO staining of lipids in sagittal cryosections (Fig. 30B, C) confirmed these effects. To address whether the lipid stores are directly affected, the adult fat body tissue of female flies was analyzed for the effects of *Gαq, Gγ1, Plc21C, Stim, Akh* and *AkhR* gene modulation in the fat storage tissues but also the effect of *Akh* gof in the cc (Fig. 30D). An RNAi-mediated fat storage-restricted knockdown of *Gαq, Gγ1, Plc21C* and *Stim* increases the amount of lipids stored in fat body cells, compared to control flies. In addition, similar effects could be observed in *AkhR* deletion mutants, in fat storage-restricted *AkhR* RNAi flies and in cc-targeted *Akh* RNAi flies. Conversely, the fat body lipid stores are largely depleted in fat storage-restricted *Akh* or *AkhR* gof flies. In summary, a modulation of *Gαq, Gγ1, Plc21C* and *Stim* causes changes in lipid storage in the whole organism as well as on the cellular level of fat body cells. Moreover, these data gives rise to the question whether Akh/AkhR-signaling in body fat control of adult *Drosophila* flies might be transmitted over the G-proteins Gαq and Gγ1 to the Phospholipase Plc21C, which finally activates SOCE causing body fat depletion.
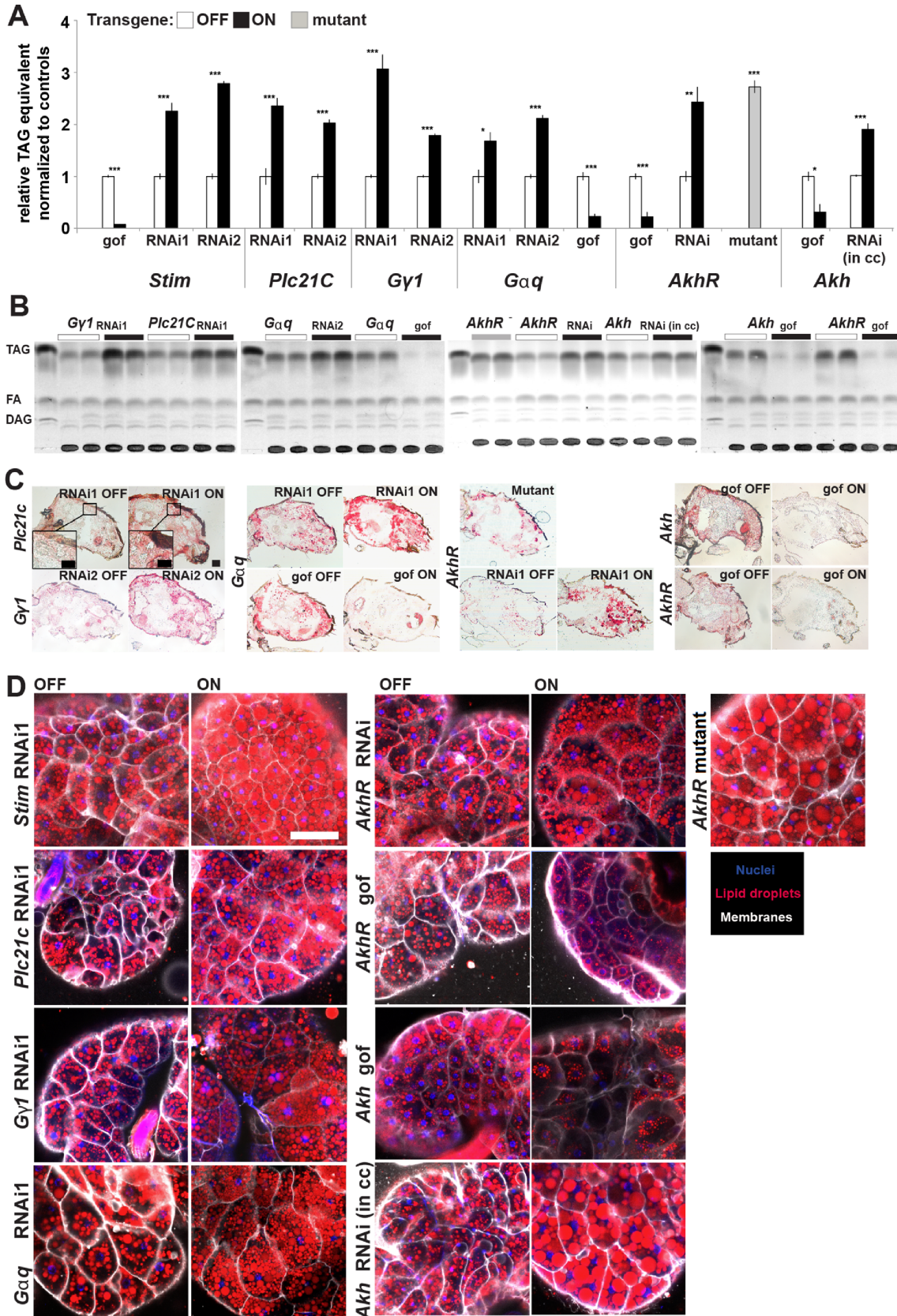
(Fig. 30 legend on next page)   64

Fig. 30: Body fat storage control by *Gαq, Gγ1, Plc21C, Stim, Akh* and *AkhR* gene modulation.
An RNAi-mediated gene knockdown of *Stim, Plc21C, Gγ1, Gαq, AkhR* (in the adult fat storage tissue) and *Akh* (in cc cells) or an *AkhR*- deletion mutant causes body fat accumulation in adult male flies. Conversely, a fat storage-restricted overexpression (gof) of *Stim, Gαq* and *Akh* leads to leanness in flies. Body fat changes were either assayed by total body fat analysis (**A**), by thin layer chromatography (**B**), by Oil Red O staining on sagittal cryosections of adult male fly abdomen (**C**) or by imaging of adult female fat bodies using confocal fluorescence microscopy (**D**; lipids [red], DNA [blue], membranes [white]). Note that image details in (**C**) show magnifications of the subcuticular fat body of *Plc21C* knockdown flies and controls. TLCs in (**B**) were done by Philip Hehlert. Fly husbandry and fat body images in (**D**) were done by Yanjun Xu (Baumbach and Xu *et al.*, 2014, accepted). Statistical significance: *$p \leq 0.05$, **$p \leq 0.01$ and *** $p \leq 0.001$. Scale bar represents (50 µm for image details) 100 µm in **C** and 50 µm in **D**. Figure is after Baumbach and Xu *et al.* (2014, accepted).

2.5.2 An impairment of *AkhR*, *Gαq*, *Gγ1* and *Plc21C* causes decreased iCa²⁺ in adult fat body cells

Previous results identified *Gαq, Gγ1* and *Plc21C* as body fat storage regulators and raised the question whether they are involved in the Akh-dependent storage lipid mobilization *via* SOCE and the key second messenger Ca^{2+}. It was already shown for a variety of insects including the tobacco hornworm *Manduca sexta* that Akh-dependent storage lipid mobilization is mediated at least in part *via* Ca^{2+} (Arrese *et al.*, 1999). For a fat storage-restricted *Stim* KD, I already showed a decrease in iCa²⁺ directly in the adult fat body cells (Fig. 17A) by using the CaLexA system, which translates the iCa²⁺ concentrations to a membrane-targeted GFP reporter expression (Masuyama *et al.*, 2012). To test whether *Gαq, Gγ1, Plc21C, Stim and AkhR* KDs are all able to modulate the iCa²⁺ concentrations in the fat body, they were subjected to similar conditions. Consistently, a fat storage-restricted impairment of *Stim* caused the expected decrease in iCa²⁺ (Fig. 17A and Fig. 31A, B). Similarly, an impairment of *Gαq, Gγ1, Plc21C* and *AkhR* under the same conditions also resulted in a strong reduction of iCa²⁺ in adult fat body cells (Fig. 31A, B). Collectively, these results implicate an involvement of *Gαq, Gγ1, Plc21C* and *AkhR* in body fat storage control *via* iCa²⁺, likely by the modulation of SOCE in the fat storage tissues. These results add further evidence for the hypothesis that *Gαq, Gγ1, Plc21C, Stim* and *AkhR* act in the same signaling pathway.

Results
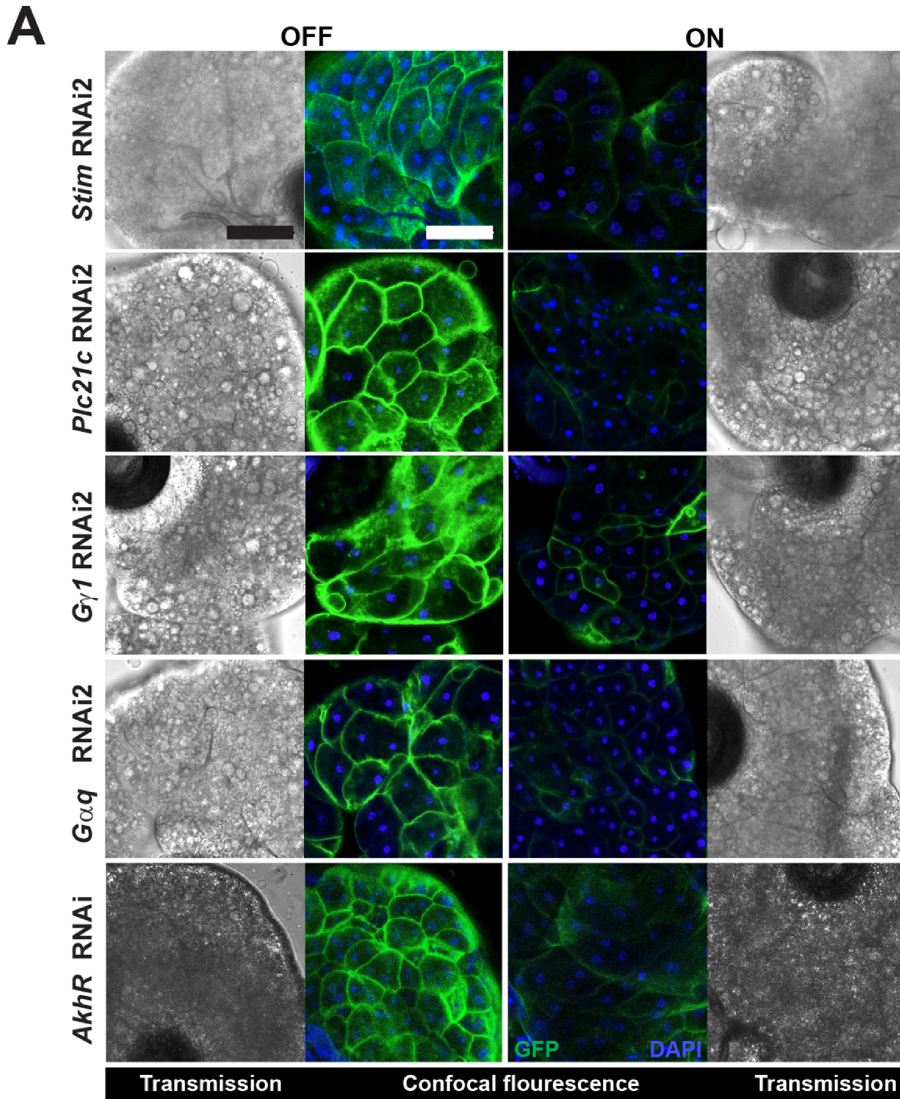
Fig. 31: An impairment of *Stim, Plc21C, Gγ1, Gαq* and *AkhR* causes decreased iCa²⁺ concentrations. (**A**) The CaLexA system, which is based on the iCa²⁺-dependent transcription of membrane-targeted GFP reporter protein (green), was used to image the iCa²⁺ concentration of fat body cells by confocal fluorescence microscopy (inner panels). In addition, transmission microscopy (outer panels) was used to show that imaged cells are LD-containing fat body cells. Nuclei are stained with DAPI (blue). (**B**) GFP-signal quantification (=iCa²⁺) of confocal images based on the CaLexA system. Fat body images were done by Yanjun Xu (Baumbach and Xu *et al.*, 2014, accepted).Scale bar is 50 µm. Fly husbandry and fat body images were done by Yanjun Xu (Baumbach and Xu *et al.*, 2014, accepted). Figure is after Baumbach and Xu *et al.* (2014, accepted).

66
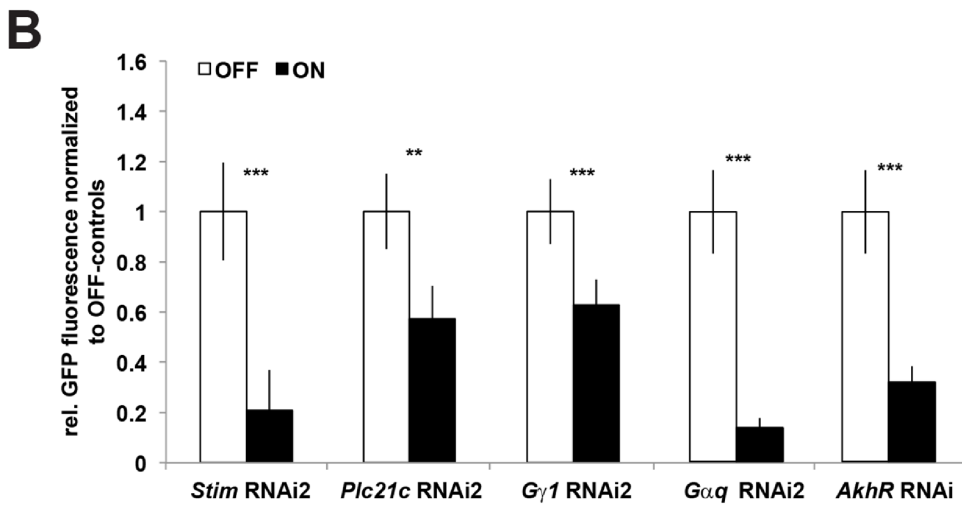
2.5.3 *Gαq*, *Gγ1* and *Plc21C* control the expression of the lipogenic *midway* and the lipolytic *brummer* gene

As shown in previous chapters, a conditional fat storage-restricted short-term (34 h) *Stim* KD causes mild body fat accumulation (Fig. 26B) and an obesogenic transcriptional response (Fig. 26C). In order to test the hypothesis that *Gαq, Gγ1, Plc21C, Stim* and *AkhR* act in the same pathway, the experimental setup was repeated with the remaining factors. Consistently, a *Stim* KD caused the onset of obesity (+22% body fat; Fig. 32A) by up-regulation of the lipogenic *mdy* gene (+52%) and down-regulation of the lipolytic *bmm* gene (-37%) (Fig. 32B). Interestingly, a similar *mdy/bmm*-expression pattern could be observed, when *Plc21C, Gαq* or *Gγ1* are short-term impaired (34 h) in the adult fat storage tissue. A *Plc21C* RNAi also resulted in mild body fat accumulation (+43% body fat; Fig. 32A), while *mdy* was up-regulated by 68% and *bmm* was down-regulated by 76% (Fig. 32B). Similarly, a *Gγ1* RNAi mediated body fat increase (+34%, Fig. 32A) could be observed, which correlated with a nearly doubled expression of *mdy* and the down-regulation of *bmm* by 57% (Fig. 32B). The fat storage-restricted short-term *Gαq* RNAi led to a mild body fat increase (+29%), while *mdy* was up- (+102%) and *bmm* was down-regulated (-32%). On the other hand, overexpression of *Gαq* caused a body fat decrease (-69%), while a down-regulation of *mdy* (-40%) and the up-regulation of *bmm* (+57%) could be observed (Fig. 32A, B).

In summary, the modulation of *Stim, Plc21C, Gγ1* and *Gαq* gene activities resulted in comparable body fat changes and transcriptional obesogenic responses, which suggests that *Stim/Plc21C/Gγ1/Gαq* act as a module in the same signal transduction pathway. Additionally, a fat storage-restricted short-term *AkhR* RNAi also caused mild body fat accumulation(+27% body fat; Fig. 32A) and up-regulation of *mdy* by 65%, while *bmm* expression is not significantly changed (Fig. 32B). This implicates that the GPCR AKHR might employ the *Gαq/Gγ1/Plc21C/Stim* module in addition to other pathways for body fat storage control.

Results
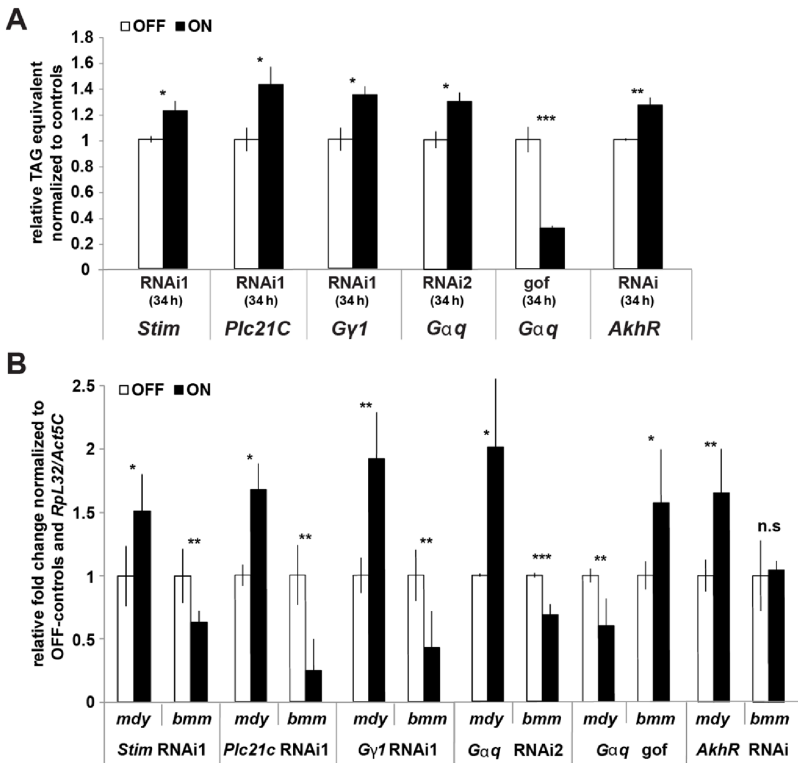
**Fig. 32: A short-term modulation of *Stim, Plc21C, Gγ1, Gαq* and *AkhR* causes transcriptional regulation of the lipogenic *mdy* and the lipolytic *bmm* genes accompanied by correlating body fat changes.** (**A**) The whole body fat content was quantified by CCA. A fat storage-restricted short-term RNAi (34 h) of *Stim, Plc21C, Gγ1, Gαq* and *AkhR* caused a comparable increase of total body fat (22-43%). Conversely, a fat storage-restricted short-term overexpression (gof) of *Gαq* resulted in depletion of body fat stores by 69%. (**B**) Modulation of body fat content by *Stim, Plc21C, Gγ1, Gαq* and *AkhR* RNAi as well as *Gαq* gof led to transcriptional regulation of the lipogenic *mdy* and the lipolytic *bmm* genes. Relative *mdy* and *bmm* transcript levels from total fly abdomen were measured by qRT-PCR and compared to control flies lacking a driver transgene (OFF). The fly husbandry and parts of the RNA extraction as well as the qRT-PCRs were done by Yanjun Xu (Baumbach and Xu *et al.*, 2014, accepted). n.s. non-significant, *p≤0.05, **p≤0.01 and ***p≤0.001. Figure is after Baumbach and Xu *et al.* (2014, accepted).

2.5.4 The Akh-mediated lipolysis can be suppressed by impairment of the *Gαq/Gγ1/Plc21C/Stim*-module

As shown in Fig. 30, a fat storage-restricted *Gαq, Gγ1, Plc21C* or *Stim* RNAi causes obesity in flies. Conversely, a fat storage-restricted overexpression of *Akh* depleted the body fat stores ((Grönke *et al.*, 2007); Fig. 30 and Fig. 33). To test if *Akh/AkhR* acts upstream of the *Gαq/Gγ1/Plc21C/Stim*-module, a genetic interaction experiment was performed to suppress the *Akh*-mediated body fat depletion in mature adult flies. Interestingly, a simultaneous overexpression of *Akh* and down-regulation of *Stim* by RNAi caused a more than doubled body fat content (Fig. 33), which is comparable to the body fat accumulation of single *Stim* RNAi flies (Fig. 30A). Consistently, a fat storage-restricted RNAi of *Gαq, Gγ1* and *Plc21C* in flies overexpressing *Akh* in the fat storage tissue, also suppressed the *Akh*-

68

mediated depletion of body fat stores (Fig. 33). In detail, a fat storage-restricted *Gαq* and *Plc21C* RNAi in an *Akh* gof background caused a mild body fat accumulation by 34% and 47%, while *Gγ1* RNAi normalized the body fat content to the level of control flies, lacking the fat storage-restricted driver transgene (ts-FB-Gal4).
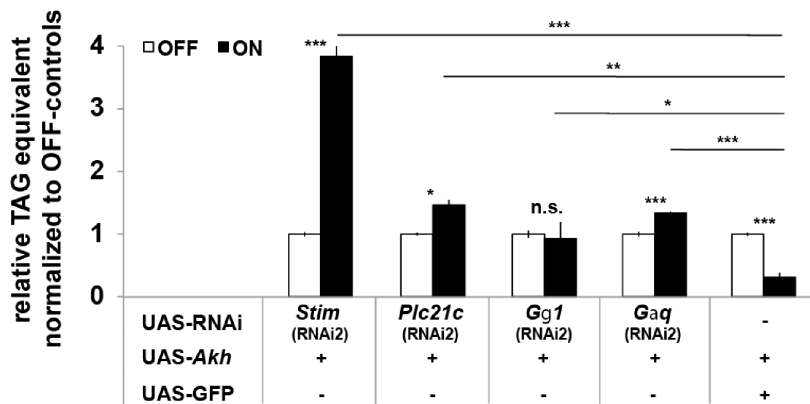

Fig. 33: A fat storage-restricted *Stim, Plc21C, Gγ1* and *Gαq* gene knockdown suppresses Akh-induced body fat depletion. The total body fat contents of male flies carrying an *Akh* over-expression effector and RNAi effector transgenes against *Stim, Plc21C, Gγ1* and *Gαq* in the presence (ON) or absence (OFF) of a conditional fat storage-restricted driver (ts-FB-Gal4) were quantified by using a CCA. Note that an UAS-GFP was crossed in the UAS-*Akh* line to match the number of transgenes. n.s. non-significant, *p≤0.05, **p≤0.01 and ***p≤0.001. Figure is after Baumbach and Xu *et al.* (2014, accepted).

In summary, the genetic interaction analysis in the adult *Drosophila* fat storage tissue supports a hypothesis in which Akh/AkhR-signaling causes the depletion of lipid stores *via* the downstream *Gαq/Gγ1/Plc21C/Stim*-module. In detail, AkhR activation might activate the Plc21C *via* the G-proteins Gαq and Gγ1, which consequently leads to synthesis of IP3, the activation of SOCE, elevated iCa^{2+} and lipid mobilization. However, other GPCRs next to AkhR might employ Gαq, Gγ1 and Plc21C to increase iCa^{2+} *via* STIM and SOCE in adult fat body cells, too. Therefore, further studies are necessary to unveil a possible role of other GPCR in the body fat storage regulation.

3 Discussion

The steady progress of humanity leads to a strong improvement of living conditions especially in industrial nations. People can reach different locations all over the world by car, ship or plane and a flood of new products, *e.g.* from the food industry, seems to make life more pleasant. However, for these particular reasons there are other problems emerging. As the consequence of mobility and the food situation, people move less on their own and consume more high caloric food (WHO, Fact sheet N°311, March 2013). This situation is a challenge for our body and metabolism, which tries to keep an energy homeostatic state. The higher energy intake and less energy consumption is normally compensated by modulating central regulators of energy homeostasis (see chapter 1.1 and 1.2). An interference of energy homeostasis by impairment or mutation of central regulators can cause a disease pattern, which is known as obesity (see chapter 1.1). The pandemic outspread of obesity in the last decades, especially in industrial nations, rises the need to understand the genetic reasons behind this disease pattern. The search and characterization of central energy homeostasis regulators is a promising way to understand the genetic reasons for obesity and to provide a base for therapeutic treatments.

In this work, I identified and characterized new regulators of energy homeostasis by a body fat-based *in vivo* RNAi knockdown screen in the fruit fly *Drosophila melanogaster*. Interestingly, the screen revealed novel pathways, which are involved in the regulation of energy homeostasis in the fly, whereby most of the identified genes and processes are conserved up to humans.

3.1 A conditional *in vivo* fat storage-restricted RNAi screen in *Drosophila* reveals new insights in body fat regulation

Different genetic screens with the aim to identify new fat storage regulators were done in a variety of invertebrate model organisms. Besides screens in yeasts (Daum *et al.*, 1999; Natter *et al.*, 2005) and *Caenorhabditis elegans* (Ashrafi *et al.*,

2003) also screens in *Drosophila* tissue culture cells were done (Beller *et al.*, 2008; Guo *et al.*, 2008).

These screens indicated that a complex regulatory network is necessary to control lipid storage. Furthermore, both *Drosophila* screens covered nearly the whole genome. While Beller *et al.* (2008) identified 526 genes causing over-/under-storage of lipid droplets due to RNAi, Guo *et al.* (2008) identified 227 genes. The major finding of both screens was the identification of genes involved in the COPI vesicle trafficking from the Golgi to the endoplasmic reticulum (ER), respectively the retrograde transport. An interference of the genes *Arf79F*, *garz* (*garz* only in Guo *et al.* (2008)) or most genes coding for COPI subunits, resulted in increased lipid storage or changed lipid droplet morphology. Since both studies were based on tissue cultures, it was not clear, which effect an interference of vesicle trafficking in whole organisms can cause. In 2010, *in vivo* screens for body fat changes were done in *Drosophila* larvae (Reis *et al.*, 2010) and adult flies (Pospisilik *et al.*, 2010). In detail, Reis *et al.* (2010) used a buoyancy-based screen on 870 homozygous-viable mutants, which identified 66 genes as regulators. Due to technical limitations, only genetic mutants, which caused a body fat accumulation, could be analyzed. The major finding of this screen was the identification of the *Sir2* gene, which regulates the storage and metabolism of carbohydrates and lipids by deacetylation of regulatory proteins. On the other hand, Pospisilik *et al.* (2010) analyzed the ubiquitous RNAi knockdowns of 10,489 distinct open reading frames (ORFs) in the adult fly resulting in 516 candidate genes. By this effort, they were able to identify a pathway, which was previously unknown to regulate the body fat content, respectively the "regulation of smoothened [hedgehog] signaling". Although all these screens unveiled new fat storage regulators, they had a limitation. All these screens were based on ubiquitous knockdowns or mutations. However, it is very likely that obesity is also based on a time- and tissue-dependent interference of gene modulation, since one gene can have many functions dependent on the expressing tissue.

3.1.1 Screening approach and candidates in body fat regulation

By using an alternative screening approach, based on the determination of body fat in adult flies with a conditional fat storage tissue targeted *in vivo* RNAi knockdown against 6796 genes, I was able to identify and validate 77 candidates, whereby most of them (74%) were previously not connected to the regulation of body fat (Baumbach *et al.*, 2014). Surprisingly, all screens outlined under chapter 3.1 showed only a very limited overlap in their identified candidate genes. In detail, a comparison to Beller *et al.* (2008) resulted in six, to Guo *et al.* (2008) in three and to Pospisilik *et al.* (2010) in eight overlapping candidates, while no overlap to Reis *et al.* (2010) could be observed. These differences in the identified candidate genes could be explained by the different model system and by the specificity of our novel screening approach, where only the adult fat storage tissues were targeted by RNAi knockdown (Fig. 8). These conditions were necessary, since I showed that almost half of the identified genes (35; 45%) caused pre-adult lethality (Table S2), indicating that about half of the obesity and anti-obesity genes are essential in a cellular context different from adult adipose tissue. Accordingly, these genes would have escaped identification as body fat regulators by conventional mutant analysis. In Pospisilik *et al.* (2010), a time-specific system was used for the primary screen, which did not specifically target the fat storage tissue. In this study, the fraction of candidate genes resulting in decreased fat content upon knockdown (360 of 516; 70%) exceeded that of obesity-causing candidates (216 of 516; 30%) (Pospisilik *et al.*, 2010), while our study (Baumbach *et al.*, 2014) showed 47 anti-obesity (61%) and 30 obesity genes (39%) out of 77 candidates. The fact that more lean candidates were identified in the primary screen of Pospisilik *et al.* (2010) might be due to the ubiquitous knockdown, which interferes with several processes, which are unrelated to body fat storage control. These interferences might decrease the fitness of the flies, whereby the reduced body fat storage is just a secondary effect. With our novel time- and tissue dependent screening approach, we circumvented this problem and found more anti-obesity than obesity genes, which could be validated by different drivers and RNAi constructs. Interestingly, fifty-seven novel body fat regulator genes including

45 (79%), which are sequence-conserved in evolution up to humans, were identified. This high conservation of candidate genes connected to body fat storage regulation was also observed in Pospisilik *et al.* (2010), which emphasizes the adult *Drosophila* model system as a starting point for the elucidation of novel body fat storage regulators in mammals.

The identification of twenty already known fly anti-obesity and obesity genes provides the proof of concept for the validity of our novel screening approach. In detail, gene regulators of glycerolipid homeostasis, such as *mdy* (Buszczak *et al.*, 2002), and *bmm* (Grönke *et al.*, 2005) were identified and validated as obesity-/anti-obesity genes. In addition, the fat storage-restricted *mdy* and *bmm* RNAi compared to mutants revealed their specificity in body fat storage control, since both approaches caused similar body fat storage effects (Fig. 11A, B, C). To uncover the possible biological function of the remaining 57 identified obesity- and anti-obesity genes, gene ontology (GO) analysis and functional classification based on manually edited GO term assignments were done.

Beside miscellaneous pathways and general metabolism regulators, also other signaling pathways could be identified (Fig. 9C, D and Fig. 10). An identified member of the kinase/phosphatase-signaling is the *multiple ankyrin repeats single KH domain* (*mask/DmANKHD1*) gene, which was highly validated in the screen (Fig. S2). Interestingly, this gene was shown to be involved in apoptosis and proliferation since the loss of Mask increases programmed cell death and reduces proliferation, *e.g.* in the L3 eye imaginal discs (Smith *et al.*, 2002). Therefore, one can suggest that also adult fat storage tissue-expressed *mask* controls the cell number and conclusively the organ size that contributes to the body fat storage, which is in accordance with Pospisilik *et al.* (2010). They also showed that fat body-restricted interference of organ size regulators contribute to the body fat storage.

Furthermore, it could also be shown that regulators of autophagy and the proteasome are able to modulate the body fat storage on the cellular level. In addition, cellular transcriptional and translational control regulators were identified. The *ftz transcription factor 1* (*ftz-f1/DmNR5A2*) gene was described as an NR5A-type orphan nuclear receptor, whereby a KD of *ftz-f1* in the follicle cells causes a

depletion of the lipid content (Talamillo *et al.*, 2013), which is consistent with the lean phenotype due to a fat storage-restricted RNAi KD (see Fig. S2).

The major finding of the RNAi screen was the identification of pathways involved in vesicle-mediated trafficking, Ca^{2+}-/G-protein coupled receptor (GPCR)-signaling and lipid metabolism (Fig. 9C, D and Fig. 10), which will be further described in the following. An adult fat storage-restricted knockdown of the *wunen-2* (*wun2*) gene, which encodes a lipid phosphate phosphatase that is capable of dephosphorylating lysophosphatidic acid (LPA) and phosphatidic acid (PA) to DAG *in vitro* (Renault *et al.*, 2004), causes lean flies (Fig. 13A, B, C). The majority of Wun2 localizes to the plasma membrane. Here it dephosphorylates extracellular lipid phosphates, which can act as signaling lipids in cell guidance and survival (Renault *et al.*, 2004). In addition, a cytoplasmic pool of Wun2 was shown (Starz-Gaiano *et al.*, 2001), which can potentially contribute to the glycerol-3-phosphate pathway of TAG biosynthesis (Fig. 12A). Taken together, the lean phenotype of *wun2* RNAi KD flies could be explained by either an improper processing of signaling lipids followed by fat body cell death or by a direct contribution to TAG biosynthesis. Further research is necessary to unveil the role of the newly identified body fat storage regulator *wun2* in lipid metabolism.

3.1.2 Interference of the phospholipid metabolism affects body fat

An impairment of the phospholipid metabolism by a fat storage-restricted interference of the *Pect* gene causes body fat accumulation in adult flies (Fig. 12B, C, D). Furthermore, genes involved in lipogenesis, namely *mdy*, *Fas*, *ACC* and *ACS* are collectively up-regulated (Fig. 12E). On the other hand, a main intermediate in lipolysis/lipogenesis which can possibly connect these processes to the Kennedy pathway of PE synthesis (Fig. 12A), respectively DAG, is also accumulated (Fig. 12B).

Previous studies observed that a global *Pect* knockdown led to lipotoxic cardiomyopathy and obesity in flies (Lim *et al.*, 2011), which gives further support for the possible link between the phospholipid and the glycerolipid metabolism *via* DAG. Interestingly, $Pcyt2^{-/+}$ knockout mice are obese (Fullerton *et al.*, 2009) and a

Pcyt2 knockout in hepatocytes causes liver steatosis (Leonardi *et al.*, 2009). In addition, an up-regulation of lipogenic genes, *e.g. Srebf1*, *Fasn*, and *Dgat1*, could also be observed in mice due to the *Pcyt2* knockout, which leads to DAG accumulation (Fullerton *et al.*, 2009; Leonardi *et al.*, 2009). These observations provide strong evidence for the evolutionary conservation of the coupling between phospholipid and glycerolipid metabolism between flies and mammals.

While this work was still under progress, it was shown that a global *Pect* knockdown in adult flies as well as mutations of the ethanolamine kinase gene *easily shocked* (*eas/DmETNK1*) causes procession of the transcriptional activator *Drosophila* sterol regulatory element-binding protein (HLH106/*Dm*SREBF1), which results in the up-regulation of the lipogenic genes *ACC* and *Fas* (Lim *et al.*, 2011). In agreement with earlier tissue culture studies (Dobrosotskaya *et al.*, 2002), it was proposed that PE inhibits the proteolytic *Dm*SREBF1 cleavage (=activation) in *Drosophila* as a feedback regulation. Since we confirmed the TAG/DAG accumulation and the lipogenic response due to an interference of the PE pathway in Baumbach *et al.* (2014), there is independent evidence for a model in which a *Pect* KD results in accumulation of PE and DAG, whereby dropping PE levels release the inhibitory effects on the cleavage of *Dm*SREBF1. Conclusively, this results in a nuclear localization of the cleaved *Dm*SREBF1 followed by activation of a lipogenic response. This finally results in accumulation of TAG and the development of obesity. Interestingly, a tissue-specific knockdown of the *CTP:phosphocholine cytidylyltransferase* (*Cct1*) gene, which is the functional homolog of *Pect* in the phosphatidylcholine (PC) synthesis, causes the formation of giant lipid droplets (LDs) in the larval fat body and an increased body TAG content (Krahmer *et al.*, 2011). This might implicate that a similar mechanism exists for the PC pathway. Furthermore, an up-regulation of the FA transporter FATP4 in the intestine of *Pcyt2*$^{+/-}$ deficient mice could be observed, which results in an increased FA pool and consequently an increased TAG formation (Singh *et al.*, 2012). Since a mutation of the *Drosophila* homolog *Fatty acid (long chain) transport protein* (*dFatp*) also leads to increased fat storage (Sujkowski *et al.*, 2012), there is additional evidence for a conserved role of Pect as a body fat

storage regulator. In addition, these results implicate a second model, whereby a *Pect* KD results in an increased dietary FA uptake in the intestine, which results in increased TAG formation and obesity.

Taken together, the identification of phospholipid metabolism genes acting as body fat regulators provides a strong support for the *in vivo* importance of the evolutionarily conserved intersection between the glycerolipid and the phospholipid metabolism pathways in the control of body fat storage. Furthermore, a mixture of regulations seems to cause the observed obesity in response to impairment of the phospholipid synthesis. Further studies could give a deeper insight in the importance of phospholipids in body fat storage regulation and might reveal a possible inter-organ communication between the fat body tissue and the intestine *via* the phospholipid regulator *Pect*.

3.1.3 The vesicle trafficking and its importance in obesity

The GO analysis indicates that genes involved in vesicle-mediated transport between the ER and Golgi participate in adiposity control (Fig. 9D). It was suggested that lipid droplets are involved in intracellular transport processes including the vesicular transport, since known components of vesicle trafficking were found to be located at lipid bodies in human epithelial cells (Umlauf *et al.*, 2004). Interestingly, the small GTPase RAB1b was found to be located at lipid droplets. A protein BLAST revealed that *Drosophila* Rab1 shows a 83% identity and covers the complete human RAB1b protein sequence, while human RAB1a shows 84% identity. Furthermore, *Rab1/DmRAB1AB* acts as anti-obesity gene in adult flies (Fig. 15A, B, C) and was previously identified as embryonic lipid-droplet associated protein (Cermelli *et al.*, 2006), while its yeast homolog Ypt1p was shown to participate in anterograde, COPII-mediated transport and cis-Golgi vesicle trafficking (Wang *et al.*, 2000). Controversially, *Rab1* DN was found to result in small lipid droplets, whereby *Rab1* CA increased lipid droplet size in *Drosophila* larval fat body (Wang *et al.*, 2012a). Since this is in contrast to adult flies, *Rab1* seems to connect body fat storage and vesicle trafficking in a context-

dependent manner. In contrast to *Rab1*, other components of vesicle trafficking were directly identified in the RNAi screen (see Tab. S2). Among the identified genes, *Arf79F/DmARF1* acts as anti-obesity gene (Fig. 15A, B, C). The small GTPase Arf79F is involved in Golgi integrity. In *Drosophila* tissue culture cells, a knockdown of *Arf79F* causes accumulation of storage lipids, shown by enlarged lipid droplets (Beller *et al.*, 2008; Guo *et al.*, 2008). The mammalian ortholog ARF1 acts as key regulator of COPI-mediated retrograde transport between Golgi and ER, whereby ARF1 is regulated by guanine nucleotide exchange factors (GEFs): at the cis-Golgi by the Golgi-specific Brefeldin A resistance factor 1 (GBF1) and at the trans-Golgi by ARFGEF1 and ARFGEF2. Interestingly, the *Drosophila* orthologue of GBF1 encoded by *garz/DmGBF1* (Wang *et al.*, 2012) and *sec71/DmARFGEF1/2* (the fly homolog of mammalian *ArfGEF1/2*) were both identified as anti-obesity genes (Fig. 15A, B, C). Human GBF1 can restore Garz function in tracheal cells, indicating that the relevant functions of Garz and GBF1 proteins have been evolutionarily conserved (Armbruster and Luschnig, 2012). In addition, GBF1 and its effector COPI are required for delivery of ATGL (adipose triglyceride lipase) to lipid droplets (LDs) (Ellong *et al.*, 2011). This was shown by a yeast two-hybrid co-immunoprecipitation, whereby GBF1 and ATGL interact directly. Furthermore, genome-wide screens in *Drosophila* tissue culture also identified *garz* and *Arf79F* as anti-obesity genes (Beller *et al.*, 2008; Guo *et al.*, 2008). Moreover, Beller *et al.* (2008) revealed that COPI components are evolutionary conserved and COPI perturbation increases stored TAG by decreasing the lipolysis rate. Conclusively, it was suggested that COPI directly or indirectly promotes ATGL localization to the droplet surface, resulting in increased lipolysis.

Taken together, impairment of the retrograde (Golgi-ER) transport causes obesity in adult flies *via* an evolutionary conserved mechanism, which is likely mediated by ATGL localization on LDs. On the other hand the RNAi screen also implicates the importance of the anterograde (ER-Golgi) and the trans-Golgi vesicle trafficking.

In contrast to earlier whole-genome *Drosophila* tissue culture screens (Beller *et al.*, 2008; Guo *et al.*, 2008), adiposity in flies can also be triggered by knockdown of the COPII-dependent vesicle trafficking components *Sec24CD/DmSEC24C* and *Ykt6/DmYKT6* (Fig 14 and Tab. S2). The R/v-SNARE *Ykt6* gene is involved in ER-Golgi trafficking (McNew *et al.*, 1997), whereby *Ykt6* orthologues contribute to macroautophagy (Nair *et al.*, 2011). Since it was described for mammals that macroautophagy of lipid droplets can regulate TAG storage (Singh *et al.*, 2009), *Drosophila Ykt6* might also regulate body fat storage in adult flies by this mechanism. As mentioned above, ARF1 is regulated by the GEFs ARFGEF1 and ARFGEF2 at the trans-Golgi. Impairment of the *Drosophila ARFGEF1/2* homolog *sec71* in the fat storage tissue causes body fat accumulation in adult flies (Fig. 15A, B, C). Sec71 is associated to LDs (Beller *et al.*, 2006) and basal for proper ER function and integrity, since a loss of *sec71* results in a changed ER morphology (Norum *et al.*, 2010).

In summary, the identification of already known and novel vesicle-mediated trafficking regulators in the *in vivo* RNAi screen emphasizes the importance of cellular trafficking processes in fat storage tissues for the body fat storage regulation and energy homeostasis.

3.2 The connection between the store-operated calcium entry and lipid metabolism

The body fat-based *in vivo* RNAi screen unveiled several genes, which showed strong effects on the body fat content. The GO analysis of the single obesity/anti-obesity genes uncovered the "regulation of ion transport" as the most prominent GO term (Table S3). Interestingly, all core components of the SOCE were identified (Fig. 16A, B, C), whereby this process was so far unrelated to lipid metabolism and body fat storage regulation.

The canonical SOCE is initiated by the activation of the Itp-r83A at the ER. A fat storage-restricted KD of the major SOCE core component *Stim* causes a depletion

of iCa^{2+} (Fig. 17A). Ca^{2+} is a known second messenger molecule, which was described in a high variety of contexts. These includes cellular functions like secretion, excitation, contraction, motility, metabolism, transcription, growth, cell division and apoptosis (reviewed in Soboloff *et al.* (2012)). Therefore, the finding that Ca^{2+} seems also to regulate the body fat content was of high interest. So far, only one publication pointed into the same direction. During this ongoing study, an obese phenotype of global *Itp-r83A* mutants was observed (Subramanian *et al.*, 2013), which highlights the importance to reveal the link between SOCE and lipid metabolism.

Furthermore, several studies revealed a high conservation of SOCE during evolution. Rat Itpr1, which is the major neuronal isoform, can functionally complement *Drosophila* Itp-r83A functions at cellular and systemic levels, when expressed in the pan-neuronal domain in *Drosophila*. In detail, rat Itpr1 rescues the established neuronal phenotypes of *Itp-r83A* mutants in *Drosophila*, including wing posture, flight, electrophysiological correlates of flight maintenance, and intracellular calcium dynamics (Chakraborty and Hasan, 2012). In addition, a *Drosophila* S2 cell screen for SOC influx revealed Stim as a core-component, which is conserved from *Drosophila* to mammals. In human cells STIM1, but not STIM2, regulates SOC influx. Conclusively, STIM1 represents a conserved component regulating SOC influx and CRAC channel activity (Roos *et al.*, 2005; Zhang *et al.*, 2006) and a characterization of the SOCE and Stim impairment may lead into new insights in the development of obesity.

3.2.1 The role of store-operated calcium entry in body fat regulation

The *in vivo* RNAi screen and further results of this study revealed genetic manipulations of SOCE genes that cause high and low iCa^{2+} concentrations in fat storage tissues and lead to lean and obese flies, respectively (Fig. 16A, B, C). The expected iCa^{2+} concentrations are based on the following widely established model of SOCE (reviewed in Soboloff *et al.* (2012)). In a non-triggered basal state,

extracellular Ca^{2+} concentrations are very high (2000 µM), while intracellular Ca^{2+} is mainly stored in the ER and the Golgi (0.4-0.8 µM; (Pizzo *et al.*, 2011)) with only low concentrations in the cytoplasm (0.1 µM; (Brini and Carafoli, 2009; Roos *et al.*, 2005)) (Fig. 34, left). This regulation is tuned by Itp-r83A and Ca-P60A. The canonical SOCE is triggered by an IP3 signaling molecule, which can bind and activate Itp-r83A. It was shown that IP3 activates the Ca^{2+} release from the ER Ca^{2+} stores (Streb H, Irvine RF, Berridge MJ, 1983), which in turn activates the ER calcium sensor encoded by *Stim*. Activated Stim interacts with the plasma membrane Ca^{2+} channel Olf186-F, which in turn is opened (Yuan *et al.*, 2009). This results in an efflux of extracellular Ca^{2+} in the cytoplasm, which is mainly driven by the gradient between extracellular and cytoplasmic Ca^{2+} concentrations. Subsequently, the iCa^{2+} rises from 0.1 µM to 1.5 µM (Roos *et al.*, 2005). Those high intracellular Ca^{2+} (iCa^{2+}) concentrations (>500 nm) can trigger a plethora of downstream effectors such as Cam (Chin and Means, 2000) (Fig. 34, right). On the other hand, SOCE can be terminated by the calcium pump Ca-P60A, which is counteracting the ER calcium release by pumping Ca^{2+} from the cytoplasm to the ER (Manjarrés *et al.*, 2010) followed by a dissociation of the Stim-Olf186-F complex (Stathopulos *et al.*, 2008).

Discussion
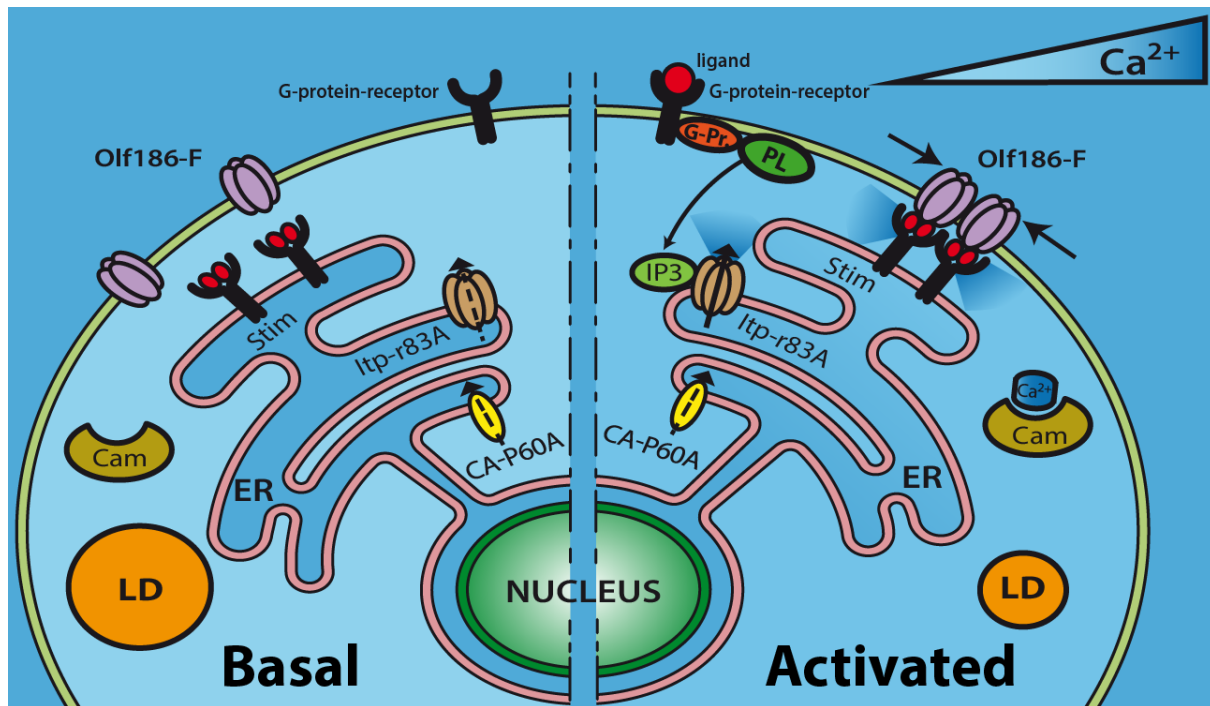
Fig. 34 Model of the store-operated calcium entry (SOCE)-mediated body fat control. In a basal state, Itp-r83A and Ca-P60A are keeping the iCa^{2+} concentration low (~0.1 µM) and the concentration in the endoplasmic reticulum (ER) stores high (~0.4-0.8 µM). SOCE activation is mediated by an IP3 signaling molecule, which is synthesized by a Phospholipase (PL). The PL is under control of G-proteins (G-Pr.) and their G-protein coupled receptor. The synthesized IP3 causes the activation and opening of Itp-r83A, resulting in a depletion of ER Ca^{2+} stores. This depletion is sensed by Stim and results in a dimerization and interaction of Stim and Olf186-F. Consequently, Olf186-F opens followed by Ca^{2+} influx from the extracellular space (~2mM Ca^{2+}) to the cytoplasm. The increased iCa^{2+} concentration (~1.5 µM) can activate effectors such as Cam, which leads to a reduction in cellular fat stores (LD = lipid droplet). Figure modified after Baumbach *et al.* (2014).

A fat storage-restricted *Stim* KD leads to a depletion of iCa^{2+} (Fig. 17A) and body fat accumulation, while a *Ca-P60a* KD, which should lead to an increase in iCa^{2+} concentrations, causes depletion of body fat (Fig. 16A, B, C). In addition, knockdown of the downstream target gene *Cam* mimics the effect of a *Stim* KD on the body fat content (Fig. 16A). Conclusively, the hypothesis that SOCE-mediated modulations in iCa^{2+} can regulate body fat levels *via* Cam is in accordance with the current model and the observed changes in body fat.

Discussion

Interestingly, some SOCE components were already described in a context, which might explain the observed body fat changes. It was shown that KD of mammalian *Stim2* or *ORAI1* caused a decrease in iCa^{2+}, which correlated with enhanced proliferation and increased expression of microphtalmia-associated-transcription-factor, which is a known marker for proliferative melanoma phenotype (Stanisz *et al.*, 2014). Theoretically, enhanced proliferation of the fat storage tissue should lead to more fat body cells, which can store more storage lipids. On the other hand, Ca-P60A was found to be associated with lipid droplets (Cermelli *et al.*, 2006), which implicate an role in body fat storage regulation. Furthermore, it was shown that a mutation of *Itp-r83A* causes increased food intake and reduced Dilp2 levels in the IPCs of *itpr*[ku]-mutant brains. This hyperphagia was accompanied by deposition of excess neutral lipids in the midgut epithelium. In support of these findings, the obese phenotype of *Itp-r83A* mutants can be partially rescued by a fat body-specific *Itp-r83A* gof (Subramanian *et al.*, 2013). Since hyperphagia consequently resulted in an increased energy intake, this might explain how an impairment of SOCE causes body fat accumulation. In addition, the authors claimed that reduced insulin signaling (=reduced Dilp2) appears to be only partially responsible for the metabolic phenotypes of *itpr*[ku]- mutant flies. However, it still remains unclear how an SOCE impairment contributes to the body fat content.

Several observations implicate an evolutionary conservation in the iCa^{2+}-mediated body fat regulation from flies to mammals. It was shown that the *in vitro* differentiation of mouse 3T3-L1 pre-adipocytes can be triggered by depletion of murine Stim1 (Graham *et al.*, 2009), which should cause low iCa^{2+} concentrations. Consistently, rise of iCa^{2+} by activation of the Transient Receptor Potential Vanniloid 1 calcium channel or by inhibition of SERCA, inhibits both the 3T3-L1 (Ntambi and Takova, 1996; Zhang *et al.*, 2007) and human (Shi *et al.*, 2000) pre-adipocyte differentiation into mature adipocytes. Interestingly, high iCa^{2+} concentrations appear to exert a biphasic regulatory role in human adipocyte differentiation, whereby high iCa^{2+} inhibits the early stages and promotes the late stage of differentiation and lipid filling (Shi *et al.*, 2000) *via* up-regulation of lipogenic genes (Jones *et al.*, 1996) and inhibition of lipolysis (Xue *et al.*, 1998).

Discussion

Since the role of iCa^{2+} on fat storage cells stills seems contradictory, further studies are necessary to unveil the potential of SOCE members to act not only as obesity-associated genes in flies, but also in mammals.

One of the potential targets of SOCE-mediated iCa^{2+} changes is the transcription factor NFAT, which belongs to a family of heavily phosphorylated proteins that reside in the cytoplasm of resting cells. Increased Ca^{2+} influx results in NFAT de-phosphorylation by the Calmodulin-dependent protein phosphatase Calcineurin and promotes NFAT translocation to the nucleus (Feske *et al.*, 2003; Hogan *et al.*, 2003), where it acts as transcription factor. In *Drosophila* S2R+ tissue culture cells, the thapsigargin-induced nuclear translocation of a NFAT1:GFP-reporter could be suppressed by knockdown of either the fly anti-obesity gene *Cullin-4* (*Cul-4/DmCUL4A*), which encodes an ubiquitin E3 ligase subunit (Higa *et al.*, 2003)*, Stim*, *olf186-F* or *Cam* (Gwack *et al.*, 2007). These genes were all identified as body fat storage regulators in the *in vivo* RNAi screen (see Tab. S2). Since, *NFAT* was identified as an anti-obesity gene in a *Drosophila* L3 larval screen (Reis *et al.*, 2010), this emphasizes the role of *NFAT* as a downstream factor in SOCE. Furthermore, mammalian studies showed a link from the Calmodulin-Calcineurin-NFAT pathway to adipogenesis. In detail, mouse 3T3-L1 pre-adipocyte differentiation is enhanced by inhibition of Calcineurin (Neal and Clipstone, 2002) and NFATc2/NFATc4 compound knockout mice are lean and resistant to diet induced obesity (Yang *et al.*, 2006).

Collectively, the *in vivo* RNAi screen and previous results emphasize the role of SOCE in body fat storage regulation. However, it is currently unknown whether SOCE-mediated body fat regulations are transmitted *via* Calmodulin, NFAT or other factors and how the lipid metabolism is affected. Therefore, a detailed characterization of central SOCE components is necessary to understand, which cellular and organismal processes cause the observed changes in the body fat content.

3.2.2 The Stromal interaction molecule (Stim) and body fat regulation

SOCE components were identified by genome-wide RNAi screening for SOC influx in *Drosophila* S2 cells (Cahalan, 2009), whereby Stim and Olf186-F are the core components of this process. To characterize the link between SOCE and body fat storage regulation, I focused on the characterization of fat storage-restricted *Stim* KD effects. A fat storage-restricted *Stim* KD triggers obesity in both mature adult male and female flies of different ages, by different *Stim* RNAi transgenes and also in response to different transgene systems (Fig. 18C). I was able to show that a fat storage-restricted *Stim* RNAi KD causes a decrease in Stim protein (Fig. 16A) and the iCa^{2+} concentration (Fig. 17A). Imaging of the fat body cells of those flies also revealed a massive accumulation of lipids directly in this tissue (Fig. 17A, B, D, F) that is accompanied by larger LDs (Fig. 17E), which leads to an increase in cell sizes (Fig. 17C). So far, a direct effect of *Stim* on the body fat content of flies was not described in the literature. Interestingly, no body fat accumulation could be observed in L3 larvae or even immature adult flies (4 h old; Fig. 18B) due to a chronic fat storage-restricted *Stim* KD. This could be explained by the different life styles of L3 larvae and adult flies. In contrast to adult *Drosophila* flies that exhibit a discontinuous feeding behavior, *Drosophila* larvae are continuous feeders to support the rapid growth and differentiation processes. Moreover, *Drosophila* larvae accumulate large amounts of TAG during their development. Conclusively, there is a hint for a fat storage specific function of Stim in regulating the energy uptake/consumption, which might be connected to the discontinuous feeding behaviour and therefore the lifestyle of mature adult flies. Much in contrast to the striking effect in body fat storage, a *Stim* KD has no effect on the organismal carbohydrates. Neither the circulating sugars in the hemolymph, the response to dietary sugars on the body fat nor the glycogen storage and mobilization are affected by a fat storage-restricted *Stim* KD (Fig. 24A, B).

Beside effects, which may involve the regulation the energy intake and/or expenditure, this work showed first evidence that *Stim* might also influence the fat body cell number by regulation of proliferation and cell death *via* apoptosis. The change in fat body cell number could consequently lead to body fat accumulation

(higher cell number) or depletion of body fat due to smaller storage tissues (lower cell number). It is known that apoptosis can be triggered at high iCa^{2+} *via* mitochondria degradation (Kroemer *et al.*, 2007). A fat storage-restricted *Stim* gof causes a dramatic and rapid decrease in body fat (Fig. 16A, B and Fig. 22A, C) and lower fat body-restricted GFP-signals, which may indicate a loss of fat body tissue *via* cell death. Since a *Stim* gof should lead to high iCa^{2+} concentrations and a major effect of increased iCa^{2+} in many cell types is the induction of apoptotic cell death (Rizzuto *et al.*, 2003), this might explain the body fat depletion due to a *Stim* gof. To proof this hypothesis, I used the *Drosophila* eye as a model system, since it is widely used to observe changes in cell number by proliferation and cell death (Hay, Wolff, and Rubin 1994; Leevers *et al.* 1996). An eye-specific *Stim* gof results in rough eyes with a significant smaller size (Fig. 23A, B). Interestingly, previous studies observed larval lethality, when *Stim* was overexpressed with an ubiquitous *da*-Gal4 driver (Eid *et al.*, 2008). In addition, this study also observed abnormally shaped ommatidia and an eye size reduction, when *Stim* was overexpressed. However, it was not shown if these effects are due to cell death. Therefore, I co-expressed the apoptotic cell death/caspase inhibitor p35 (Hay *et al.*, 1994) with *Stim*. This co-expression rescues the reduced eye size and the abnormally shaped ommatidia back to control levels, which indicates a role of cell death mediated *via* the *Stim* gof. A widely used marker for cell death is the gene *reaper* (*rpr*). An overexpression of *rpr* causes a similar effect as observed due to a *Stim* gof, whereby this effect can also be rescued by p35 co-expression (Fig. 23A, B). *Drosophila* Rpr can be localized to the mitochondria, where it can induce mitochondrial fragmentation and apoptotic cell death (Thomenius *et al.*, 2011). Therefore, one can speculate that an increased iCa^{2+} concentration, caused by a *Stim* gof, activates this mitochondria fragmentation *via* Rpr. This is supported by the observation of degraded mitochondria due to a fat storage-restricted *Stim* gof (Fig. 22D). Another possible mode of action for iCa^{2+}-mediated cell death is the mitochondrial Krebs cycle. Ca^{2+}-sensitive dehydrogenases of the Krebs cycle can be stimulated by increased mitochondrial Ca^{2+}, which leads to a boost in ATP production. A side effect of the increased ATP production is the formation of

reactive oxygen species, which are effective but nonselective cell death mediators (Clapham, 2007). Collectively, a *Stim* gof can cause cell death, which causes a decrease in body fat storage. Interestingly, a transient *Stim* gof shows a direct effect on the body fat content, which can be reverted. If *Stim* is not overexpressed anymore, the body fat starts to recover back to control levels (Fig. 22E). Since a *Stim* gof controls the body fat levels *via* cell death, which can be recovered, it seems plausible that the fat storage tissue can also undergo proliferation in order to recover and to adapt the fat storage depots to the energy demands of the fly. This would be supported be the antagonistic effect of a fat storage-restricted *Stim* KD in adult flies, which resulted in obesity instead of body fat depletion (Fig. 17). Previous publications indirectly showed that the adult *Drosophila* fat body might undergo proliferation. In detail, adipocyte cell number and triglyceride storage/fat mass can be controlled by insulin signaling as a conserved process *via* dFOXO and Shaggy (Sgg/*Dm*GSK3B) (DiAngelo and Birnbaum, 2009). In addition, Hippo (Hpo/*Dm*STK3) can control the fat cell number and affects fat storage, whereby *hpo* under the control of the ubiquitous *Dcg*-Gal4 driver resulted in a decrease of the total DNA content in the fat body and knockout of *hpo* promotes fat cell proliferation, shown by mosaic analysis with a repressible cell marker in larvae (Huang *et al.*, 2013). Since these publications indicate that the fat body is able to undergo cell division-mediated fat mass increase, I used two different approaches to validate the cell division in control flies and checked whether a fat storage-restricted *Stim* KD causes a change. By labelling single cell clones with GFP, I was able to show that the control fat body undergoes cell divisions, whereby the cell division rate in *Stim* KD seems to be much higher. This is shown by the size of single cell clones. While control fat bodies have only single cell clones with the size of 1-4 cells, the *Stim* KD cell clone size can not be determined anymore after 5 days, since the single cell clones are already fused with neighboring cell clones (Fig. 20). This indicates that a *Stim* KD leads to the rapid proliferation of fat body cells and the formation of new fat body tissue. In agreement with these observations, the mitotic marker pHis3(S10) shows stronger signals directly in the cell nuclei of *Stim* KD fat body tissue, compared to controls (Fig. 21). Interestingly,

a transient fat storage-restricted *Stim* KD causes chronic obesity in adult flies of different ages (called "programmed obesity"; Fig. 19A, B), which is associated with an enlarged abdomen and a gain in body weight (Fig. 19C, D). The programmed obesity-effect can not be observed by interference of the central lipid metabolism regulator *brummer*, which indicates that the *Stim* KD-mediated effect is specific and not due to a general transient disturbance of lipid metabolism or body fat storage. Notably, it was observed that SOCE shuts down during cell division by a complex mechanism involving redistribution and internalization of Orai1 channels as well as phosphorylation and inactivation of STIM1, whereby the physiological significance of SOCE down-regulation during cell division is not fully understood (reviewed in Smyth and Putney (2012)). This may indicate that SOCE serves as a kind of actuator during cell division and that a disturbance can cause uncontrolled proliferation. Taken together, these observations emphasizes the importance of SOCE and its core components for cell division and supports a model in which *Stim* KD-mediated obesity might be due to proliferation of fat body cells followed by the over-storage of body fat. Further studies are still ongoing to reveal if the "programmed obesity" is due to a permanently impaired fat body proliferation or if other factors are involved. These ongoing studies will lead into new and promising insights in the progression of obesity.

Beside a possible role of *Stim* in the fat body cell number control, different approaches revealed that a *Stim* KD causes a lipid mobilization defect (Fig. 25A, B, C, D). Furthermore, analysis of several energy metabolism regulators (data not shown) revealed strong transcriptional regulation of lipogenesis *via* *mdy/DmDGAT1* (Beller *et al.*, 2010; Buszczak *et al.*, 2002) and lipolysis *via* *bmm/DmATGL* (Grönke *et al.*, 2005) due to a fat storage-restricted *Stim* KD (Fig. 26C). Nevertheless, it is currently unknown, whether mammalian *DGAT1* and *ATGL* transcription is acutely regulated in response to reduced iCa^{2+} levels of the adipose tissues as shown here for *Drosophila*. Interestingly, a comparison between the *bmm/mdy* transcription profiles of *Stim* KD, *Cam* KD and *CrebB* DN flies, revealed similar regulations of body fat and *bmm/mdy* transcripts after a short induction (Fig. 26B, C). Therefore, the increased iCa^{2+} might also trigger the

Calmodulin-Calcineurin-Crtc-CrebB pathway, whereby Crtc/*Dm*TORC2 acts as a CrebB coactivator in *Drosophila* (Bittinger *et al.*, 2004; Chorna and Hasan, 2012). In a non-stimulated state, mammalian TORC2 is restricted to the cytoplasm by a phosphorylation-dependent interaction with 14-3-3 proteins. Increasing iCa^{2+} concentrations will be sensed by Calmodulin and activate Calcineurin to dephosphorylate TORC2, which enables the dephosphorylated TORC2 to enter the nucleus (Screaton *et al.*, 2004), where it affects CREB. In *Drosophila*, CrebB/*Dm*CREB acts as a transcriptional activator and is described to regulate body fat levels (Iijima *et al.*, 2009), whereby a fat storage-restricted overexpression of *CrebB* DN results in body fat accumulation (Fig. 26B and Iijima *et al.* (2009)). Taken together, the transcriptional activator CrebB might be a mediator in *Stim* KD-dependent obesity but further studies are necessary to unveil the connection between *Stim*, *CrebB,* and the lipid metabolism regulators *mdy/bmm*. However, another similarity occurs between *Stim* KD and *CrebB* DN flies. Both showed an enriched food intake due to a fat storage-restricted KD (Fig. 27D and Iijima *et al.* (2009)), which gives further evidence for *CrebB* as a target of *Stim* KD-dependent obesity and also implicates an inter-organ communication, since the food intake is mainly controlled in the brain.

3.2.3 *Stim* controls food intake and the onset of obesity *via* an inter-organ communication

The fat storage-restricted induction of a *Stim* KD causes a rapid body fat accumulation, whereby the locomotor activity is not changed (Fig. 27C). In addition, the average metabolic rate of *Stim* KD flies is un-affected in comparison to control flies (Fig. 27A, B). Hence, the reduced energy expenditure can be excluded as a major cause of *Stim* KD-dependent obesity. Interestingly, flies become hyperphagic from two days of *Stim* KD induction onwards (Fig. 27D). Furthermore, adapting the food intake of *Stim* KD flies to the level of control flies by pair feeding strongly rescues the *Stim* KD-mediated body fat accumulation (Fig. 27E), which implicates that adiposity of *Stim* KD flies is mainly driven by hyperphagia. Since hyperphagia indicates the impairment of normal food intake

control by the central nervous system, I tested the expression pattern of the *Drosophila insulin like peptide* (*dilp*) *2* and *5* genes, which are described as anorexigenic in *Drosophila* larvae (Wu *et al.*, 2005). On the other hand, I tested the expression pattern of the starvation-induced *short neuropeptide F* (*sNPF/DmNPY*) gene, which is described as orexigenic in flies as well as its mouse homolog *neuropeptide Y* (*Npy*) (Hong *et al.*, 2012; Nässel and Wegener, 2011). When *Stim* was specifically impaired in the fat storage tissue, brain *dilp2* and *dilp5* expression is unaffected, while *sNPF* was up-regulated (Fig. 28A), which increases the food intake (Fig. 27D) and causes body fat accumulation (Fig. 27C). In addition, overexpression of *sNPF* directly in the *sNPF*-producing cells leads to an increased food intake and body fat accumulation (Fig. 28D). Conversely, down-regulation reduces food intake (Lee *et al.*, 2004), increases starvation sensitivity (Kahsai *et al.*, 2010) and resulted in lean flies (Fig. 29A). Interestingly, brain *sNPF* becomes up-regulated from one day of fat storage-restricted *Stim* KD induction onwards, while the previously observed *mdy* and *bmm* regulations become apparent after 34 hours (Fig. 28E). This temporal progress of transcriptional regulations indicates that a fat storage-restricted *Stim* KD controls *sNPF* expression in the brain, which in turn causes hyperphagia, resulting in the obesogenic transcriptional regulations of *mdy* and *bmm* in the fat storage tissue. Notably, the *Stim* KD-mediated *mdy/bmm*-regulations could also be triggered by overexpression of *sNPF* in the brain (Fig. 28F), which indicates that *Stim* KD-mediated regulation of *mdy* and *bmm* expression in fat storage tissue requires *sNPF* activity in the brain. Furthermore, the *Stim* KD-mediated *mdy/bmm*-regulations can be almost rescued back to control levels, when *Stim* KD flies were pair fed. Only *mdy* transcripts are still marginally up-regulated, which is in agreement with previous experiments, where pair fed *Stim* KD flies still accumulate slightly more body fat (Fig. 27E). In addition, transgenic correction of *sNPF*, *mdy* and *bmm* gene dysregulation in *Stim* KD flies *via* co-expression of *sNPF* RNAi in the brain (Fig. 29A), *mdy* RNAi (Fig. 29B) and *bmm* gof (Fig. 29C) in the fat storage tissue, attenuates the *Stim* KD-mediated obesity. Since the fat storage tissue-restricted *Cam* KD regulates the *sNPF*, *mdy*, and *bmm* expression very similar in comparison to *Stim* KD flies (Fig.

Discussion

28G), it is likely that the *Stim* KD-mediated decrease in iCa^{2+} is sensed by Cam, which participates in inter-organ communication and brain *sNPF* regulation.

Interestingly, it was shown that the *sNPF* gene expression level is controlled in the brain (Hong *et al.*, 2012), whereby fly sNPF or mammalian NPY signaling up-regulates the Dual specificity tyrosine-phosphorylation-regulated kinase 1, which in turn deacetylates (=activates) FOXO *via* Sirtuin. The activated FOXO binds to the *NPY* and *sNPF* promoter regions and consequently increases expression in the brain. This evolutionary conserved autoregulatory loop may indicate that aspects of *Stim* KD-mediated obesity progression, including inter-organ communication, are conserved from flies to mammals. Further studies might unveil a role of *Stim* in the inter-organ communication and body fat storage regulation in mammals.

However, the signal that transmits *Stim* regulations in the fat body to the *sNPF* regulation in the brain is currently unknown. Since several lipid metabolism regulators can be induced by starvation, *e.g. brummer* in the fat body (Grönke *et al.*, 2005) or *dFOXO* in the brain, which in turn induces *sNPF* expression (Hong *et al.*, 2012), it is important to learn whether *Stim* expression can also be regulated by starvation. Notably, the abdominal *Stim* expression is not significantly changed after 24 h water-only starvation or during a 24 h re-feeding, while body fat is mobilized and refilled, respectively (Fig. 35). However, it is not known how the post-translational Stim activity is controlled on starvation.
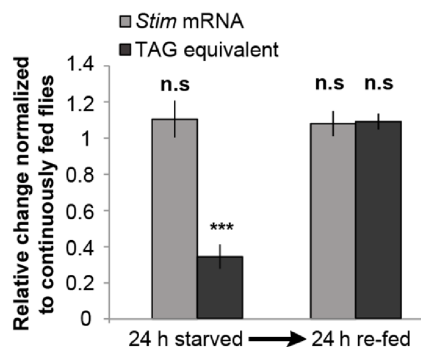
Fig. 35 The *Stim* gene is not transcriptionally regulated in response to starvation. While a severe body fat depletion/re-accumulation of 6 days old male *w*-control flies subject to a 24 h starvation → 24 h re-feeding regimen could be observed, the *Stim* gene expression levels were unchanged. Body fat was measured by a CCA, while relative *Stim* mRNA levels, normalized to fed controls and *RpL32/Act5C* gene expression, was measured from total abdomen mRNA by qRT-PCR. ***p≤0.001, n.s. not significant

Discussion

Noteworthy, the fat body expressed *dilp6* (Grönke *et al.*, 2010) was down-regulated after a 34 h fat storage-restricted *Stim* KD (data not shown). The *dilp6* was shown to be induced in the fat body by starvation and/or activated dFOXO, whereby a reduced expression of *sNPF* in the brain was observed (Bai *et al.*, 2012). Conclusively, the fat body *dilp6* down-regulation in a *Stim* KD might also down-regulate systemic Dilp6 levels and thereby release its inhibitory effect on the *sNPF* expression in the brain, which causes increased *sNPF* levels and hyperphagia. However, it is not shown so far whether fat body-derived Dilp6 is directly acting on the *sNPF* expression in the brain, whether it regulates a downstream adipokine or whether it leads to general metabolic changes, which are affecting the brain. Another potential mediator of the *Stim* KD-mediated inter-organ communication is the fat body expressed cytokine Unpaired 2 (Upd2). Upd2 acts as a functional homolog of mammalian leptin and signals the "fed state" of the fat body to the central nervous system, where it remotely controls the release of Dilps from the insulin producing cells (IPCs; (Rajan and Perrimon, 2012)). In detail, a fat storage-restricted *upd2* KD resulted in flies which are normophagic, hyperglycemic and lean. In addition, these flies accumulate Dilp2 in the IPCs, which implicates that systemic insulin signaling is reduced in such flies. As shown in this work, a fat storage-restricted *Stim* KD causes a down-regulation of abdominal *upd2* transcripts by 49% (Fig. 28A). Controversially, *Stim* KD flies are hyperphagic (Fig. 27D), euglycemic (Fig. 24A) and have significantly lower Dilp2 levels in IPCs compared to controls (Fig. 28B), which is much in contrast to *upd2* knockdown flies. Nevertheless, decreased Upd2 levels might release an inhibitory effect on the brain *sNPF* expression, since it was shown that mammalian mice hypothalamic *Foxo1* expression is reduced by leptin (Kim *et al.*, 2006). This would implicate a model in which a fat storage-restricted *Stim* KD leads to reduced systemic Upd2 levels, which in turn causes higher *dFOXO* expression in the brain and the induction of *sNPF*.

Taken together, the results from this and previous works implicate that a fat storage-restricted impairment of SOCE (represented by its central component Stim) resulted in a change in iCa^{2+} levels of fat body cells, which is sensed by Cam.

Discussion

In consequence of low fat body iCa^{2+}, a yet unknown inter-organ communication pathway is used to enhance *sNPF* expression in the brain. Since excess food intake but no change in the metabolic rate or the locomotor activity was observed under these conditions, reduced energy expenditure can be excluded as a major cause of *Stim* KD-mediated obesity, while the observed hyperphagia causes the observed obesogenic *mdy/bmm* gene regulations in the fat body leading to a rapid increase of fat storage (Fig. 36). By the identification of novel obesity and anti-obesity genes and the finding of SOCE mediated inter-organ communication, the way is now open to address further key questions regarding the orchestration of energy homeostasis in flies, the fat tissue-brain communication process and the evolutionary conservation of the factors and mechanisms underlying fat storage control in animal organisms. However, it is currently not known whether Dilp6, Upd2 or so far unknown signals participate in the *Stim* KD-mediated inter-organ communication. The identification of factor(s) and mechanisms underlying this process awaits further studies.
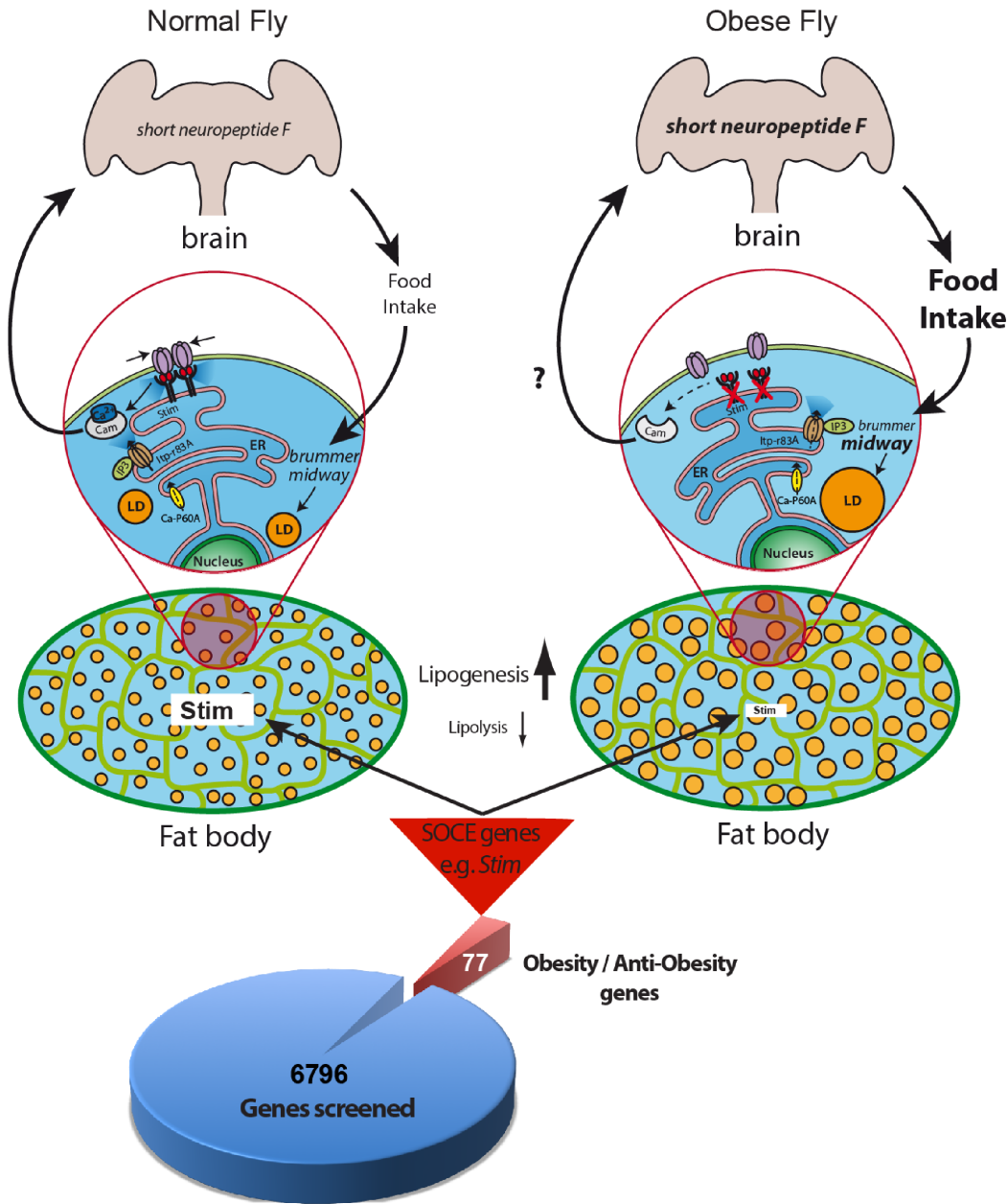
Fig. 36 A conditional *in vivo* RNAi screen in *Drosophila* identifies Stim as regulator of body fat storage and inter-organ communication. By a body fat based screen (6796 genes, 49% of the whole *Drosophila* genome), 77 obesity/anti-obesity genes were identified, whereby the store-operated calcium entry (SOCE) was the highest enriched process. A knockdown of the central SOCE component *Stromal interaction molecule* (*Stim/DmSTIM1*) leads to a decrease in intracellular Ca^{2+} levels, which can be sensed by Calmodulin (Cam/*Dm*CALM). As a consequence, a so far unknown signal from the fat body to the brain becomes impaired, which causes up-regulation of the *short neuropeptide F* (*sNPF/DmNPY*) gene expression in the brain. Since *sNPF* is an orexigenic regulator, the food intake increases due to the up-regulation causing hyperphagia. Conclusively, the energy intake also increases, which leads to an obesogenic response in the fat body by the up-regulation of lipogenesis *via midway/DmDGAT1* and down-regulation of lipolysis *via brummer/DmATGL*. This transcriptional regulations cause the onset of obesity, which is visible by massive body fat accumulation in the obese fly. Figure modified after Baumbach *et al.* (2014).

3.3 The Adipokinetic hormone receptor (AkhR) is coupled *via* Gαq, Gγ1 and Plc21C to SOCE-mediated body fat regulation

A major finding of the screen was the identification of the *Gαq/DmGNAQ* and *Gγ1* G-protein subunit coding genes, which dramatically increases the body fat content due to a fat storage-restricted KD. These two subunits were shown to interact by anti-tag co-immunoprecipitation and a peptide mass fingerprinting (Guruharsha *et al.*, 2011). Additional screening revealed the phospholipase Plc21C/*Dm*PLCB1 as a body fat storage regulator. In addition, two G-protein coupled receptors were identified in the screen, respectively the Adipokinetic hormone receptor (AkhR/*Dm*GNRHR) and the Leucine-rich repeat-containing G protein-coupled receptor 1 (Lgr1/*Dm*LHCGR). While *Lgr1* is mainly expressed in the hindgut, the highest *AkhR* expression could be detected in the fat body (http://flyatlas.org/). Interestingly, the KD of *AkhR*, *Gαq*, *Gγ1 and Plc21C* causes body fat accumulation (Fig. 30). Therefore, one can propose a model where the G-protein coupled receptor AkhR acts *via* the G-protein-activated Phospholipase C and IP3-mediated SOCE activation to regulate fat body iCa^{2+} concentrations and finally the body fat content in *Drosophila*.

Interestingly, the AkhR was already described to act *via* the second messengers cAMP and Ca^{2+} in the *Manduca sexta* fat body (Arrese *et al.*, 1999) and was also shown to act as a body fat storage regulator in *Drosophila* (Grönke *et al.*, 2007). Biochemical *in vitro* data from other insect species also showed that the lipid mobilization from *Schistocerca gregaria* fat bodies, which can be initiated by Akh-containing cc extracts, depends on cAMP and extracellular Ca^{2+} (Spencer and Candy, 1976), which can also be mimicked by injection of Ca^{2+} ionophores in adult *Locusta migratoria* (Lum and Chino, 1990; Vroemen *et al.*, 1995). Furthermore, the need for extracellular Ca^{2+} in the cAMP-dependent response to Akh was shown in *Manduca sexta* (Arrese *et al.*, 1999) and *Locusta migratoria* (Wang *et al.*, 1990) fat body cells, which emphazises the hypothesis that the second messengers Ca^{2+} and cAMP are interconnected and Akh-depended body fat depletion integrates

both signals. In addition, studies from *Manduca sexta* showed that pharmacological elevation of the fat body iCa^{2+} concentrations increases the activity of the Pka, which depends on cAMP (Arrese *et al.*, 1999). Since Pka was shown to phosphorylate Plin1 in *Manduca* and *Drosophila* (Arrese *et al.*, 2008; Patel *et al.*, 2005), whereby phosphorylated Plin1 facilitates lipid mobilization in *Manduca* (Patel *et al.*, 2005) and *Drosophila plin1*-mutants are obese (Beller *et al.*, 2010), one can speculate whether $G\alpha q$, $G\gamma 1$, *Plc21C* and *Stim* KD flies also involve the Plin1 phosphorylation *via* the proposed $cAMP/Ca^{2+}$-crosstalk to modulate body fat levels. This would be supported by the observation that a KD of any of these components reduces the iCa^{2+} concentrations (Fig. 31A, B) and facilitates body fat accumulation (Fig. 30A, B, C, D). Conversely, overexpression of either *Akh*, *AkhR* or $G\alpha q$ causes depletion of body fat (Fig. 30A, B, C, D), which is consistent with a model where these novel regulators act *via* the same pathway.

However, the knowledge about transcriptional targets of Akh-signaling, which may contribute to Akh-dependent lipid mobilization, is very limited. The transcriptional activator CrebB was shown in tissue culture studies to be depended on the Ca^{2+}-controlled protein phosphatase Calcineurin and the second messengers $cAMP/iCa^{2+}$ (Yang *et al.*, 2013). Interestingly, overexpression of *CrebB* DN or an *AkhR* KD leads to body fat accumulation (Fig. 28B, Fig. 30A, B, C, D and Iijima *et al.* (2009)), which suggests that AkhR might cause transcriptional changes *via* cAMP and CrebB. However, the Calcineurin activity depends on Calmodulin (Cam), whereby a *Cam* KD causes body fat accumulations similar to a *Creb* DN or a *Stim* KD (Fig. 26B; (Baumbach *et al.*, 2014)), which is accompanied by the obesogenic up-regulation of the *mdy* gene and down-regulation of the *brummer* gene (Fig. 26C). Compared to the observed obesogenic *mdy/bmm*-responses due to interference of *Stim*, *Cam* or *CrebB*, the functional impairment of $G\alpha q$, $G\gamma 1$ and *Plc21C* showed similar regulations (Fig. 32B), while an *AkhR* KD resulted in the up-regulation of *mdy* with no effect on *bmm*. Conversely, a fat storage-restricted overexpression of $G\alpha q$, which mimics the lean phenotype of an Akh pathway hyperactivation (Fig. 32A), causes reduced *mdy* expression and increases *bmm*

transcripts (Fig. 32B). Conclusively, the transcription of *mdy* and *bmm* depends on *Gαq*, *Gγ1*, *Plc21C* and *Stim*, while the *AkhR* KD-mediated regulation is limited to *mdy*, which is in support with the finding that Akh/AkhR and Bmm act in separate lipolytic systems. In detail, Akh/AkhR-dependent lipolysis was shown to be mediated by cAMP signaling and Pka activity, while the Bmm is responsible for most of the basal and part of the induced lipolysis (Grönke *et al.*, 2007). However, since a reduction of *mdy* activity leads to lean flies (Fig. 11A, B, C, Fig. 29B and Beller *et al.* (2010)) and an overexpression causes fat flies (Fig. 29B), this gene is a candidate factor to transmit the Akh-induced lipogenesis inhibition, e.g. observed in *Gryllus bimaculatus* (Lorenz, 2001).

Interestingly, Akh-signaling was also shown to regulate the spontanous activity in *Drosophila* (Katewa *et al.*, 2012) and food intake of *Gryllus bimaculatus* (Konuma *et al.*, 2012), *e.g.* hyperphagia has been reported in response to *AkhR* gene knockdown in *Gryllus bimaculatus* (Konuma *et al.*, 2012), which reduces fat body iCa^{2+} in *Drosophila* (Fig. 31A, B; (Baumbach and Xu *et al.*, 2014)). Since a *Stim* KD-dependent obesity is mediated *via* reduced fat body iCa^{2+} levels (Fig. 17), up-regulation of the orexigenic gene *sNPF* in the central nervous system (Fig. 28A, E) and subsequent hyperphagia (Fig. 27D), it is feasible that the observed obesity due to a fat storage-restricted *AkhR* KD might be mediated in a similar way. Therefore, systemic Akh might activate SOCE in the fat body *via* AkhR, Gαq, Gγ1 and Plc21C to coordinate organismal energy demands, which involves a crosstalk of the brain and the fat body. The close relationship between *AkhR* KD- and *Stim* KD-mediated obesity is further supported by the finding that the occurrence of programmed obesity after a transient KD can be observed for both genes (Fig. 19E). However, also other GPCRs might involve the *Gαq/Gγ1/Plc21C*-module to regulate SOCE and body fat, *e.g.* the stimulation of the GPCR cysteinyl leukotriene type I receptors in rat basophilic leukemia (RBL)-1 cells induces extensive store depletion (Kar *et al.*, 2012) and *Drosophila Lgr1* was identified in the screen as an anti-obesity gene (Fig. 10 and Table S2). Therefore, additional body fat based

screens are still ingoing and may identify additional GPCRs which act *via* SOCE to regulate energy homeostasis in flies.

Summarized, the observed body fat accumulation, which is accompanied by decreased iCa^{2+} concentrations, and the obesogenic *mdy/bmm*-regulations adds evidence for the novel body fat storage regulators *Gαq, Gγ1* and *Plc21C* to act upstream of *Stim* and SOCE. In addition, an *AkhR* KD shows similar trends in body fat storage increase and iCa^{2+} decrease, whereby only the lipogenic *mdy* gene was up-regulated and the lipolytic *bmm* gene regulation is unchanged. However, since *AkhR* acts not only *via* iCa^{2+} but also *via* an additional cAMP second messenger branch, this might cause the different obesogenic regulations. The fact that KDs of *Gαq, Gγ1, Plc21C* and *Stim* can prevent the lipolytic actions of an *Akh* overexpression in the fat body (Fig. 33), adds further evidence that *AkhR* is connected *via* G*αq*, G*γ1* and *Plc21C* to SOCE (Fig. 34). Notably, the programmed obesity effect could be observed in a transient *AkhR* and *Stim* KD, whereby I also could get first evidence that at least a transient KD of *Gαq* causes similar effects (data not shown). Therefore, further characterization of the SOCE upstream regulators will lead into new and promising insights of obesity progression and might be a way to describe the so far not understood programmed obesity effect. Furthermore, a better understanding of Akh/AkhR-signaling might reveal further links to the SOCE-mediated inter-organ communication processes, whereby a potential feedback regulation between fat body and brain during the Akh-induced lipid mobilization deserves future research attention.

In general, the possibility to do a thermogenetic conditional gene knockdown directly in the fat storage tissue of adult flies, established the *Drosophila* model system for future research in the context of organ-autonomous functions as well as inter-organ communication processes underlying organismal storage lipid homeostasis. Future research will also reveal the relevance for SOCE-mediated inter-organ communication processes in mammals, which might be an approach for a better understanding of obesity progression and could lead to further progress

in the development of novel therapies with the ambition to overcome human obesity.

4 Materials and Methods

4.1 Genetics

4.1.1 Modulation of gene activity *via* the GAL4/UAS-system

The expression of genes can be modulated *in vivo* using the GAL4/UAS-system. In this work mainly two different techniques of this system were used for the targeted expression of RNAi KD, gof or DN constructs which contain an UAS binding motif (Brand and Perrimon, 1993). Both systems make use of a tissue-specific yeast transcrption factor GAL4 expression, depending on the promoter in front of the GAL4 coding sequence. If GAL4 is expressed, it can bind to the UAS-element and activates the expression of constructs, which are under the control of the UAS-element. In the Gene Switch system the GAL4 expression is controlled by the binding of the drug RU486 (Roman *et al.*, 2001), which can be applied by adding it to the food. In the TARGET system the GAL4 expression is controlled by a GAL80ts (McGuire *et al.*, 2003, 2004). The GAL80ts prevents GAL4-mediated activation of the UAS-element. Since GAL80ts is a temperature-sensitive allele, the UAS activation can be controlled by a temperature shift, whereby the GAL80ts will be degraded. In this work, 18 °C were used to prevent (repressed conditions) and 25 °C or 30 °C were used to activate (active-conditions) the TARGET system. Taken together, both systems can be independently used in *Drosophila* for the *in vivo* modulation of gene activity in a time- and tissue-specific manner.

4.1.2 A fat storage tissue-restricted *in vivo* RNAi screen

In *Drosophila*, a targeted gene KD by RNAi is mediated by the expression of a long double-stranded 'hairpin' RNA from a transgene containing a gene fragment cloned as an inverted repeat. This inverted repeat is processed by the endogenous RNAi mechanism and leads to the degradation of the target gene mRNA, which causes a reduction in gene activity (Kennerdell and Carthew, 2000).

In extension to this work, 7524 *Drosophila* lines representing 6796 reference genes of 13781 *Drosophila* coding genes (coverage 49%) from an UAS-RNAi library were

used (VDRC GD library; (Dietzl *et al.*, 2007); see digital supplement Table S4 for a list of all tested genes/fly lines, modified after Baumbach *et al.* (2014)). By crossing these lines against a conditional fat storage driver line (ts-FB-Gal4; RKF805), a progeny could be generated, which includes a gene specific UAS-RNAi element and the ts-FB-Gal4 driver. By using the properties of the TARGET system (see chapter 4.1.1), target gene activities could be modulated in a time- and tissue-dependent manner. Subsequently, the progeny was screened for changes in body fat in order to identify new obesity/anti-obesity genes. The screen was done by J. Baumbach, I. Bickmeyer, K.M. Kowalczyk, M. Frank, K.Knorr and R. P. Kühnlein (Baumbach *et al.*, 2014).

4.1.2.1 Selection of obesity and anti-obesity genes

In the primary screen, the UAS-RNAi lines from the VDRC GD library were crossed in cohorts (co) of 200 lines against the ts-FB-Gal4 driver-line. The progeny was raised under gene knockdown repressed conditions (18 °C) until hatching of the flies. Male flies (females for X-chromosomal RNAi transgene integrations) were collected 0-24 h after hatching and kept under gene knockdown active-conditions (30 °C) for six days. Subsequently, the flies were quick-frozen and the body fat content (FC) was determined in duplicate groups of five flies by a coupled colorimetric assay (CCA). Primary candidate (c) lines, which resulted in very high or low FC within their cohort (criteria: FC_c < average FC_{co} - 1.5 x standard deviation FC_{co} for obesity gene candidates and FC_c > average FC_{co} + 1.5 x standard deviation FC_{co} for anti-obesity gene candidates) were re-tested in two additional rounds of screening:

In the first round, the c lines, which were identified in the primary screen were re-tested under primary screen conditions, whereby cohorts (co) of 100 lines were used and *Z* scores were determined ($Z\ score\ = \frac{FC(c) - average\ FC(co)}{standard\ deviation\ FC(co)}$). The lean or obese c lines with a *Z* score ≤-1.5 or ≥1.5, respectively, were defined as class I regulators (see Fig. 9B, left panel).

In the second round, the c lines were re-tested by crossings against the ts-FB-Gal4 and a driverless *w*-control (control; RKF1084) line under primary screen conditions. Due to this approach, transgene integration effects on the FC could be excluded by determination of the relative FC changes (RFC) compared to control flies, respectively (RFC = FC$_{\text{ts-FB-Gal4}}$ - FC$_{\text{control}}$). Subsequently, the *Z* scores were determined ($Z\ score\ = \frac{\text{RFC(c)} - \text{average RFC(c)}}{\text{standard deviation RFC(c)}}$) and c lines causing a *Z* score ≤2.06 or ≥1.49 for males and ≤1.45 or ≥1.19 for females, were defined as class II regulators (see Fig. 9B, right panel).

4.1.2.2 Validation of obesity and anti-obesity genes

Most class I and II regulators (87%) were validated by re-testing their effect on the FC in two independent experiments. (i) The primary screen RNAi effector fly line was expressed in response to an alternative adult fat body driver (*to*-Gal4 for autosomal and *yolk*-Gal4 for X-chromosomal GD lines compared to control crosses [RKF1192]) by raising the progeny on 25 °C until the adult flies were 6 days old. (ii) Alternatively, a second transgenic RNAi line (VDRC KK or Harvard TRiP collection) targeting the same gene was used to avoid false positive identifications by RNAi off-target effects, whereby the progeny was raised on primary screen conditions. Gene knockdowns, which changed the RFC by more than 25% received a positive validation score (+1).

Candidate genes, which (i) reached a validation score of ≥2 (out of up to four independent experiments), which (ii) were represented by at least one high quality RNAi transgenic lines (s19 score ≥ 0.79 and CAN repeats ≤ 6) and which (iii) were not predicted to function in general RNA interference, qualified as confirmed fly obesity or anti-obesity genes (see Table S2).

4.1.2.3 *In silico* analysis by Gene Ontology and InParanoid

For the identified and validated obesity/anti-obesity genes, all available gene ontology (GO) terms in the categories "biological process" and "molecular function" were retrieved. Statistically significant over- or underrepresented GO terms in the obesity/anti-obesity gene set as compared to the reference gene set were identified using the GOToolBox suite (at http://genome.crg.es/GOToolBox/; last update: 2009-07-22) with hypergeometric calculation mode, level cutting 5 and Benjamini & Hochberg correction. Enriched GO terms in the category "biological process" were filtered according to $p < 0.012$, reference gene set range 4-100, enrichment factor >3 and manually clustered into functional classes (Table S3 and Fig. 9C, D). Gene Ontology analysis was done by Petra Hummel (Baumbach *et al.*, 2014).

Human orthologs (inparalog score 1) of *Drosophila* genes (Table S2) were either identified using InParanoid 7 (Ostlund *et al.*, 2010) done by PD Dr. Ronald P. Kühnlein (Baumbach *et al.*, 2014) or by a NCBI HomoloGene search (http://www.ncbi.nlm.nih.gov/homologene).

4.2 Physiology

4.2.1 Fly stocks

Transgenic RNAi fly strains used in this study were received from either the VDRC (GD and KK library; (Dietzl *et al.*, 2007) and www.vdrc.at) or the BDSC (Harvard TRiP library; www.flyrnai.org) fly stock centers. In addition, the following fly stocks were used in this study:

Short name	Stock number	Genotype	Reference/ source
ts-FB-Gal4	RKF805	*y*w* ; P{w[+mW.hs]=GawB}FB P{w[+m*] UAS-GFP 1010T2}#2; P{w[+mC]=tubP-GAL80[ts]}2*	(Beller *et al.*, 2010)

FB-Gal4	RKF125	*w*; P{w[+mW.hs]=GawB}FB+SNS*	(Grönke *et al.*, 2003)
w-control	RKF1084	*w[1118]*	VDRC60000
to-Gal4	RKF1088	*w*; to-Gal4 (II)*	(Dauwalder *et al.*, 2002)
	RKF1192	*w*; rev[to-Gal4 (II)]#1*	(Baumbach *et al.*, 2014)
yolk-Gal4	RKF1091	*w*; yolk-Gal4 (II)*	(Georgel *et al.*, 2001)
FBI-26-Gal4	RKF1045	*P{Switch1}FBI-26; UAS-GFP*	(Suh *et al.*, 2007)
double balancer	RKF1365	*w[*]; Kr[If-1]/CyO; D[1]/TM3, Ser[1]*	BDSC7198
mdy⁻	RKF1004	*w*; mdy[QX25] cn[1] bw[1] / CyO float.*	(Buszczak *et al.*, 2002)
mdy RNAi			VDRC6367
mdy gof	RKF560	*w*; P{w[+mC]UAS-mdy} / TM3 Sb[1] e[1] float.*	(Baumbach *et al.*, 2014)
bmm⁻	SGF529	*w*; bmm[1] / TM3, Sb[1] float.*	(Grönke *et al.*, 2005)
bmm gof	SGF533	*w*; + / +; P{w[+mC] bmm[Scer\UAS]=UAS-bmm}#2d*	(Grönke *et al.*, 2007)
bmm RNAi			VDRC37880
	JBF1246	*w*; UAS-dStim[RNAi]2; bmm[1] / TM3 Sb[-]*	(Baumbach *et al.*, 2014)
	JBF1247	*w*; UAS-dStim[RNAi]2; bmm[1] plin1[1] / TM3 Sb[-]*	(Baumbach *et al.*, 2014)
nuclear lacZ:eGFP reporter	GÖ1048	*y[1] w[67c23]; P{UAS-GFP::lacZ.nls}2-1; P{GAL4-btl.S}3-1 / TM3 Sb[1] Ser[1]*	(Shiga *et al.*, 1996)
Pect RNAi1			VDRC27459
Pect RNAi2			VDRC109802
Itp-r83A RNAi1			VDRC106982
Itp-r83A RNAi2			BDSC25937
Itp-r83A DN	RKF1139	*UAS-itpr[Ka901] cDNA on II*	(Srikanth *et al.*, 2006)
Ca-P60A RNAi1			VDRC4474

Ca-P60A RNAi2			VDRC107446
Ca-P60A RNAi3			BDSC25928
Stim RNAi1	RKF1112	w[1118]; UAS-dStim[RNAi]1 / CyO	(Eid *et al.*, 2008)
Stim RNAi2	RKF1113	w[1118]; UAS-dStim[RNAi]3 / TM3, Sb*	(Eid *et al.*, 2008)
Stim RNAi3			VDRC47073
Stim gof	RKF1114	w[1118]; UAS-dStim[FL]#290 / CyO	(Eid *et al.*, 2008)
ey-Gal4>*Stim* gof	JBF1251	w*; UAS-dStim[FL]#290 / CyO; ey3.5-GAL4 / TM3 Sb[-], UAS-lacZ	(Baumbach *et al.*, 2014)
rpr	RKF177	w*; P{w[+m*]UAS-reaper} / CyO, P{w[+mC]=ActGFP}JMR1; +/+	BDSC5824
p35		w*; UAS-p35; +/+	BDSC5072
ey-Gal4	RKF173	w*; ey-Gal4; +/+	(Carrera *et al.*, 1998)
Stinger GFP	RKF1171	+; UAS-StingerII; +	(Barolo *et al.*, 2000)
olf186-F RNAi			VDRC12221
olf186-F gof	RKF1191	w*; Orai-pUAST#3 / TM3, Sb[1] e[1]	(Venkiteswaran and Hasan, 2009)
wunen-2 RNAi			VDRC4176
sec71/DmARFGEF1/2 RNAi1			VDRC33634
sec71/DmARFGEF1/2 RNAi2			VDRC100300
Arf79F/DmARF1 RNAi1			VDRC23082
Arf79F/DmARF1 RNAi2			VDRC103572
garz/DmGBF1 RNAi			VDRC42140
Rab1 RNAi			VDRC27299
Cam RNAi			VDRC102004
Creb DN		w[1118]; + / +; P{w[+mC]=dCREB-B-UAS}94	BDSC7220
	JBF1246	w*; UAS-dStim[RNAi]1; bmm [1] / TM3 Sb [-]	(Baumbach *et al.*, 2014)
	JBF1247	w*; UAS-dStim[RNAi]1; bmm[1] plin1[1] / TM3 Sb [-]	(Baumbach *et al.*, 2014)

	JBF1387	w*; UAS-dStim[RNAi]1 / CyO float.; UAS-mdy RNAi / TM3 Ser[-]	(Baumbach et al., 2014)
CG9825 RNAi			VDRC1712
CG14205 RNAi			VDRC6198
CG14205 gof		y[1] w*; P{w[+mC]=UAS-CG14205}attB / CyO; +/+	unpublished
Hippi RNAi			VDRC106927
CG14406 RNAi			VDRC107523
Cyp4d1 RNAi			VDRC109341
Stim RNAi2 CG14205 gof		w*;UAS-CG14205 gof / CyO; UAS-dStim[RNAi]3 / TM3, Sb*	unpublished
Stim RNAi2 CG14406 RNAi		w*; UAS-CG14406 RNAi / CyO;UAS-dStim[RNAi]3 / TM3, Sb*	unpublished
	JBF1385	w*; UAS-dStim[RNAi]1 / CyO float.; P{w[mc]UAS-GFP.nls} / TM3 Ser[-]	(Baumbach et al., 2014)
	JBF1386	w*; P{w[mc]UAS-GFP.nls}; UAS-mdy RNAi	(Baumbach et al., 2014)
Act-cd2-Gal4 line	JBF1377	hs-FLP; stau-GFP; Act-cd2-Gal4, UAS-GFP	(Pignoni and Zipursky, 1997)
sNPF gof	JBF1393	w*; UAS-sNPF; UAS-sNPF	(Hong et al., 2012)
sNPF RNAi	RKF1320	w*;+/+; UAS-sNPF.RI III	(Hong et al., 2012)
sNPF-Gal4	RKF1321	w*; +/+; sNPF.RI-GAL4	(Hong et al., 2012)
CaLexA reporter	JBF1324	LexAop-CD8-GFP-2A-CD8-GFP / LexAop-CD8-GFP-2A-CD8-GFP; UAS-mLexA-VP-NFAT C del (4-2), LexAop-CD2-GFP / TM6B	(Masuyama et al., 2012)
Akh-Gal4	RKF694	w*; akhp-GAL4, UAS-mCD8 GFP ; akhp-GAL4/ SM5a-TM6 Tb[-]	(Kim and Rulifson, 2004)
Akh RNAi		y[1] sc[*] v[1]; P{y[+t7.7] v[+t1.8]=TRiP.HMS00477}attP2	BDSC34960
Akh gof	RKF656	y[1] w[*]; P{w[+mC]=UAS-Akh.L}2	(Lee and Park, 2004)
AkhR gof	RKF592	w*;P{w[+mC]AkhR[Scer\UAS]=UAS-AkhR}#32A / TM3 Sb[1] e[1] float.	(Grönke et al., 2007)

AkhR RNAi		*w[1118]; +/+; P{GD586}v9546/TM3 Sb[-]*	VDRC9546
AkhR[1]	RKF639	*y* float. w*; AkhR[1] / CyO float.*	(Grönke *et al.*, 2007)
Gαq gof	RKF1140	*UAS-Gqα3 on II*	(Banerjee *et al.*, 2006)
Gαq RNAi1		*w[1118]; P{GD8609}v19088*	VDRC19088
Gαq RNAi2		*y[1] v[1]; P{y[+t7.7] v[+t1.8]=TRiP.JF02390}attP2*	BDSC33765
Gγ1 RNAi1		*w[1118]; P{GD13720}v28844/CyO*	VDRC28844
Gγ1 RNAi2		*y[1] v[1]; P{y[+t7.7] v[+t1.8]=TRiP.JF01954}attP2*	BDSC25934
Plc21C RNAi1		*w[1118]; P{GD11359}v26558*	VDRC26558
Plc21C RNAi2		*y[1] sc[*] v[1]; P{y[+t7.7] v[+t1.8]=TRiP.HMS00600}attP2*	BDSC33719
FB-Gal4 *AkhR* RNAi	YXF1417	*w[*]; P{w[+mW.hs]=GawB}FB+SNS /CyO; AkhR RNAi/TM3,Ser[*]*	(Baumbach and Xu *et al.*, 2014, accepted)
FB-Gal4 *Gαq* RNAi2	YXF1418	*w[*]; P{w[+mW.hs]=GawB}FB+SNS; Gαq RNAi2/TM3, Ser[*]*	(Baumbach and Xu *et al.*, 2014, accepted)
FB-Gal4 *Gγ1* RNAi2	YXF1419	*w[*]; P{w[+mW.hs]=GawB}FB+SNS; Gγ1 RNAi2/TM3, Ser[*]*	(Baumbach and Xu *et al.*, 2014, accepted)
FB-Gal4 *Plc21C* RNAi2	YXF1420	*w[*]; P{w[+mW.hs]=GawB}FB+SNS; Plc21C RNAi2/TM3, Ser[*]*	(Baumbach and Xu *et al.*, 2014, accepted)
FB-Gal4 *Stim* RNAi2	RKF1397	*w[*]; P{w[+mW.hs]=GawB}FB+SNS; Stim RNAi2/TM3, Ser[*]*	(Baumbach *et al.*, 2014)
Akh gof GFP-control	JBF1426	*w[*]; P{w[+mC]=UAS-Akh.L}2 / CyO; P{w[+mC] UAS-GFP}3 / TM3-Sb, P{w[+] Ubx-lacZ}*	(Baumbach and Xu *et al.*, 2014, accepted)
Akh gof *Gαq* RNAi2	JBF1427	*w[*]; P{w[+mC]=UAS-Akh.L}2 / CyO; Gαq RNAi2 / TM3-Sb, P{w[+] Ubx-lacZ}*	(Baumbach and Xu *et al.*, 2014, accepted)

Akh gof *Gγ1* RNAi2	JBF1428	*w[*]; P{w[+mC]=UAS-Akh.L}2 / CyO; Gγ1 RNAi2 / TM3-Sb, P{w[+] Ubx-lacZ}*	(Baumbach and Xu *et al.*, 2014, accepted)
Akh gof *Plc21C* RNAi2	JBF1429	*w[*]; P{w[+mC]=UAS-Akh.L}2 / CyO; Plc21C RNAi2 / TM3-Sb, P{w[+] Ubx-lacZ}*	(Baumbach and Xu *et al.*, 2014, accepted)
Akh gof *Stim* RNAi2	JBF1430	*w[*]; P{w[+mC]=UAS-Akh.L}2 / CyO; Stim RNAi2 / TM3-Sb, P{w[+] Ubx-lacZ}*	(Baumbach and Xu *et al.*, 2014, accepted)

4.2.2 Fly husbandry

Young flies (24-48 h after hatching) were kept for 5-6 days on standard food (20 l H_2O, 125 g agar, 360 g dry yeast, 200 g soy flour, 440 g treacle, 1.6 kg cornmeal, 1.6 kg malt, 125 ml propionic acid and 30 g nipagine). Progeny containing the ts-FB-Gal4 driver was raised under repressed conditions (18 °C). After hatching, young flies were induced for further 6 days at active-conditions (30 °C). Alternatively, freshly hatched flies were kept for 6 additional days on repressed conditions followed by the exposure to 30 °C at short-term (34-48 h) or long-term (6 days) conditions. Furthermore, the transient *Stim* KD effect was analyzed on *Stim* KD flies, which were raised for 6 days on repressed conditions, induced on active-conditions for 34 h and shifted for 5/10/20/30 additional days on repressed conditions in order to recover the *Stim* RNAi knockdown.

Flies containing the FBI-26-, *yolk-* or the FB-Gal4 drivers were continuously kept at 25 ºC. For low/medium/high sugar experiments flies were placed for 5 days on a 10% yeast, 1.5% agar food (Skorupa *et al.*, 2008) including preservatives (see above) containing low (2.3%), medium (8.7%) or high (30.6%) sucrose concentrations. For conditional fat body-restricted transgene (FBI-26-Gal4 driver) induction using the Gene Switch system (Roman *et al.*, 2001) the flies were kept for 5 days on standard food containing either 200 µM RU486 (mifepristone; Sigma M8046; stock solution 10 mM in 80% ethanol; ON-condition) or solvent only (OFF-condition).

For clonal analysis of the adult fat body, the *Act*-cd2-Gal4 line was crossed against the *Stim* RNAi1 line or a *w*-control on 25 °C. Freshly hatched female virgins were raised for 4-5 days on 25 °C. Afterwards these flies were either induced by a heat shock in a 37.5 °C prewarmed water bath for 30 min or left on room temperature in parallel as a non-induced control. After the heat shock, flies were recovered and further incubated at 25 °C for 3, 5 and 8 days prior to analysis of the fat body.

4.2.3 Lipid analysis

Organismal fat content (expressed as glycerides) of migrating L3 larvae, 0-4 h old freshly hatched and 6 days old male flies was quantified by an coupled colorimetric assay (Grönke *et al.*, 2003; Hildebrandt *et al.*, 2011). Samples were collected in 0.5 ml or 2 ml tubes and directly snap frozen in liquid nitrogen. A 7 mm ceramic cylinder (or 6.8 mm ceramic bead) and 600 µl 0.05% Tween-20 were added, samples were homogenized for 10 sec at 5000 rpm (peqlab Precellys 24 instrument), incubated for 5 min on 70 °C, centrifuged for 3 min at 3500 rpm (Beckman, GS6KR) and 500 µl of the supernatant was transferred to a 96-deepweel Masterblock. The samples were afterwards either stored on -20 °C for later use or pre-heated to 37 °C, centrifuged for 3 min at 2500 rpm (Heraeus, Megafuge 1.0R) and loaded (50 µl) to two 96 well microtiter plates. Blank values were measured at either 540 nm for quantification of organismal fat or 570 nm for protein loading control. Two hundred µl of Thermo Infinity Triglyceride solution (prewarmed to 37 °C) or Pierce BCA protein assay kit (#23225) were added, samples were incubated for 30 min at 37 °C with mild shaking (120 rpm) and re-measured. In parallel, Thermo Trace Triglyceride standard (organismal fat) or BSA (protein) in 0.05% Tween-20 were used for generation of standard curves. Standard curves were used to determine TAG equivalent per fly or TAG equivalent per mg protein. Depicted are representative experiments with average values of triplicate measurements (on five larvae or flies per replicate) and corresponding standard deviations. Experiments were repeated at least twice.

Fly lipids were extracted according to Bligh and Dyer (1959). The wet weight of duplicate samples of 3-8 six days old male flies was determined and the flies were homogenized in 150 µl methanol, 75 µl chloroform and 60 µl water in a Bioruptor sonifier (www.diagenode.com). Lipids were extracted for 1 h at 37 °C before adding 75 µl chloroform and 75 µl 1 M KCl. Phases separation was achieved by centrifugation (3000 rpm for 2 min) and the chloroform phase solvent was evaporated in a SpeedVac concentrator. Lipid pellets were resuspended in 25-50 µl chloroform/methanol (1:1). Lipids extracted from 1-3.5 mg fly wet weight were now separated on high performance thin layer chromatography plates (Merck, 105633) using n-hexane/diethylether/acetic acid (70:30:1, v/v/v; Merck) for unpolar lipids TAG, DAG, FA or chloroform/methanol/water (60:25:4, v/v/v; Merck) for phospholipids, respectively. Along with this, the following standard lipids were used: trioleoylglycerol (TAG; Sigma T7140), pentadecanoin (DAG; Sigma D8508) and stearic acid (FA; Fluka 85679). Plates were air dried, dipped into 8% (w/v) H_3PO_4 containing 10% (w/v) copper (II) sulfate pentahydrate and charred for 10 min at 180 °C. Fly lipid classes were quantified by photo densitometry (LAS-1000 and Image Gauge V3.45, FujiFilm) and scaled to a dilution series of the corresponding lipid standard. TLC experiments were either done by Anja Hildebrand (Fig. 11B, 12C, 13B, 15B and 16B; (Baumbach *et al.*, 2014)) or Philip Hehlert (Fig. 30B; (Baumbach and Xu *et al.*, 2014)).

For the lipid mobilization analysis, *Stim* RNAi1 flies were crossed against *w*-control and ts-FB-Gal4, respectively. Afterwards, F1 males were raised for 6 days on repressed conditions, induced for further 6 days on active-conditions and subsequently subjected to water-only starvation. Triplicates of five male flies were collected and quick-frozen in liquid nitrogen at different time points during the starvation paradigm until the median starvation time was reached. The body fat content of these flies was quantified by a coupled colorimetric assay as described above.

Starvation-induced *post mortem* body fat content was determined by a coupled colorimetric assay for male adult flies, which were monitored for their survival every 5-8 h (see Fig. 25C, D).

4.2.4 Carbohydrate analysis

For circulating sugar analysis from hemolymph, 15 male flies were subjected to thorax perforation (10 pricks with a fine needle). Perforated flies were placed in a 0.5 ml-tube (with a hole in the bottom, covered with a cotton plug) caged in a 1.5 ml tube and hemolymph was extracted by centrifugation (2 min, 14.000 rpm, 4 °C). Hemolymph (0.5 µl per assay) was used immediately for sugar determination. Hemolymph glucose levels were determined with Infinity Glucose Hexokinase solution (Thermo Electron TR15421) and by measuring the absorbance at 340 nm (T_1). For the determination of hemolymph trehalose levels, trehalase (Sigma T8778; final: 0.05 U/ml) was added and the samples were incubated at 37 ºC overnight followed by a second reading of absorbance at 340 nm (T_2). The amount of trehalose is equal to the final absorbance reading (T_2) minus that of the first reading (T_1). Final glucose and trehalose concentrations were determined by reference to standard curves (Glucose standard: Sigma G7528, Trehalose standard: Sigma T3663).

Glycogen levels of whole flies were determined according to protocols (Iijima *et al.*, 2009; Palanker *et al.*, 2009) with minor modifications. Five male flies were quick frozen in liquid nitrogen and homogenized in 1 ml 0.5% Tween 20 (in 1x PBS). Homogenates were immediately incubated at 70 °C for 5 min and centrifuged at 12.000 rpm for 3 min. Thirty µl aliquots of the supernatant were added to either 100 µl 1x PBS, 100 µl Glucose Assay Kit solution (Sigma, GAGO20-1KT) and 100 µl Glucose Assay Kit solution + 0.3 U Amyloglucosidase (Sigma, 10115-1G-F) in a 96-well microplate format. Microplates were incubated for 30 min at 37 °C and absorbance at 540 nm was determined in a microplate reader (BioRad Microplate Reader Benchmark). Glucose and glucose plus glycogen content were determined using a standard curve (Glycogen standard: Sigma G0885). The amount of glycogen was determined by subtracting the glucose from the glucose plus glycogen values.

Flies for the glycogen mobilization analysis were treated identical to flies subjected to lipid mobilization analysis (see above). Glycogen levels were quantified as described above.

4.2.5 Feeding and food intake

Food intake quantification of adult male flies under *ad libitum* feeding and restricted food conditions was achieved by a modified CAFE system (Ja *et al.*, 2007). In detail, freshly hatched F1 male progeny of *Stim* RNAi1 flies crossed against *w*-control and ts-FB-Gal4, respectively, were raised for 6 days on repressed-conditions (18 °C). Afterwards flies (n=22) were transferred into individual chambers of a modified CAFE system (24-well plate) with 100% humidity at 25 °C (active-condition) and 12 h/12 h-light/dark cycle. Flies were *ad libitum* fed on liquid diet (5% sucrose/5% dry yeast) in 5 µl capillaries (ringcaps, Hirschmann, Ref 9600105) and food intake was determined daily when fresh food was provided. Food consumption reads were corrected by an evaporation control (empty fly chamber).

For food restriction (pair feeding), flies of the same genotypes were provided with the daily food ration consumed by *ad libitum* fed control flies only. Capillaries were loaded with the respective food volume overlaid by 2 µl of mineral oil (Sigma, M-5904). After 6 days of feeding, body fat content was measured as described above (see Fig. 31E).

4.2.6 Determination of body weight

For the determination of body weight, groups of 10 male flies were weighted at least twice with a weighing scale (Mikrowaage MC5, Sartorius) in a 1.5 ml Eppendorf-Tube in 5 replicates. Statistical analysis was done in Excel with the students T-test.

4.2.7 Determination of Energy expenditure

The metabolic rate of male progeny flies of *Stim* RNAi1 crossed against *w*-control and ts-FB-Gal4 flies raised and analyzed on repressed (18 °C)- and active (25 °C)-conditions was estimated on the basis of manometric measurement of the CO_2 production as described in (Kucherenko *et al.*, 2011). This was done for four different 2 h-periods during the circadian light cycle (dark/light phase: 12 h/12 h). Triplicates of three male flies of each genotype were placed in a sealed fly chamber

with CO_2 absorber (Soda lime: Wako, 196-10525), connected to an eosin-stained (Sigma-Aldrich, HT110232-1L) H_2O reservoir by a 50 µl capillary (Brand, 708733) in a closed TLC running chamber. The change in the meniscus of the capillaries was determined every 30 min during the 2 h-periods. Data sets were normalized against the respective genotypes under OFF-conditions and daily averages were calculated on the basis of four different time points in the light cycle (Zeitgeber time: 0, 3, 5, 7.5 h; see Fig. 27A, B). The so-called "Zeitgeber time" is defined as the time point after beginning of the light phase.

4.2.8 Starvation assay

Young male flies (aged 0-24 h) were kept for 6 days at 25 °C on standard food. Afterwards triplicates of 15 male flies per genotype were subjected to water-only starvation. The number of survivors was determined every 5-12 h until all flies were starved to death and the median survival time was determined. The median survival time is defined as the time point were only 50% survivors remain.

4.2.9 Measurement of locomotor activity

Male progeny flies (32 per genotype, aged 0-24 h) of *Stim* RNAi1 crossed against *w*-control and ts-FB-Gal4 flies were analyzed in the TriKinetics DAM2 system (http://www.trikinetics.com/) on standard food. This system measures the cumulative laser passes of individual flies. The activity was monitored for 6 days at 18 °C (repressed-condition) followed by further 6 days at 25 °C (active-condition). The cumulative activity was determined and normalized to the activity on repressed-conditions.

4.2.10 Climbing assays

For climbing assays, see supplement chapter 5.2 for experimental procedures.

4.2.11 Longevity assays

For longevity assays, see supplement chapter 5.2 for experimental procedures.

4.3 Molecular biology

4.3.1 Extraction of total RNA

Five to ten larvae or adult flies were snap frozen and the total RNA of whole larvae or abdomen of adults was extracted. For RNA extraction of adult brains, fifty brains were dissected from adult male flies and RNA was extracted as described below. Samples were homogenized in 500-700 µl peqGold TriFast reagent (www.peqlab.de) or TRIzol Reagent (Ambion, cat. no. 15596-026) by using a 0.5 or 2 ml screw tube with small beads (2 mm) or a ceramic-cylinder in a Precellys 24 (5000 rpm, 10 sec). Alternatively, the Direct-zol RNA MiniPrep-kit (Zymo Research, cat. no. R2050) was used according the instructions of the manufacturer. Afterwards, samples were centrifuged for 1min at 5000 rpm, supernatant (500 µl) was transferred to a 1.5 ml Phase Lock Gel Heavy tube, 200 µl Chloroform was added, the samples were shaken for 15 sec and centrifuged for 30 min (12000 rpm, 4 °C). The upper phase was transferred to a 1.5 ml tube, 500 µl Isopropanol was added, vortexed and incubated for 10 min at room temperature. Next, samples were centrifuged for 10 min (12000 rpm, 4 °C) and the supernatant was discarded. The resulting pellet was washed twice with 1 ml 70% ethanol, vortexed and centrifuged for 10 min (12000 rpm, 4 °C). Subsequently, the pellet was dried for 3 min in a Speed Vac (concentrator setting: medium) and resuspended in 25-50 µl water (RNase free). RNA concentration was measured with a NanoDrop ND-8000 (peQlab) for quality control and in preparation for cDNA synthesis.

4.3.2 Synthesis of cDNA from total RNA

The cDNA was synthesized from total RNA using the QuantiTect Reverse Transcription Kit (www.qiagen.com).

Therefore total RNA (800-1000 ng) was mixed with 2 µl 7x gDNA Wipeout Buffer and filled up to 14 µl with H_2O (RNase free water). Still present gDNA was digested by incubating the solution for 2 min in a water bath on 42 °C followed by a shift on ice.

Afterwards, 6 µl of the following mastermix was added:

      1 µl Quantiscript Reverse Transcriptase

      4 µl 5x Quantiscript Reverse Transcriptase Buffer

      1 µl Reverse Transcriptase Primer Mix

The cDNA was now synthesized by incubating the mix in a PCR machine (ABI9700) with the following settings:

      15 min, 42 ºC

      3 min, 95 ºC

      4 ºC

After the synthesis, the cDNA was either stored at -20 °C or -80 °C.

4.3.3 Quantitative reverse transcriptase polymerase chain reaction

The qRT-PCR analysis was performed on an Applied Biosystems StepOnePlus or a Qiagen Rotor-Gene Q using Applied Biosystems Fast SYBR Green Master Mix (www.appliedbiosystems.com) or the Qiagen SYBR Green Master Mix (Qiagen, cat. no. 204056) with the normalization genes *Ribosomal protein L32* (*RpL32*) and/or *Act5C* as internal controls. These normalization genes were shown to be stable between different genotypes and conditions (Ponton *et al.*, 2011).

Technical triplicates of synthesized cDNA (2 µl) in a 1:5 or 1:25 dilution were loaded in Micro Amp Fast Optical 96 well reaction plate (StepOnePlus) or 0.1 ml tube-stripes (Qiagen, cat. no. 981103; for Rotor Gene Q) and mixed with primer-specific master mixes on ice:

<u>Sybr Green Mix, for self-designed primers (Eurofins MWG Operon)</u>

    10 µl Sybr Green

    1.5 µl Primer 1 (10 µM)

    1.5 µl Primer 2 (10 µM)

    5 µl water (RNase free water)

    2 µl cDNA

<u>Sybr Green Mix, for bought primer-mixes (Qiagen)</u>

    10 µl Sybr Green

    2 µl Primer Mix (10x)

    6 µl water (RNase free water)

    2 µl cDNA

Plates/stripes were then loaded to the according qRT-PCR instrument and runs were started with the following cycle conditions:

    1.) 5 min at 95 °C

    2.) 5 sec at 95 °C   ⬑ Step 2.) and 3.) were

    3.) 10 sec at 60 °C   ⬏ repeated for 40 times

    4.) From 65-95 °C

       in 1 °C –steps (5 sec each)

Quantifications of mRNA abundance are shown with standard deviations representing 2-3 independent biological replicates. Following primers were used:

Detected gene	Sequence/Identity	Reference
RpL32	QT00985677	www.qiagen.com
Fas (CG3523)	5` CCCCAGGAGGTGAACTCTATCA 3` 5` GACTTGACCGATCCGATCAAC 3`	(Seegmiller et al., 2002)
mdy	5` AAGACAGGCCTCTACTATTGT 3` 5` CCCATCATGCCCATAAATGCC 3`	this study
Stim	QT00923020	www.qiagen.com
ACS	5` AAATCCCATGGACCGATGAC 3` 5` TGTAGAGCATGAACAATGGATCCT 3`	(Seegmiller et al., 2002)
ACC	5` GTGCAACTGTTGGCAGATCAGT 3` 5` TTTCTGATGACGACGCTGGAT 3`	(Seegmiller et al., 2002)
bmm	QT00964460	www.qiagen.com
Act5c	5` GTGCACCGCAAGTGCTTCTAA 3` 5` TGCTGCACTCCAAACTTCCAC 3`	(Bauer et al., 2009)
upd2	5` CGGAACATCACGATGAGCGAAT 3` 5` TCGGCAGGAACTTGTACTCG 3`	(Rajan and Perrimon, 2012)
sNPF	5` CCCGAAAACTTTTAGACTCA 3` 5` TTTTCAAACATTTCCATCGT 3`	(Hong et al., 2012)
Dilp2	5` ACGAGGTGCTGAGTATGGTGTGCG 3` 5` CACTTCGCAGCGGTTCCGATATCG 3`	(Wang et al., 2008)
Dilp5	5` GAGGCACCTTGGGCCTATTC 3` 5` CATGTGGTGAGATTCGGAGCTA 3`	(Broughton et al., 2005)
RpL32	5` GTCGATACCCTTGGGCTTGC 3` 5`AAGATGACCATCCGCCCAGC 3`	(Marrone et al., 2011)
Akh	QT00957859	www.qiagen.com
AkhR	QT00931210	www.qiagen.com
$G\alpha q$	QT00945357	www.qiagen.com
$G\gamma 1$	QT01170596	www.qiagen.com
Plc21C	QT00926877	www.qiagen.com
CG14205	QT00925435	www.qiagen.com
CG14406	QT00922180	www.qiagen.com

4.3.4 Western blot analysis

For western Blot analysis, protein homogenates from adult fly abdomen corresponding to one fly/lane were separated on a 12% SDS-PAGE gel and blotted on a nitrocellulose membrane (Thermo scientific #88018). Blots were washed in 1x PBT (Tween-20 0.1% in 1x PBS) and blocked overnight at 4 °C in 1x PBT/5% BSA and incubated with primary antibodies for 1 h. After washing in 1x PBT, blots were incubated with secondary antibodies for 30 min, washed in 1x PBT and developed in Super Signal West Pico Chemiluminescent solution (Thermo scientific #34080) for 2 min. Signals were visualized on X-ray films (Kodak BioMax XAR Film, CAT 1651454), and scanned images were processed with Adobe Photoshop CS3. For signal intensity normalization against ß-Tubulin, developed blots were washed in PBT, restored in Restore Solution (Thermo scientific #21059) and then processed as described above.

Antibodies were used at the following final concentrations: guinea pig anti-Stim and mouse anti-ß-Tubulin (1:2000 and 1:1.000; this study and Developmental Studies Hybridoma Bank #E7); goat anti-mouse IgG-HRP (1:40.000; Pierce #31430) and donkey anti-guinea pig IgG-HRP (1:20.000; IR Europe 706-055-148). Guinea pig anti-Stim antibodies were generated against the HRQLDDDDNGNIDLSESDDFLRC peptide and affinity-purified (for the generation of a corresponding sheep antibody see Eid *et al.* (2008)). To reduce unspecific binding, anti-Stim antibody (diluted 1:2.000) was pre-incubated to a blot with proteins from *Stim* RNAi knockdown flies prior to use. Signal intensities were quantified in a Fujifilm Intelligent Dark Box II using Fujifilm LAS-1000 Pro 2.11 and Fujifilm Sciencelab99 L Process 1.95. For the Stim protein quantification (see Fig. 18A and 19A), Stim protein signals were normalized to ß-Tub protein signals and OFF-controls.

4.3.5 Transformation of fly lines by P-element insertion

Transgenic fly lines were generated by using a P-element insertion (Spradling and Rubin, 1982). In detail, constructs were cloned in a *w⁺*-containing pUASTattB vector, directly downstream of an UAS-sequence (cloning done by PD Dr. Ronald

Kühnlein and Iris Bickmeyer). Afterwards, the Plasmid DNA was injected in y^1w* embryos (BDSC24482) by using P[acman] docking sites. Injection, generation and identification of transformants was done to identify positive transformants by red eye color (done by BestGen Inc., http://www.thebestgene.com). Positive transformants were balanced *via* a double balancer line (RKF1365) to generate the final stocks.

4.4 Histology and microscopy

4.4.1 Confocal microscopy

For the analysis of the adult fat body by confocal microscopy, female abdomens were opened to remove the gut and the reproductive organs. The fat body-enriched carcass was embedded in 1x PBS containing LD540 (Spandl *et al.*, 2009) or BODIPY 493/503 (Invitrogen D3922; for lipid droplets), DAPI (Invitrogen D1306; for nuclei) and CellMask (Invitrogen C10046; for membranes) dyes. Pictures were taken with a Zeiss LSM-780 at 25x magnification in fixed gain mode. Single optical sections of 15 cells from four independent fat body preparations were analyzed for the lipid area and the cell area quantification by using ImageJ (in Fig. 17B, C).

For the estimation of intracellular Ca^{2+} concentrations (iCa^{2+}), female progeny of CaLexA reporter crossed against FB-Gal4>*Stim* RNAi2 flies were raised for 10 d on 25 °C (Fig. 17A). Alternatively, female progeny containing the non-conditional FB-Gal4 fat body driver (ON) in combination with the CaLexA reporter and a specific UAS-RNAi construct (controls without UAS-RNAi) were raised on 25 °C until hatching and kept on 18 °C for 6-7 days prior to use for the CaLexA imaging (Fig. 31A, B; fly husbandry and imaging by Yanjun Xu; (Baumbach and Xu *et al.* 2014, accepted)). The CaLexA reporter works with a cytoplasmic Ca^{2+} induced nuclear import of the chimeric transcription factor LexA-VP16-NFAT, which in turn drives a CD8-tagged (membrane localization signal) GFP reporter expression (Masuyama *et al.*, 2012). Hence, the GFP expression represents cytoplasmic Ca^{2+} levels. For the imaging fat body enriched carcasses were prepared and images were taken as described above.

For the quantification of iCa^{2+} from the CaLexA-based images (Fig. 31A, B), the GFP intensities of abdominal deep fat body tissue from at least five females per genotype were determined in 134x134 µm^2 areas and quantified by using ImageJ. Intensity values were normalized against intensities of RNAi OFF control genotypes.

4.4.2 Preparation and imaging of adult fly guts

Flies carrying the ts-FB-Gal4 were crossed to nuclear lacZ:eGFP reporter flies and male progeny was kept for 6 days at 30 °C (active condition) or 18 °C (repressed condition), respectively. Subsequently, adult fly guts were manually dissected in 1x PBS and reproductive tract structures removed. Afterwards, guts were mounted in 1x PBS/30% glycerol with DAPI (1:1000; Invitrogen D1306) for at least 10 min and imaged as described below. Alternatively, guts were stained with 0.5% Oil Red O (Sigma O-0526; solved in propylenglycol) for 30 min at 65 °C, washed three times with propylenglycol and 1x PBS before mounting in 1x PBS/30% glycerol. Specimens were imaged with a Zeiss Axiovert 200M equipped with a Hamamatsu ORCA ER camera or a Zeiss Axiophot equipped with a ProgRes 3012 camera at 5x magnification. Images were assembled using Adobe Photoshop CS3.

4.4.3 Preparation and imaging of adult fly eyes

For the estimation of growth and/or proliferation effects, the adult *Drosophila* eye is a widely used model system (Böhni *et al.*, 1999; Oldham *et al.*, 2002; Puig *et al.*, 2003). Flies containing an imaginal disc/eye-specific driver (*ey*-Gal4) were crossed against lines carrying UAS-*reaper* (*rpr*, inducer of apoptotic cell death; (Thomenius *et al.*, 2011)), UAS-p35 (p35, prevents apoptotic cell death; (Hay *et al.*, 1994; Zoog *et al.*, 1999)) and UAS-Stinger (Stinger GFP) constructs as controls. Also flies carrying the *ey*-Gal4 and an UAS-*Stim* gof (*ey*-Gal4>*Stim* gof) were crossed against Stinger GFP and p35 flies. The progeny was raised on 25 °C and aged for 6 days after hatching. Afterwards, flies were frozen on -20 °C and thawed for at least 10 min on room temperature. These flies were fixed with a needle in the

119

thorax and images of the eyes were captured with a 8x magnification on a Zeiss Discovery V8 stereomicroscope (see Fig. 23B). Eye sizes of 5-10 male flies per genotype were determined as arbitrary units (see Fig. 23A) by using the polygon selection tool of ImageJ and analyzed by using Excel 2010. Statistical analysis was done with a student's t-test.

4.4.4 Immunohistochemistry

Male progeny flies of *Stim* RNAi1 crossed against *w*-control and ts-FB-Gal4 flies were raised for 6 days on repressed-conditions (18 °C) and induced for further 6 days on active-conditions (30 °C). Brains were dissected in 0.3% Triton-X100 /1x PBS and fixed in 4% paraformaldehyde for 25 min. Fixed brains were intensively washed in 0.3% Triton-X100/1x PBS, blocked for 2 h in 5% BSA (in 0.3% Triton-X100/1x PBS) and incubated with an anti-Dilp2 antibody (1:400; (Géminard *et al.*, 2009)) overnight at 4 °C. After further washing, brains were incubated with an Alexa Fluor 568-labeled anti-rat IgG antibody (1:500, Invitrogen A-11077) for 2 h at room temperature. Brains were washed, embedded in VECTASHIELD mounting medium (Vector laboratories, contains DAPI, H-1500) and imaged with a Zeiss LSM-780 confocal microscope. To quantify the Dilp2-dependent fluorescence, maximum intensity projections of 10 brains per genotype were generated using ZenLite 2011. Images were then quantified by calculation of the mean gray value using ImageJ.

For clonal analysis, the fat body-enriched carcasses of male flies were washed and processed as described above with the following changes. An anti-pHis3S10 antibody was used as the primary antibody (1:500, US Biomol, cat. no. H5110-13J) and an Alexa Fluor 568-labelled anti-rabbit IgG antibody (1:500 for 4 h on room temperature, Invitrogen, cat. no. A-11036) was used as a secondary antibody. Afterwards, the fat body-enriched carcass were embedded in a 1x PBS staining solution containing the following dyes: BODIPY 493/503 (Invitrogen

D3922; for lipid droplets), DAPI (Invitrogen D1306; for nuclei) and CellMask (Invitrogen C10046; for membranes).

4.4.5 Histology of adult flies

Cryosections were done on adult male fly progeny of RNAi transgenic flies crossed against ts-FB-Gal4 and the *w*-control, raised under repressed-conditions and fed for 6 days under repressed- or active-conditions. Wings were removed and whole flies were incubated in OCT medium (www.leica-microsystems.com) for 6 h prior to freezing on dry ice. 18 µm sections at -16 °C/-13 °C chamber/object-temperature were done on a Leica CM 3050 S cryostat (www.leica-microsystems.com) and transferred on coated slides (Superfrost Plus; www.thermoscientific.com). Sections were dried for 5 min at 30 °C prior to staining.

For ß-galactosidase activity staining, cryosections were thawed and specimens were fixed for 10 min in 0.5% glutaraldehyde/1x PBS. Fixation was stopped by washing specimens three times in 1x PBS and slides were exposed to staining solution (5 mM $K_3[Fe^{III}(CN)_6]$, 5 mM $K_4[Fe^{II}(CN)_6]$, 2 mg/ml X-Gal in 1x PBS) at 37 °C. After completion of color development, specimens were washed three times in 1x PBS, post-fixed for 30 min in 5% paraformaldehyde/1x PBS, washed as above and mounted in 30% glycerol/1x PBS.

For Oil Red O staining, cryosections were thawed and fixed for 30 min in 5% paraformaldehyde/1x PBS. Specimens were washed three times in 1x PBS and covered with propylenglycol (SAFC W294004-K) for 10 min. Sections were stained in 0.5% Oil Red O (Sigma O0625) in propylenglycol for 3 h and staining solution was replaced by propylenglycol for 10 min followed by three washing steps in 1x PBS. Sections were mounted and imaged as described above.

For paraffin sections, flies were put in a collar and fixed with Carnoy`s solution (60% EtOH, 30% chloroform, 10% acidic acid) overnight on 4 °C. Afterwards, samples were washed with increasing EtOH concentrations (40%: 2x 10 min, 70%:1x 10 min, 100%: 2x 10 min) and prepared with methyl benzoate (30 min at 65 °C), methyl benzoate+paraffin (30 min at 65 °C) and paraffin only (2x 45min at 65 °C). The prepared samples were now embedded in paraffin and cured on room

temperature overnight. The cured paraffin blocks were cut on a Zeiss Hyrax M25 rotary mikrotome in 10 µm slices, which were absorbed by paraffin-coated slides (Superfrost Plus; www.thermoscientific.com). After the slides dried, they were washed with xylene (2x 4min) and decreasing EtOH concentrations (100%: 2x 4 min; 95%: 3 min; 70%: 2 min; 0%: 1 min). Washed slides were now stained in Mayer`s Hematoxylin solution (nuclei staining; Sigma-Aldrich, cat. no. MH516), washed with water for 2x 10min and stained with Eosine Y solution (cytoplasm staining; Sigma-Aldrich, cat. no. 110232). Stained slides were washed by rising EtOH concentrations (70%: 18 dips; 95%: 30 sec; 100%: 1x 2 min + 1x 4 min) and xylene prior to mounting in DPX Mountant (Sigma-Aldrich, cat. No. 06522).

Microscopic analysis and image acquisition were done using a Zeiss Axiophot (www.zeiss.com) microscope in bright field mode equipped with a ProgRes 3012 camera (www.progres-camera.com).

4.4.6 Electron microscopy

Electron microscopy pictures were done on abdomen of adult male fly progeny from *Stim* RNAi1 transgenic flies crossed against ts-FB-Gal4 and the *w*-control. The progeny was raised for 6 days under repressed-conditions followed by feeding for 6 days under active-conditions (30 °C). For this purpose abdomen were placed on a 150 µm flat embedding specimen holder using 1-hexadecen (Engineering Office M. Wohlwend GmbH, Sennwald, Switzerland). Afterwards, samples were frozen in a Leica HBM 100 high pressure freezer (Leica Microsystems, Wetzlar, Germany) and embedded by using an Automatic Freeze Substitution Unit (Leica) on vitrified samples.

The substitution was done at -90 °C in a mix of anhydrous acetone, 0.1% tannic acid and 0.5% glutaraldehyde over 72 h and in anhydrous acetone, 2% OsO_4, 0.5% glutaraldehyde for additional 8 h and 18 h at -20 °C. Afterwards, samples were warmed up to 4 °C and washed with anhydrous acetone followed by embedding in Agar 100 (Epon 812 equivalent) at room temperature and polymerization at 60 °C for 24 h. A Philips CM120 electron microscope (Philips Inc.) equipped with a TemCam 224A slow scan CCD camera (TVIPS, Gauting,

Germany) was used for image acquisition. The diameter of lipid droplets (LD) were determined and statistical analyzed by Excel 2010 for LD with a diameter ≥8 µm. The preparation of flies and the electron microscopy images were done by Dr. Dietmar Riedel (Max Planck Institute for biophysical chemistry, Facility for Transmission Electron Microscopy; (Baumbach *et al.*, 2014).)

5 Supplement

5.1. A transcriptome analysis of *Stim* KD flies reveals potential downstream factors mediating the onset of obesity

An interference of SOCE causes severe changes in body fat storage (Fig. 16A, B, C). A fat storage-restricted knockdown of the core component *Stim* leads to massive body fat accumulation (Fig. 17). This effect is at least in part mediated *via* an unknown factor, which drives the expression of the food intake regulator short neuropeptide F (sNPF) in the brain causing higher food intake (Fig. 27D, E, Fig. 28A, D, E, F and Fig. 29A). To unveil, which fat body to brain-mediator might be transcriptionally affected by an adult fat storage tissue-specific *Stim* KD and which other processes might be interfered, the transcriptome of fly abdomen (enriched for fat storage tissue) was determined under different knockdown conditions and by different techniques. In detail, *Stim* RNAi1 flies were crossed against a conditional fat storage-restricted driver line (ON, ts-FB-Gal4) and driverless *w*-controls (OFF) under repressed conditions (18 °C). After hatching of the progeny, male flies were raised for additional 6d under repressed conditions and afterwards shifted for short-term (34 h) or long-term (6 d) on active-conditions (30 °C) to induce the *Stim* KD. Afterwards, flies were directly frozen in liquid nitrogen and the total RNA was extracted.

Microarray analysis of total RNA from long-term induced *Stim* KD flies and controls were done with three biological replicates by the "Transkriptionsanalyselabor (TAL) Göttingen" (http://www.uni-bc.gwdg.de/index.php?id=661) on the basis of an Agilent Microarray Platform (Wolber *et al.*, 2006). In detail, cDNA was synthesized and labeled with Cy3 and Cy5 in an ozone free environment (hybridization, washing and scanning). Cy3 and Cy5 intensities are detected by simultaneous two-color scanning using an Agilent DNA microarray scanner at 2-5 micron resolution and normalized against normalization genes. The fold changes (FC) were calculated by normalization to controls.

Supplement

For RNAseq analysis, total RNA extractions of three biological replicates from short-term induced *Stim* KD flies and controls were used by the "TAL Göttingen" to generate fragmented cDNA. A HiSeq 2000 Sequencing System (Illumina) was used to generate up to 100 bp read-outs of the cDNA fragments, which were aligned to the whole *Drosophila* genome allowing an isoform specific gene identification. Samples were normalized to the sum of all read-outs and fold changes of the genes were determined by normalization of the *Stim* KD read-outs against control read-outs.

By this effort, the following six genes could be identified, which are ectopically expressed in fat storage tissues and highly regulated due to a short- and long-term fat storage-restricted *Stim* KD: *CG14205, CG9825, Hippi, CG16775, Cyp4d1* and *CG14406* (Table S1).

Table S1 Regulated candidate genes in a short- and long-term fat storage-restricted *Stim* KD. Shown are 41 candidate genes from an RNAseq analysis of short-term *Stim* KD flies with a fold change of >1.47 (green font: up-regulation; red font; down-regulation) and a false discovery rate <5% (with some exceptions). Fold changes of short-term *Stim* KD flies (34 h) were compared to fold changes on long-term conditions (6d). Overlapping trends with an ectopic gene expression in adult fat storage tissues (targeted by a ts-FB-Gal4 driver) were highlighted with a green background (6 candidates). Candidates with a false discovery rate of 5% - 10% or an ectopic gene expression in other tissues were marked with a yellow background (7 candidates) and candidates, which do not show an overlap between short- and long-term conditions were marked with an red background (27 candidates). Information about expressing tissues were achieved by comparison against the FlyBase database (www.flybase.org) separately for each gene. n.s.: not significantly regulated

(Table S1 on next page)

Supplement

(Table S1 legend on previous page)

gene name	Fold change after 34 h	Fold change after 6 d	false discovery rate	expressing tissues
CG14406	10,88	297,24	0,00%	fat body, heart
CG14205	-2,43	-10,24	0,25%	midgut
CG9825	-1,98	-3,88	1,40%	midgut, testis
Hippi	-1,93	-2,95	2,51%	fat body
CG16775	-2,13	-2,45	0,00%	midgut
Cyp4d1	-2,42	-2,43	6,66%	midgut, fat body
Dpt	2,34	24,97	7,09%	weak expression in all tissues
CG6106	3,58	2,74	0,32%	weak in hindgut
RabX2	46,29	2,97	0,00%	weak in all tissues, more in testis
CG10089	-2,44	-3,16	0,05%	testis
Cpr50Ca	-2,01	-4,31	0,00%	male accessory gland, weak in hindgut
Cyp310a1	-1,57	-2,55	6,27%	larval fat body, malpighian tubules
W	1,68	27,14	0,02%	eye, malpighian tubules
CG10182	-7,28	3,27	0,00%	midgut
CG42825	-5,36	n.s.	0,00%	midgut, hindgut
LysX	-3,47	2,88	0,00%	midgut, hindgut
Muc68D	-3,47	n.s.	0,02%	adult midgut
CG34220	-2,95	n.s.	0,29%	adult expression
Cp1	-2,89	n.s.	0,00%	ubiquitous, very high in heart/fat body
Jon66Cii	-2,72	n.s.	5,76%	midgut
CG14219	-2,58	n.s.	0,29%	midgut
CG9016	-2,32	n.s.	0,00%	testis
CG32050	-2,27	n.s.	2,29%	very weak in all tissues
Sdic3	-2,21	n.s.	0,22%	high expression in all tissues
CG5550	-1,85	n.s.	2,45%	hindgut, midgut
CG15043	-1,80	17,69	0,50%	midgut
CG10943	-1,67	2,69	1,56%	midgut, hindgut
CG32368	-1,64	14,00	0,12%	midgut, hindgut, fat body
CG11671	-1,60	2,11	6,19%	midgut, hindgut
CG42782	-1,55	n.s.	0,60%	no expression data available
Mur29B	-1,47	6,66	4,63%	midgut, hindgut
Cyp4p2	1,66	n.s.	3,55%	midgut, hindgut
RpS21	1,80	n.s.	0,09%	ubiquitous very high expression
CG34327	2,36	n.s.	6,78%	no expression data available
Hsp70Bb	2,42	n.s.	0,01%	very weak in all tissues
CheA75a	2,69	n.s.	0,04%	carcass
CG13428	2,70	n.s.	0,00%	carcass
CheA7a	2,85	n.s.	0,13%	carcass
Dro	5,92	n.s.	0,01%	very weak in midgut
sisA	12,16	n.s.	0,00%	weak in all tissues

Supplement

5.1.1 An RNAi KD of *CG14205* or *CG14406* causes changes in body fat storage

In order to get further evidence, that the identified genes (see chapter 5.1 and Tab. S1) are potential downstream targets of *Stim,* a fat storage-restricted KD was done against those genes under long-term conditions (6 days) to mimic the *Stim* KD-mediated down-regulation of transcripts. Afterwards, the body fat content was determined by CCA. While a KD against *CG9825* showed no significant regulation, interference against *Hippi* and *Cyp4d1* showed small but significant changes in the body fat content (Fig. S1). Interestingly, a KD of *CG14205* resulted in a more than doubled body fat accumulation, which is comparable to a *Stim* KD (Fig. S1 and Fig. 16A). In addition, RNAi against *CG14406* depletes body fat stores, which is antagonistic to the obese *Stim* KD flies with up-regulated *CG14406* expression levels.
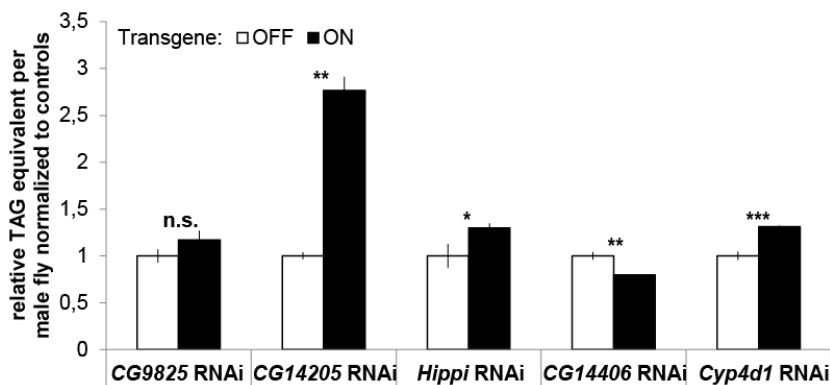
Fig. S1 A fat storage-restricted KD of potential *Stim* down-stream candidates results in changed body fat storage. The expression levels of the identified candidate genes were down-regulated by RNAi to mimic the *Stim* KD-mediated transcript levels (see Tab. S1). Subsequently the body fat content was determined by a CCA. Note that *CG14406* was up-regulated in *Stim* KD flies but down-regulation by RNAi caused an antagonistic body fat depletion. ***p<0.001, **p<0.01, *p<0.05, n.s. non-significant

In summary, these results introduce *CG14205* and *CG14406* as body fat storage regulators, which potentially act downstream of *Stim* in the body fat storage regulation of adult flies.

5.1.2 The *Stim* KD-mediated obesity can be partially rescued by *CG14406* KD or *CG14205* gof

Since a *Stim* KD in the adult fly fat body causes down-regulation of *CG14205* and up-regulation of *CG14406*, which finally leads to massive body fat accumulation, I want to analyze if these effects can be rescued by antagonistic regulations of *CG14205* and *CG14406*. Therefore, a *CG14406* RNAi-construct or an UAS-*CG14205* (*CG14205* gof) construct were crossed in a *Stim* RNAi1 background and stocks were established. Both combinations were crossed against a ts-FB-Gal4 line or *w*-controls and raised under repressed conditions. Freshly hatched male flies were raised for additional 6 days on repressed-conditions and thereafter induced for 6 days on active-conditions. Afterwards, the body fat content was determined by a CCA (Fig. S2).
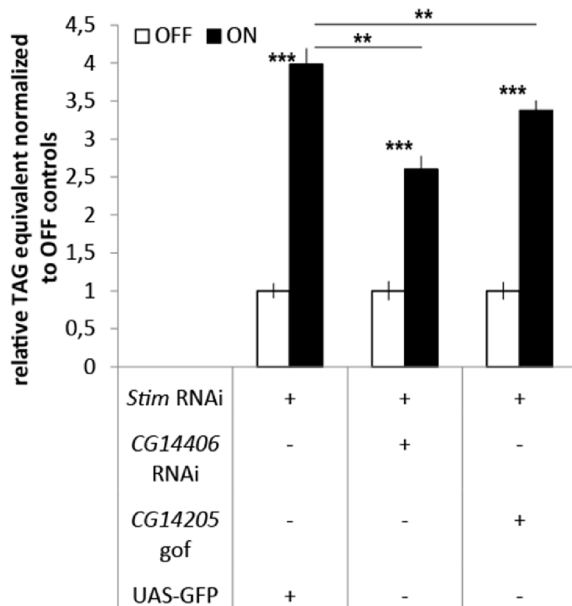
Fig. S2 The *Stim* KD-mediated body fat accumulation in adult male flies can be partially rescued by RNAi against *CG14406* or overexpression of *CG14205*. Shown are whole body fat contents (measured by CCA) from the male progeny of *Stim* RNAi1 as well as combinations of *Stim* RNAi with *CG14406* RNAi or *CG14205* gof flies crossed against a ts-FB-Gal4 (ON) or *w*-controls (OFF). Note that *Stim* RNAi1 flies include an UAS-GFP to match the number of UAS-inducible transgenes. **p<0.01, ***p<0.001

A *Stim* RNAi caused a nearly 4-fold body fat accumulation, while simultaneous RNAi against *CG14406* or a *CG14205* gof leads only to a 2.5-3.5 fold body fat accumulation. Conclusively, the *Stim* KD-mediated body fat accumulation can be partially suppressed by either *CG14406* RNAi or *CG14205* gof, which supports the hypothesis that these factors are possible downstream targets of SOCE and *Stim*.

5.1.3 A *CrebB* DN causes a strong up-regulation of *CG14406*

A *Stim* KD causes massive body fat accumulation at least in part *via* transcriptional regulations of *CG14205* and *CG14406*. Since *Stim* is a known core component of SOCE and regulates cytoplasmic Ca^{2+} concentrations, one can speculate that a Ca^{2+}-responsive transcriptional activator is in charge of those regulations. CrebB is a transcriptional activator, which is described to regulate body fat levels (Iijima *et al.*, 2009). In detail, a fat body-restricted overexpression of *CrebB* DN by a *to*-Gal4 driver results in body fat accumulation. In addition, CrebB is regulated by Crtc, which responds to cAMP and Ca^{2+} followed by Crtc translocation to the nucleus where it can activate CrebB (Bittinger *et al.*, 2004). To get additional evidence that *CrebB* might be modulated by low cytoplasmic Ca^{2+} levels in a fat storage tissue-specific *Stim* KD, *CrebB* DN flies were induced for 50h and *Stim* RNAi flies for 34 h using a conditional fat body-restricted driver (ts-FB-Gal4), which results in 30-50% body fat accumulation (see Fig. 26B). Abdomen of male flies were prepared, RNA was extracted, cDNA was synthesized and a qRT-PCR was done to determine the *CG14205* and *CG14406* transcripts in a *Stim* KD and a *CrebB* DN (Fig. S3).
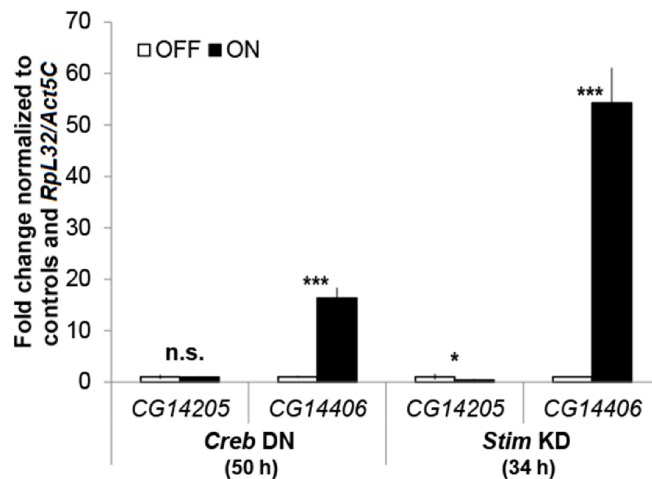
Fig. S3: A *CrebB* DN causes a strong up-regulation of *CG14406*. Male progeny of *CrebB* DN or *Stim* RNAi crossed against a ts-FB-Gal4 driver (ON) or *w*-controls (OFF) were induced for 34 h (*Stim* RNAi) or 50 h (*Creb* DN) to adapt their physiological body fat levels (+30-50% body fat). Abdomen of induced male flies were prepared in three biological replicates, RNA was extracted and a qRT-PCR was done to determine the transcript levels of *CG14205* and *CG14406*. n.s. not significant, *p<0.05, ***p<0.001.

In *Stim* KD flies, *CG14205* was down-regulated by more than 50%, while *CG14406* was up-regulated by more than 50 times. On the other hand, a *Creb* DN has no effect on *CG14205* transcripts but causes a fold change of >15 for *CG14406*.

In summary, RNAseq results for a 34 h *Stim* KD (see Table S1) were validated for the *CG14406* up- and the *CG14205* down-regulation by qRT-PCR. Similar effects could be observed in a 50 h *Creb* DN for *CG14406*, while *CG14205* was not significantly regulated.

The analysis of *Stim* KD-mediated obesity in adult flies by microarrays and RNAseq reveals several regulated genes (Table S1). Among the highest regulated genes are *CG14205* and *CG14406*, whereby the function of these genes are largely unknown. The *CG14205* is expressed highly specific in the larval and adult midgut (http://flyatlas.org/) and was described to be a concentration-dependent sugar responsive ten transmembrane receptor in L3 larvae (Zinke *et al.*, 2002), which is likely dependent on the metabolic flux of glycolysis as a potential signaling receptor. Also *CG14205* shows high homology to other *Drosophila* genes like *CG14219*, *CG14204* and *CG10182*, whereby these genes are not sugar-responsive. Interestingly, *CG14219* and *CG10182* were down-regulated due to a short (34 h) fat storage-restricted *Stim* KD, which is overlapping with the *CG14205* regulation (Table S1). On the other hand *CG14219* and *CG10182* were not down- or even up-regulated with an extended *Stim* KD (6 days). This implicates that they may share similar functions but they also consists of independent functions. The most interesting fact is that an RNAi-mediated KD of *CG14205* causes massive body fat accumulation, which supports its function as a metabolic key player (Fig. S1). The gene *CG14406* was the most up-regulated gene in a *Stim* KD, which also shows changes in global body fat levels due to interference (Fig. S1). Since *CG14406* is ectopically expressed at low levels specifically in the fat body and the heart, this might explain why the difference in body fat is only low (-20%) after a KD. Little is known so far about this gene in the literature. No homologs are known (http://www.ncbi.nlm.nih.gov/homologene) and a protein blast shows only low conservation to the "insulin-like growth factor 2 mRNA binding protein 2" in *Mus musculus.* Interestingly, CG14406 shows a distinct similarity to the *Drosophila* protein Girdin, which was described to act as a substrate of Akt1, a central regulator of insulin signaling. Therefore it also plays a role in the regulation of cell

growth and proliferation, shown by a KD of *Girdin* in the *Drosophila* wing imaginal disc cells, which resulted in the reduction of cell size (Puseenam *et al.*, 2009). This might implicate that CG14406 could also acts as a substrate for central metabolic pathways. Furthermore, *CG14406* is up-regulated due to infection (Short and Lazzaro, 2013), which emphasizes its function in the fat body.

Since *CG14205* and *CG14406* contribute to the *Stim* KD-mediated body fat accumulation (Fig. S2), I further asked the question which transcriptional activator (TA) mediates these effects. The TA CrebB was described to regulate carbohydrate and TAG metabolism in *Drosophila* (Iijima *et al.*, 2009) and mice *via* the second messenger Ca^{2+} (Wang *et al.*, 2012b). Interestingly, a fat storage-restricted interference of *Stim* or *CrebB* in the adult fly causes body fat accumulation, similar expression patterns for the lipogenesis regulator *midway* (Beller *et al.*, 2010) or the lipolysis regulator *brummer* (Grönke *et al.*, 2005)(Fig. 26B, C), a higher food intake (Fig. 27D and Iijima *et al.* (2009)) and a strong up-regulation of *CG14406* (Fig. S3). These facts implicate *CrebB* as a downstream effector of *Stim* and *CG14406* as a downstream effector of *Stim* and *CrebB*, whereby *CrebB* seems to activate the transcription of an unknown transcription repressor, which keeps the ectopic *CG14406* transcripts at low levels. Further research on *CG14406* might lead into new insights how this newly described body fat storage regulator contributes to the control of energy homeostasis and body fat storage control.

5.2 A *Stim* KD-mediated obesity has no effect on the fitness or the longevity of adult flies

A transient or chronic fat storage-restricted interference of *Stim* in flies causes a massive body fat accumulation (Baumbach *et al.* (2014), Fig. 16A and Fig. 18B). In order to test if the adult fly's fitness is affected under these conditions and if it contributes to the *Stim* KD-mediated body fat accumulation, climbing and locomotor activity assays were done.

Supplement

For climbing assays, *Stim* RNAi1 flies were crossed against a conditional fat storage-restricted driver line (ts-FB-Gal4; ON) or a *w*-control (OFF). Progeny was raised under repressed-conditions (18 °C) as well as freshly hatched male flies (0-24 h). The male flies were aged for 6 days followed by a shift to active-conditions (30 °C) for another 6 days in order to induce a fat storage-restricted *Stim* KD. Male flies were tested in a climbing/mobility assay according to (Greene *et al.*, 2003). In detail, four technical and two biological replicates of twenty male flies were placed in the first chamber of a countercurrent apparatus (Benzer, 1967). The flies were tapped to the bottom of the first chamber, which was then connected to a second chamber. Flies, which managed to climb the 10 cm from the first into the second chamber in 5 sec, were used for additional rounds. After five rounds (6 chambers), the number of flies in each chamber was counted and the climbing index calculated as the sum of the number of flies in each chamber multiplied by the number of the chamber and divided by 100 (Fig. S4).
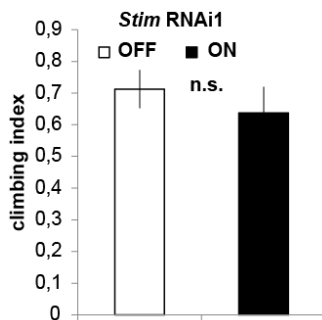
Fig. S4 Climbing fitness is not affected in obese fat storage-restricted *Stim* KD flies. The climbing index was determined as a fitness indicator in 6 d fat storage induced (ts-FB-Gal4) *Stim* KD males (ON) or in controls without the driver (OFF). No significant (n.s.) differences could be detected compared to control flies.

Stim KD flies showed a small tendency to a lower climbing index, which showed no significant changes in comparison to controls. Conclusively, the climbing index showed that the activity/fitness in *Stim* KD flies is not affected, which is in line with the results from the metabolic rate (Fig. 27A, B) and the locomotor activity measurement (Fig. 27C).

For the longevity assays, *Stim* RNAi1 flies were crossed against a chronic fat storage-restricted driver (FB-Gal4) or a *w*-control. In addition, FB-Gal4 flies were crossed against *w*-control flies as a second control. Progeny was continuously raised on 25 °C, 50% humidity and a 12 h/12 h light/dark-cycle. Freshly hatched

males (0-24 h) were then raised for 6 days in batches and afterwards split into 15 replicates with 15 males each. The number of survivors per replicate was determined every 3-4 days until all flies died. Furthermore, three replicates per genotype were incubated in parallel and aliquots for a body fat determination were collected every 10-20 days (Fig. S5).
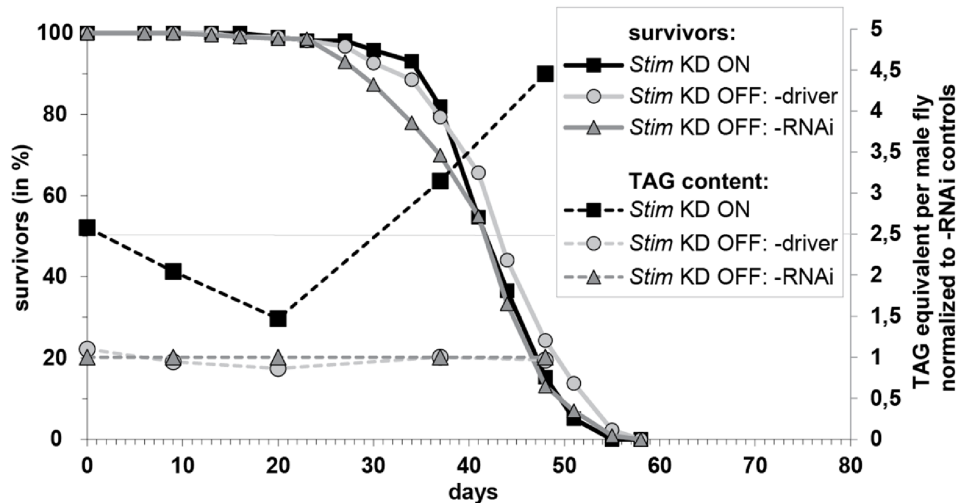
Fig. S5 The longevity is not affected in obese _Stim_ KD flies. Freshly hatched chronic fat storage-restricted _Stim_ KD flies (black, FB-Gal4>_Stim_ RNAi1) and two independent controls for the RNAi construct (dark grey) or the driver (light grey) were monitored for their survival every 3-4 d (solid lines) and their body fat content (TAG, dashed lines) every 10-20 d. While body fat levels are increased due to a fat storage-restricted _Stim_ KD, the survival shows no clear trend compared to controls.

At the starting point of the longevity observation (0 days), _Stim_ KD flies store more than the double amounts of body fat compared to controls. Interestingly, after 20 days less than 5% of the flies died in all genotypes but the body fat content of _Stim_ KD flies drops to only +47% body fat accumulation. Furthermore, after 37 days the _Stim_ KD flies store three times more body fat as controls and this trend is even increasing after 48 days. With reference to the longevity, significant differences determined by a log-rank test could be detected between _Stim_ KD and control flies (p=0.006 for the driver- and p=0.424 for the RNAi-control). The median longevity time of _Stim_ KD flies is 43.5 days, while the driver-control shows a 44.4 days and

the RNAi-control a 42.0 days median longevity time. Hence, the obesity of *Stim* KD flies shows changes concerning the body fat content during the adult life. While young flies are obese, middle age flies accumulate only small amounts of body fat. Interestingly, flies with a higher age became extremely obese in comparison to controls. Even if the differences in the median longevity time were significant in comparison to the driver-control, the *Stim* KD-mediated obesity seems not to influence the longevity of the flies, since the median longevity time of *Stim* KD flies is between both controls.

So far, the view on mechanisms underlying aging is very limited. It was previously shown that body fat accumulation and obesity are not necessarily connected to the longevity of flies (Grönke *et al.*, 2010). In detail, *dilp6*- (*drosophila insulin like peptide 6*) and *dilp2,3,5*-mutant flies accumulate +21% and +19% body fat with no significant change in the longevity, while *dilp2* and *dilp2-3* mutant flies are not obese but increased in their median life span. On the other hand, *dSH2B* mutant obese flies were also shown to have an extended lifespan, likely by binding to Chico and thereby promoting insulin signaling downstream of InR (Song *et al.*, 2010). Interestingly, a fat storage-restricted *Stim* KD causes a decrease in Dilp2 in the insulin producing cells (IPC) (see Fig. 28B, C), which results in obesity (Fig. 17) but has no effect on the longevity (Fig. S5). Since the *dilp2* and *dilp5* transcripts are not affected (Fig. 28A), the decrease in Dilp2 is likely due to a higher secretion from the IPCs. Taken together with the effects from *dilp2* and *dilp2,3,5*-mutant flies on longevity and obesity, there is evidence that a finely tuned network of Dilps and the interaction to their target tissues is central for body fat regulation and longevity (see Houtkooper *et al.* (2010) for a review). Thereby, observation of the other Dilps in *Stim* KD flies are essential for a better understanding. Conclusively, further studies are necessary to understand the role of the observed Dilp2 decrease in the IPCs of *Stim* KD flies and their possible effects on longevity and metabolism.

5.3 Additional supplemental tables

Table S2 A body fat based *in vivo* RNAi KD screen in *Drosophila* identifies 77 obesity (green)/anti-obesity (red) genes. The primary screen revealed 968 primary screen candidates, whereby 210 genes were confirmed under class I or II conditions (see 4.1.2.1 for details). Subsequently, 188 of these genes (95 obesity and 93 anti-obesity genes) were subjected to validation by an alternative driver or RNAi line and validation-scores were determined (see 4.1.2.2 for details). The final validation scores were calculated as the sum of the single experiment scores. Based on a validation score ≥2 and further criteria (see 4.1.2.2 for details) 77 anti-obesity/obesity genes were defined. Thirty-five of these gene knockdowns (45%) resulted in lethality upon pre-adult developmental gene knockdown, which emphasizes the importance of a repressible system. Fifty-seven of these genes (74%) are novel fly fat storage regulators. A comparison to human protein sequences by using NCBI (ProteinBLAST) and InParanoid7 showed that 64 (83%) of these fly genes have a human ortholog. *Note that *ltp-r83a* was not tested in the primary screens but independently validated.

FlyBase gene symbol	validation score	1 = yes; 0 = no Lethality upon pre-adult gene knockdown?	1 = yes; 0 = no Reported as cellular or organismal body fat regulator in flies?	Human ortholog (InParanoid7, inparalog score 1)
bmm	4	0	1	ATGL (PNPLA2)
CSN4	3	0	0	COPS4
Cul-4	3	1	0	CUL4B
Galphaq	3	0	0	GNAQ
AkhR	3	0	1	GNRHR
CG6937	3	1	0	MKI67IP
CG9940	3	0	0	NADSYN1
CG7770	3	0	1	PFDN6
CG9238	3	0	0	PPP1R3C
Stim	3	0	0	STIM1
Arf79F	2	1	1	ARF1
sec71	2	1	0	ARFGEF1/2
Aut1	2	0	0	ATG3
VhaM8.9/CG8444	2	0	1	ATP6AP2
Vha16-1	2	0	0	ATP6V0C
Br140/CG1845	2	0	0	BRD1
Cam	2	0	0	CALM
CG6272	2	1	0	CEBPG
CG31915	2	0	0	COLGALT2
Tbh	2	0	0	DBH
antdh	2	0	0	DHRS11

CG10166	2	0	1	DPM1
CG6750	2	0	0	EMC3
Ggamma1	2	0	0	GNG12
Rpd3	2	1	0	HDAC2
CG7379	2	0	0	ING2
*Itp-r83a**	2	n.d.	1	ITPR1
Lgr1	2	0	0	LHCGR
CG3214	2	0	0	NDUFA12
Pect	2	0	1	PCYT2
tam	2	0	0	POLG
Sec24CD	2	1	0	SEC24C
CG4743	2	0	0	SLC25A26
spen	2	1	0	SPEN
bip2	2	0	0	TAF3
RN-tre	2	0	0	TBC1D3
poe	2	0	0	UBR4
Tom34	2	0	0	UNC45B
CG5484	2	1	1	YIF1B
CAH2	2	0	0	
CG14210	2	0	0	
CG15142	2	0	0	
CG15890	2	0	0	
Eip74EF	2	0	0	
l(2)05714	2	1	0	
NKAIN	2	0	0	
Rx	2	0	0	
Ykt6	2	1	1	
mask	4	1	0	ANKHD1
Ntf-2	4	1	1	NUTF2
Rpn6	4	1	0	PSMD11
Ca-P60A	3	1	0	ATP2A2
Cas	3	1	1	CSE1L
eIF-1A	3	1	1	EIF1AX
Prosalpha5	3	0	1	PSMA5
Prosbeta3	3	1	1	PSMB3
Rpn8	3	1	0	PSMD7
how	3	1	0	QKI
Su(var)3-9	3	1	0	SUV39H2
put	2	1	0	ACVR2
CG14270	2	1	0	C19orf52
CG16903	2	1	1	CCNL1

l(2)NC136	2	1	0	CNOT3
mdy	2	0	1	DGAT1
Es2	2	0	0	DGCR14
Fbw5	2	1	1	FBXW5
ftz-f1	2	1	1	NR5A2
olf186-F	2	1	1	ORAI1
pcx	2	1	0	PCNXL
Rpn7	2	0	1	PSMD6
RpL26	2	1	0	RPL26L1
CG3500	2	1	0	TEX261
CG15618	2	1	0	THADA
Mtor	2	1	0	TPR
CG14512	2	0	0	
l(3)05822	2	0	0	
Lasp	2	1	0	
plx	2	1	0	

Table S3 Gene Ontology (GO) analysis (Biological Processes). The anti-obesity/obesity gene set (see table S2) was analyzed by Gene Ontology (http://genome.crg.es/GOToolBox/) with the following selection criteria: P value <0.012; number of ref. (reference genes, dedicated to a GO term) 4-100; Enrichment factor (EF) >3. Terms, which fullfilled the criteria were manually clustered into functional classes. Terms connected to calcium signaling, protein/nuclear transport and lipid metabolism showed the highest EF. For details, see chapter 4.1.2.3.

GO number	GO term	number of ref.	number of genes in set	EF	Identified genes in the set	functional class
GO:0006888	ER to Golgi vesicle-mediated transport	14	2	11,5	*sec71, CG10882*	Vesicle-mediated transport
GO:0006914	autophagy	12	2	13,8	*Aut1, Eip74EF*	Autophagy
GO:0040034	regulation of development, heterochronic	10	2	16,4	*Eip74EF, ftz-f1*	Transcriptional/Translational regulation
GO:0055085	transmembrane transport	63	4	5,1	*Stim, olf186-F, Cam, Vha16*	Protein transport
GO:0017038	protein import	73	7	7,8	*Stim, cul-4, Cas, Ntf-2, olf186-F, Mtor, Cam*	Protein transport
GO:0060341	regulation of cellular localization	49	5	8,3	*Stim, cul-4, Cas, olf186-F, Cam*	Protein transport
GO:0032879	regulation of localization	68	7	8,4	*Stim, cul-4, Cas, olf186-F, CG34413, Ca-P60A, Cam*	Protein transport
GO:0051049	regulation of transport	38	6	12,9	*Stim, cul-4, Cas, olf186-F, CG34413, Cam*	Protein transport

GO ID	Term				Genes	Category
GO:0032880	regulation of protein localization	29	5	14,1	*Stim, cul-4, Cas, olf186-F, Cam*	Protein transport
GO:0032386	regulation of intracellular transport	25	5	16,3	*Stim, cul-4, Cas, olf186-F, Cam*	Protein transport
GO:0046486	glycerolipid metabolic process	8	2	20,3	*bmm, mdy*	Lipid Metabolism
GO:0006639	acylglycerol metabolic process	7	2	23,0	*bmm, mdy*	Lipid Metabolism
GO:0006638	neutral lipid metabolic process	7	2	23,0	*bmm, mdy*	Lipid Metabolism
GO:0051169	nuclear transport	77	7	7,40	*Stim, cul-4, Cas, Ntf-2, olf186-F, Mtor, Cam*	Nuclear transport
GO:0042307	positive regulation of protein import into nucleus	13	5	31,9	*Stim, cul-4, Cas, olf186-F, Cam*	Nuclear transport
GO:0046824	positive regulation of nucleocytoplasmic transport	13	5	31,9	*Stim, cul-4, Cas, olf186-F, Cam*	Nuclear transport
GO:0070201	regulation of establishment of protein localization	24	5	16,9	*Stim, cul-4, Cas, olf186-F, Cam*	Calcium signaling
GO:0051223	regulation of protein transport	24	5	16,9	*Stim, cul-4, Cas, olf186-F, Cam*	Calcium signaling
GO:0051050	positive regulation of transport	19	5	21,6	*Stim, cul-4, Cas, olf186-F, Cam*	Calcium signaling
GO:0032388	positive regulation of intracellular transport	13	5	31,9	*Stim, cul-4, Cas, olf186-F, Cam*	Calcium signaling
GO:0051222	positive regulation of protein transport	13	5	31,9	*Stim, cul-4, Cas, olf186-F, Cam*	Calcium signaling
GO:0043269	regulation of ion transport	4	3	64,6	*Stim, olf186-F, CG34413*	Calcium signaling

Table S4
See digital supplement (Table_S4.xlsx) provided on a DVD.

6 References

Adams, M.D. (2000). The Genome Sequence of Drosophila melanogaster. Science (80-.). *287*, 2185–2195.

Ahmadian, M., Wang, Y., and Sul, H.S. (2010). Lipolysis in adipocytes. Int. J. Biochem. Cell Biol. *42*, 555–559.

Anand, A.N., and Lorenz, M.W. (2008). Age-dependent changes of fat body stores and the regulation of fat body lipid synthesis and mobilisation by adipokinetic hormone in the last larval instar of the cricket, Gryllus bimaculatus. J. Insect Physiol. *54*, 1404–1412.

Armbruster, K., and Luschnig, S. (2012). The Drosophila Sec7 domain guanine nucleotide exchange factor protein Gartenzwerg localizes at the cis-Golgi and is essential for epithelial tube expansion. J. Cell Sci. *125*, 1318–1328.

Arrese, E., and Soulages, J. (2010). Insect fat body: energy, metabolism, and regulation. Annu. Rev. Entomol. 207–225.

Arrese, E.L., and Wells, M.A. (1994). Purification and Properties of a Phosphorylatable Triacylglycerol Lipase from the Fat-Body of an Insect, Manduca-Sexta. J. Lipid Res. *35*, 1652–1660.

Arrese, E., Rojas-Rivas, B., and Wells, M. (1996). The use of decapitated insects to study lipid mobilization in adult Manduca sexta: effects of adipokinetic hormone and trehalose on fat body lipase activity. Insect Biochem Mol Biol. *26*, 775–782.

Arrese, E.L., Flowers, M.T., Gazard, J.L., and Wells, M. a (1999). Calcium and cAMP are second messengers in the adipokinetic hormone-induced lipolysis of triacylglycerols in Manduca sexta fat body. J. Lipid Res. *40*, 556–564.

Arrese, E.L., Rivera, L., Hamada, M., Mirza, S., Hartson, S.D., Weintraub, S., and Soulages, J.L. (2008). Function and structure of lipid storage droplet protein 1 studied in lipoprotein complexes. Arch. Biochem. Biophys. *473*, 42–47.

Ashburner, M. (1989). Drosophila: A Laboratory Handbook and Manual (New York: Cold Spring Harbor Laboratory Press).

Ashrafi, K., Chang, F.Y., Watts, J.L., Fraser, A.G., Kamath, R.S., Ahringer, J., and Ruvkun, G. (2003). Genome-wide RNAi analysis of Caenorhabditis elegans fat regulatory genes. Nature *421*, 268–272.

Bai, H., Kang, P., and Tatar, M. (2012). Drosophila insulin-like peptide-6 (dilp6) expression from fat body extends lifespan and represses secretion of Drosophila insulin-like peptide-2 from the brain. Aging Cell *11*, 978–985.

Banerjee, S., Joshi, R., Venkiteswaran, G., Agrawal, N., Srikanth, S., Alam, F., and Hasan, G. (2006). Compensation of inositol 1,4,5-trisphosphate receptor function by altering sarco-endoplasmic reticulum calcium ATPase activity in the Drosophila flight circuit. J. Neurosci. *26*, 8278–8288.

References

Barolo, S., Walker, R.G., Polyanovsky, A.D., Freschi, G., Keil, T., and Posakony, J.W. (2000). A notch-independent activity of suppressor of hairless is required for normal mechanoreceptor physiology. Cell *103*, 957–969.

Bauer, R., Voelzmann, A., Breiden, B., Schepers, U., Farwanah, H., Hahn, I., Eckardt, F., Sandhoff, K., and Hoch, M. (2009). Schlank, a member of the ceramide synthase family controls growth and body fat in Drosophila. EMBO J. *28*, 3706–3716.

Baumbach, J., Hummel, P., Bickmeyer, I., Kowalczyk, K.M., Frank, M., Knorr, K., Hildebrandt, A., Riedel, D., Jäckle, H., and Kühnlein, R.P. (2014). A Drosophila in vivo screen identifies store-operated calcium entry as a key regulator of adiposity. Cell Metab. *19*, 331–343.

Baumbach, J., Xu, Y., Hehlert, P., and Kühnlein, R.P. (2014). Galphaq, Ggamma1 and Plc21C control Drosophila body fat storage. J. Genet. Genomics accepted.

Beller, M., Riedel, D., Jänsch, L., Dieterich, G., Wehland, J., Jäckle, H., and Kühnlein, R.P. (2006). Characterization of the Drosophila lipid droplet subproteome. Mol. Cell. Proteomics *5*, 1082–1094.

Beller, M., Sztalryd, C., Southall, N., Bell, M., Jäckle, H., Auld, D.S., and Oliver, B. (2008). COPI complex is a regulator of lipid homeostasis. PLoS Biol. *6*, e292.

Beller, M., Bulankina, A. V, Hsiao, H.-H., Urlaub, H., Jäckle, H., and Kühnlein, R.P. (2010). PERILIPIN-dependent control of lipid droplet structure and fat storage in Drosophila. Cell Metab. *12*, 521–532.

Benzer, S. (1967). BEHAVIORAL MUTANTS OF Drosophila ISOLATED BY COUNTERCURRENT DISTRIBUTION. Proc. Natl. Acad. Sci. U. S. A. *58*, 1112–1119.

Bharucha, K.N., Tarr, P., and Zipursky, S.L. (2008). A glucagon-like endocrine pathway in Drosophila modulates both lipid and carbohydrate homeostasis. J. Exp. Biol. *211*, 3103–3110.

Bittinger, M.A., McWhinnie, E., Meltzer, J., Iourgenko, V., Latario, B., Liu, X., Chen, C.H., Song, C., Garza, D., and Labow, M. (2004). Activation of cAMP response element-mediated gene expression by regulated nuclear transport of TORC proteins. Curr. Biol. *14*, 2156–2161.

BLIGH, E.G., and DYER, W.J. (1959). A rapid method of total lipid extraction and purification. Can. J. Biochem. Physiol. *37*, 911–917.

Bodenstein, D. (1950). The postembryonic development of Drosophila. Demerec 275–367.

Böhni, R., Riesgo-Escovar, J., and Oldham, S. (1999). Autonomous Control of Cell and Organ Size by CHICO, a Drosophila Homolog of Vertebrate IRS1–4. Cell *97*, 865–875.

Brand, a H., and Perrimon, N. (1993). Targeted gene expression as a means of altering cell fates and generating dominant phenotypes. Development *118*, 401–415.

Brasaemle, D.L., Dolios, G., Shapiro, L., and Wang, R. (2004). Proteomic analysis of proteins associated with lipid droplets of basal and lipolytically stimulated 3T3-L1 adipocytes. J. Biol. Chem. *279*, 46835–46842.

Brini, M., and Carafoli, E. (2009). Calcium pumps in health and disease. Physiol. Rev. 1341–1378.

References

Britton, J.S., and Edgar, B. a (1998). Environmental control of the cell cycle in Drosophila: nutrition activates mitotic and endoreplicative cells by distinct mechanisms. Development *125*, 2149–2158.

Brockmann, G. a, and Bevova, M.R. (2002). Using mouse models to dissect the genetics of obesity. Trends Genet. *18*, 367–376.

Brogiolo, W., Stocker, H., Ikeya, T., Rintelen, F., Fernandez, R., and Hafen, E. (2001). An evolutionarily conserved function of the Drosophila insulin receptor and insulin-like peptides in growth control. Curr. Biol. *11*, 213–221.

Broughton, S., and Partridge, L. (2009). Insulin/IGF-like signalling, the central nervous system and aging. Biochem. J. *418*, 1–12.

Broughton, S.J., Piper, M.D.W., Ikeya, T., Bass, T.M., Jacobson, J., Driege, Y., Martinez, P., Hafen, E., Withers, D.J., Leevers, S.J., *et al.* (2005). Longer lifespan, altered metabolism, and stress resistance in Drosophila from ablation of cells making insulin-like ligands. Proc. Natl. Acad. Sci. U. S. A. *102*, 3105–3110.

Buszczak, M., Lu, X., Segraves, W.A., Chang, T.Y., and Cooley, L. (2002). Mutations in the midway gene disrupt a Drosophila acyl coenzyme A: diacylglycerol acyltransferase. Genetics *160*, 1511–1518.

Cahalan, M.D. (2009). STIMulating store-operated Ca(2+) entry. Nat. Cell Biol. *11*, 669–677.

Canavoso, L.E., Jouni, Z.E., Karnas, K.J., Pennington, J.E., and Wells, M.A. (2001). Fat metabolism in insects. Annu. Rev. Nutr. *21*, 23–46.

Carrera, P., Abrell, S., Kerber, B., Walldorf, U., Preiss, a, Hoch, M., and Jäckle, H. (1998). A modifier screen in the eye reveals control genes for Krüppel activity in the Drosophila embryo. Proc. Natl. Acad. Sci. U. S. A. *95*, 10779–10784.

Cermelli, S., Guo, Y., Gross, S.P., and Welte, M.A. (2006). The lipid-droplet proteome reveals that droplets are a protein-storage depot. Curr. Biol. *16*, 1783–1795.

Chakraborty, S., and Hasan, G. (2012). Functional complementation of Drosophila itpr mutants by rat Itpr1. J. Neurogenet. *26*, 328–337.

Chen, H.C., Stone, S.J., Zhou, P., Buhman, K.K., and Farese, R. V (2002). Dissociation of obesity and impaired glucose disposal in mice overexpressing acyl coenzyme a:diacylglycerol acyltransferase 1 in white adipose tissue. Diabetes *51*, 3189–3195.

Chin, D., and Means, A.R. (2000). Calmodulin: a prototypical calcium sensor. Trends Cell Biol. *10*, 322–328.

Choquet, H., and Meyre, D. (2011). Molecular basis of obesity: current status and future prospects. Curr. Genomics *12*, 154–168.

Chorna, T., and Hasan, G. (2012). The genetics of calcium signaling in Drosophila melanogaster. Biochim. Biophys. Acta *1820*, 1269–1282.

References

Chua, S.C., Chung, W.K., Wu-Peng, X.S., Zhang, Y., Liu, S.M., Tartaglia, L., and Leibel, R.L. (1996). Phenotypes of mouse diabetes and rat fatty due to mutations in the OB (leptin) receptor. Science *271*, 994–996.

Clapham, D.E. (2007). Calcium signaling. Cell *131*, 1047–1058.

Clement, K., Boutin, P., and Froguel, P. (2002). Genetics of obesity. Am. J. Pharmacogenomics *2*, 177–187.

Colombani, J., Raisin, S., Pantalacci, S., Radimerski, T., Montagne, J., and Léopold, P. (2003). A nutrient sensor mechanism controls Drosophila growth. Cell *114*, 739–749.

Czabany, T., Athenstaedt, K., and Daum, G. (2007). Synthesis, storage and degradation of neutral lipids in yeast. Biochim. Biophys. Acta *1771*, 299–309.

Daum, G., Tuller, G., Nemec, T., Hrastnik, C., Balliano, G., Cattel, L., Milla, P., Rocco, F., Conzelmann, a, Vionnet, C., *et al.* (1999). Systematic analysis of yeast strains with possible defects in lipid metabolism. Yeast *15*, 601–614.

Dauwalder, B., Tsujimoto, S., Moss, J., and Mattox, W. (2002). The Drosophila takeout gene is regulated by the somatic sex-determination pathway and affects male courtship behavior. Genes Dev. *16*, 2879–2892.

Demerec, M. (1994). Biology of Drosophila (Cold Spring Harbour Laboratory Press).

DiAngelo, J.R., and Birnbaum, M.J. (2009). Regulation of fat cell mass by insulin in Drosophila melanogaster. Mol. Cell. Biol. *29*, 6341–6352.

Dietzl, G., Chen, D., Schnorrer, F., Su, K.-C., Barinova, Y., Fellner, M., Gasser, B., Kinsey, K., Oppel, S., Scheiblauer, S., *et al.* (2007). A genome-wide transgenic RNAi library for conditional gene inactivation in Drosophila. Nature *448*, 151–156.

Dobrosotskaya, I.Y., Seegmiller, a C., Brown, M.S., Goldstein, J.L., and Rawson, R.B. (2002). Regulation of SREBP processing and membrane lipid production by phospholipids in Drosophila. Science *296*, 879–883.

Edgar, B.A. (2006). How flies get their size: genetics meets physiology. Nat. Rev. Genet. *7*, 907–916.

Eid, J.-P., Arias, A.M., Robertson, H., Hime, G.R., and Dziadek, M. (2008). The Drosophila STIM1 orthologue, dSTIM, has roles in cell fate specification and tissue patterning. BMC Dev. Biol. *8*, 104.

Elbashir, S.M., Harborth, J., and Lendeckel, W. (2001). Duplexes of 21 ± nucleotide RNAs mediate RNA interference in cultured mammalian cells. Nature *411*, 1–5.

Ellong, E.N., Soni, K.G., Bui, Q.-T., Sougrat, R., Golinelli-Cohen, M.-P., and Jackson, C.L. (2011). Interaction between the triglyceride lipase ATGL and the Arf1 activator GBF1. PLoS One *6*, e21889.

Fast, P.G. (1966). A comparative study of the phospholipids and fatty acids of some insects. Lipids *1*, 209–215.

References

Feske, S., Okamura, H., Hogan, P.G., and Rao, A. (2003). Ca2+/calcineurin signalling in cells of the immune system. Biochem. Biophys. Res. Commun. *311*, 1117–1132.

Fire, A., Xu, S., Montgomery, M.K., Kostas, S.A., Driver, S.E., and Mello, C.C. (1998). Potent and specific genetic interference by double-stranded RNA in Caenorhabditis elegans. Nature *391*, 806–811.

Flagg, R. (1988). Carolina Drosophila Manual (New York: Cold Spring Harbor Laboratory Press).

Flatt, J. (1995). Use and storage of carbohydrate and fat. Am. J. Clin. Nutr. *61*.

Flier, J.S. (2004). Obesity wars: molecular progress confronts an expanding epidemic. Cell *116*, 337–350.

Friedman, J.M. (2004). Modern science versus the stigma of obesity. Nat. Med. *10*, 563–569.

Friedman, J.M. (2009). Obesity: Causes and control of excess body fat. Nature *459*, 340–342.

Fullerton, M.D., Hakimuddin, F., Bonen, A., and Bakovic, M. (2009). The development of a metabolic disease phenotype in CTP:phosphoethanolamine cytidylyltransferase-deficient mice. J. Biol. Chem. *284*, 25704–25713.

Gäde, G., and Auerswald, L. (2003). Mode of action of neuropeptides from the adipokinetic hormone family. Gen. Comp. Endocrinol. *132*, 10–20.

Géminard, C., Rulifson, E., and Léopold, P. (2009). Remote Control of Insulin Secretion by Fat Cells in Drosophila. Cell Metab.

Georgel, P., Naitza, S., Kappler, C., Ferrandon, D., Zachary, D., Swimmer, C., Kopczynski, C., Duyk, G., Reichhart, J.M., and Hoffmann, J. a (2001). Drosophila immune deficiency (IMD) is a death domain protein that activates antibacterial defense and can promote apoptosis. Dev. Cell *1*, 503–514.

Gilbert, L.I., and Chino, H. (1974). Transport of lipids in insects. J. Lipid Res. *15*, 439–456.

Giorgi, C., Baldassari, F., Bononi, A., Bonora, M., De Marchi, E., Marchi, S., Missiroli, S., Patergnani, S., Rimessi, A., Suski, J.M., *et al.* (2012). Mitochondrial Ca(2+) and apoptosis. Cell Calcium *52*, 36–43.

Graham, S.J.L., Black, M.J., Soboloff, J., Gill, D.L., Dziadek, M.A., and Johnstone, L.S. (2009). Stim1, an endoplasmic reticulum Ca2+ sensor, negatively regulates 3T3-L1 pre-adipocyte differentiation. Differentiation *77*, 239–247.

Greenberg, A.S., Egan, J.J., Wek, S.A., Garty, N.B., Blanchette-Mackie, E.J., and Londos, C. (1991). Perilipin, a major hormonally regulated adipocyte-specific phosphoprotein associated with the periphery of lipid storage droplets. J. Biol. Chem. *266*, 11341–11346.

Greene, J.C., Whitworth, A.J., Kuo, I., Andrews, L. a, Feany, M.B., and Pallanck, L.J. (2003). Mitochondrial pathology and apoptotic muscle degeneration in Drosophila parkin mutants. Proc. Natl. Acad. Sci. U. S. A. *100*, 4078–4083.

References

Grönke, S., Beller, M., Fellert, S., Ramakrishnan, H., Jäckle, H., and Kühnlein, R.P. (2003). Control of Fat Storage by a Drosophila PAT Domain Protein. Curr. Biol. *13*, 603–606.

Grönke, S., Mildner, A., Fellert, S., Tennagels, N., Petry, S., Müller, G., Jäckle, H., and Kühnlein, R.P. (2005). Brummer lipase is an evolutionary conserved fat storage regulator in Drosophila. Cell Metab. *1*, 323–330.

Grönke, S., Müller, G., Hirsch, J., Fellert, S., Andreou, A., Haase, T., Jäckle, H., and Kühnlein, R.P. (2007). Dual lipolytic control of body fat storage and mobilization in Drosophila. PLoS Biol. *5*, e137.

Grönke, S., Clarke, D.-F., Broughton, S., Andrews, T.D., and Partridge, L. (2010). Molecular evolution and functional characterization of Drosophila insulin-like peptides. PLoS Genet. *6*, e1000857.

Guo, Y., Walther, T.C., Rao, M., Stuurman, N., Goshima, G., Terayama, K., Wong, J.S., Vale, R.D., Walter, P., and Farese, R. V (2008). Functional genomic screen reveals genes involved in lipid-droplet formation and utilization. Nature *453*, 657–661.

Gurley, L.R., Walters, R. a, and Tobey, R. a (1974). Cell cycle-specific changes in histone phosphorylation associated with cell proliferation and chromosome condensation. J. Cell Biol. *60*, 356–364.

Guruharsha, K.G., Rual, J.-F., Zhai, B., Mintseris, J., Vaidya, P., Vaidya, N., Beekman, C., Wong, C., Rhee, D.Y., Cenaj, O., *et al.* (2011). A protein complex network of Drosophila melanogaster. Cell *147*, 690–703.

Guyenet, S.J., and Schwartz, M.W. (2012). Regulation of food intake, energy balance, and body fat mass: implications for the pathogenesis and treatment of obesity. J. Clin. Endocrinol. Metab. *97*, 745–755.

Gwack, Y., Srikanth, S., Feske, S., Cruz-Guilloty, F., Oh-hora, M., Neems, D.S., Hogan, P.G., and Rao, A. (2007). Biochemical and functional characterization of Orai proteins. J. Biol. Chem. *282*, 16232–16243.

Haemmerle, G., Lass, A., Zimmermann, R., Gorkiewicz, G., Meyer, C., Rozman, J., Heldmaier, G., Maier, R., Theussl, C., Eder, S., *et al.* (2006). Defective lipolysis and altered energy metabolism in mice lacking adipose triglyceride lipase. Science *312*, 734–737.

Halaas, J., Gajiwala, K., Maffei, M., and Cohen, S. (1995). Weight-reducing effects of the plasma protein encoded by the obese gene. Science (80-.). *269*, 543–546.

Hapala, I., Marza, E., and Ferreira, T. (2011). Is fat so bad? Modulation of endoplasmic reticulum stress by lipid droplet formation. Biol. Cell *103*, 271–285.

Hartenstein, V. (1993). Atlas of Drosophila development (Cold Spring Harbor Laboratory Press).

Hay, B. a, Wolff, T., and Rubin, G.M. (1994). Expression of baculovirus P35 prevents cell death in Drosophila. Development *120*, 2121–2129.

Higa, L.A.A., Mihaylov, I.S., Banks, D.P., Zheng, J., and Zhang, H. (2003). Radiation-mediated proteolysis of CDT1 by CUL4-ROC1 and CSN complexes constitutes a new checkpoint. Nat. Cell Biol. *5*, 1008–1015.

References

Hildebrandt, A., Bickmeyer, I., and Kühnlein, R.P. (2011). Reliable Drosophila body fat quantification by a coupled colorimetric assay. PLoS One *6*, e23796.

Hogan, P.G., Chen, L., Nardone, J., and Rao, A. (2003). Transcriptional regulation by calcium, calcineurin, and NFAT. Genes Dev. *17*, 2205–2232.

Hong, S.-H., Lee, K.-S., Kwak, S.-J., Kim, A.-K., Bai, H., Jung, M.-S., Kwon, O.-Y., Song, W.-J., Tatar, M., and Yu, K. (2012). Minibrain/Dyrk1a regulates food intake through the Sir2-FOXO-sNPF/NPY pathway in Drosophila and mammals. PLoS Genet. *8*, e1002857.

Van der Horst, D.J., Van Marrewijk, W.J., and Diederen, J.H. (2001). Adipokinetic hormones of insect: release, signal transduction, and responses. Int. Rev. Cytol. *211*, 179–240.

Houtkooper, R., Williams, R., and Auwerx, J. (2010). Metabolic networks of longevity. Cell *142*, 1–10.

Huang, H., Wu, W., Zhang, L., and Liu, X.-Y. (2013). Drosophila ste-20 family protein kinase, hippo, modulates fat cell proliferation. PLoS One *8*, e61740.

Iijima, K., Zhao, L., Shenton, C., and Iijima-Ando, K. (2009). Regulation of energy stores and feeding by neuronal and peripheral CREB activity in Drosophila. PLoS One *4*, e8498.

Ja, W.W., Carvalho, G.B., Mak, E.M., de la Rosa, N.N., Fang, A.Y., Liong, J.C., Brummel, T., and Benzer, S. (2007). Prandiology of Drosophila and the CAFE assay. Proc. Natl. Acad. Sci. U. S. A. *104*, 8253–8256.

Jones, B.H., Kim, J.H., Zemel, M.B., Woychik, R.P., Michaud, E.J., Wilkison, W.O., and Moustaid, N. (1996). Upregulation of adipocyte metabolism by agouti protein: possible paracrine actions in yellow mouse obesity. Am. J. Physiol. *270*, E192–E196.

Kahsai, L., Kapan, N., Dircksen, H., Winther, A.M.E., and Nässel, D.R. (2010). Metabolic stress responses in Drosophila are modulated by brain neurosecretory cells that produce multiple neuropeptides. PLoS One *5*, e11480.

Kar, P., Bakowski, D., Di Capite, J., Nelson, C., and Parekh, A.B. (2012). Different agonists recruit different stromal interaction molecule proteins to support cytoplasmic Ca2+ oscillations and gene expression. Proc. Natl. Acad. Sci. U. S. A. *109*, 6969–6974.

Katewa, S.D., Demontis, F., Kolipinski, M., Hubbard, A., Gill, M.S., Perrimon, N., Melov, S., and Kapahi, P. (2012). Intramyocellular fatty-acid metabolism plays a critical role in mediating responses to dietary restriction in drosophila melanogaster. Cell Metab. *16*, 97–103.

Kennerdell, J.R., and Carthew, R.W. (2000). Heritable gene silencing in Drosophila using double-stranded RNA. Nat. Biotechnol. *18*, 896–898.

Kim, S.K., and Rulifson, E.J. (2004). Conserved mechanisms of glucose sensing and regulation by Drosophila corpora cardiaca cells. Nature *431*, 316–320.

Kim, M.-S., Pak, Y.K., Jang, P.-G., Namkoong, C., Choi, Y.-S., Won, J.-C., Kim, K.-S., Kim, S.-W., Kim, H.-S., Park, J.-Y., *et al.* (2006). Role of hypothalamic Foxo1 in the regulation of food intake and energy homeostasis. Nat. Neurosci. *9*, 901–906.

References

Kirchhausen, T. (2000). Three ways to make a vesicle. Nat. Rev. Mol. Cell Biol. *1*, 187–198.

Kodrík, D., Socha, R., Simek, P., Zemek, R., and Goldsworthy, G.J. (2000). A new member of the AKH/RPCH family that stimulates locomotory activity in the firebug, Pyrrhocoris apterus (Heteroptera). Insect Biochem. Mol. Biol. *30*, 489–498.

Konuma, T., Morooka, N., Nagasawa, H., and Nagata, S. (2012). Knockdown of the adipokinetic hormone receptor increases feeding frequency in the two-spotted cricket Gryllus bimaculatus. Endocrinology *153*, 1–12.

Krahmer, N., Guo, Y., Wilfling, F., Hilger, M., Lingrell, S., Heger, K., Newman, H.W., Schmidt-Supprian, M., Vance, D.E., Mann, M., *et al.* (2011). Phosphatidylcholine synthesis for lipid droplet expansion is mediated by localized activation of CTP:phosphocholine cytidylyltransferase. Cell Metab. *14*, 504–515.

Kroemer, G., Galluzzi, L., and Brenner, C. (2007). Mitochondrial membrane permeabilization in cell death. Physiol. Rev. *87*, 99–163.

Kucherenko, M.M., Marrone, A.K., Rishko, V.M., Magliarelli, H. de F., and Shcherbata, H.R. (2011). Stress and muscular dystrophy: a genetic screen for dystroglycan and dystrophin interactors in Drosophila identifies cellular stress response components. Dev. Biol. *352*, 228–242.

Kühnlein, R. (2011). The contribution of the Drosophila model to lipid droplet research. Prog. Lipid Res. *50*, 348–356.

Lass, A., Zimmermann, R., Haemmerle, G., Riederer, M., Schoiswohl, G., Schweiger, M., Kienesberger, P., Strauss, J.G., Gorkiewicz, G., and Zechner, R. (2006). Adipose triglyceride lipase-mediated lipolysis of cellular fat stores is activated by CGI-58 and defective in Chanarin-Dorfman Syndrome. Cell Metab. *3*, 309–319.

Lee, G., and Park, J.H. (2004). Hemolymph sugar homeostasis and starvation-induced hyperactivity affected by genetic manipulations of the adipokinetic hormone-encoding gene in Drosophila melanogaster. Genetics *167*, 311–323.

Lee, M.J., and Goldsworthy, G.J. (1995). The preparation and use of dispersed cells from fat body of Locusta migratoria in a filtration plate assay for adipokinetic peptides. Anal. Biochem. *228*, 155–161.

Lee, K.-S., You, K.-H., Choo, J.-K., Han, Y.-M., and Yu, K. (2004). Drosophila short neuropeptide F regulates food intake and body size. J. Biol. Chem. *279*, 50781–50789.

Leevers, S.J., Weinkove, D., MacDougall, L.K., Hafen, E., and Waterfield, M.D. (1996). The Drosophila phosphoinositide 3-kinase Dp110 promotes cell growth. EMBO J. *15*, 6584–6594.

Leonardi, R., Frank, M.W., Jackson, P.D., Rock, C.O., and Jackowski, S. (2009). Elimination of the CDP-ethanolamine pathway disrupts hepatic lipid homeostasis. J. Biol. Chem. *284*, 27077–27089.

Lim, H.-Y., Wang, W., Wessells, R.J., Ocorr, K., and Bodmer, R. (2011). Phospholipid homeostasis regulates lipid metabolism and cardiac function through SREBP signaling in Drosophila. Genes Dev. *25*, 189–200.

References

Lindemans, M., Janssen, T., Beets, I., Temmerman, L., Meelkop, E., and Schoofs, L. (2011). Gonadotropin-releasing hormone and adipokinetic hormone signaling systems share a common evolutionary origin. Front. Endocrinol. (Lausanne). *2*, 16.

Liu, P., Ying, Y., Zhao, Y., Mundy, D.I., Zhu, M., and Anderson, R.G.W. (2004). Chinese hamster ovary K2 cell lipid droplets appear to be metabolic organelles involved in membrane traffic. J. Biol. Chem. *279*, 3787–3792.

Londos, C., Sztalryd, C., Tansey, J.T., and Kimmel, A.R. (2005). Role of PAT proteins in lipid metabolism. Biochimie *87*, 45–49.

Lorenz, M.W. (2001). Synthesis of lipids in the fat body of Gryllus bimaculatus: age-dependency and regulation by adipokinetic hormone. Arch. Insect Biochem. Physiol. *47*, 198–214.

Lorenz, M.W., and Gäde, G. (2009). Hormonal regulation of energy metabolism in insects as a driving force for performance. Integr. Comp. Biol. *49*, 380–392.

Lum, P.Y., and Chino, H. (1990). Primary role of adipokinetic hormone in the formation of low density lipophorin in locusts. J. Lipid Res. *31*, 2039–2044.

Manjarrés, I.M., Rodríguez-García, A., Alonso, M.T., and García-Sancho, J. (2010). The sarco/endoplasmic reticulum Ca(2+) ATPase (SERCA) is the third element in capacitative calcium entry. Cell Calcium *47*, 412–418.

Marrone, A.K., Kucherenko, M.M., Wiek, R., Göpfert, M.C., and Shcherbata, H.R. (2011). Hyperthermic seizures and aberrant cellular homeostasis in Drosophila dystrophic muscles. Sci. Rep. *1*, 47.

Masuyama, K., Zhang, Y., Rao, Y., and Wang, J.W. (2012). Mapping neural circuits with activity-dependent nuclear import of a transcription factor. J. Neurogenet. *26*, 89–102.

McGuire, S.E., Le, P.T., Osborn, A.J., Matsumoto, K., and Davis, R.L. (2003). Spatiotemporal rescue of memory dysfunction in Drosophila. Science *302*, 1765–1768.

McGuire, S.E., Mao, Z., and Davis, R.L. (2004). Spatiotemporal gene expression targeting with the TARGET and gene-switch systems in Drosophila. Sci. STKE *2004*, pl6.

McNew, J.A., Sogaard, M., Lampen, N.M., Machida, S., Ye, R.R., Lacomis, L., Tempst, P., Rothman, J.E., and Söllner, T.H. (1997). Ykt6p, a prenylated SNARE essential for endoplasmic reticulum-Golgi transport. J. Biol. Chem. *272*, 17776–17783.

Meister, G., and Tuschl, T. (2004). Mechanisms of gene silencing by double-stranded RNA. Nature *431*, 343–349.

Montague, C.T., Farooqi, I.S., Whitehead, J.P., Soos, M.A., Rau, H., Wareham, N.J., Sewter, C.P., Digby, J.E., Mohammed, S.N., Hurst, J.A., *et al.* (1997). Congenital leptin deficiency is associated with severe early-onset obesity in humans.

Moran, T.H., and McHugh, P.R. (1982). Cholecystokinin suppresses food intake by inhibiting gastric emptying. Am. J. Physiol. *242*, R491–7.

References

Murphy, D.J. (2001). The biogenesis and functions of lipid bodies in animals, plants and microorganisms. Prog. Lipid Res. *40*, 325–438.

Murphy, D.J. (2012). The dynamic roles of intracellular lipid droplets: from archaea to mammals. Protoplasma *249*, 541–585.

Nair, U., Jotwani, A., Geng, J., Gammoh, N., Richerson, D., Yen, W.-L., Griffith, J., Nag, S., Wang, K., Moss, T., *et al.* (2011). SNARE proteins are required for macroautophagy. Cell *146*, 290–302.

Nässel, D.R., and Wegener, C. (2011). A comparative review of short and long neuropeptide F signaling in invertebrates: Any similarities to vertebrate neuropeptide Y signaling? Peptides *32*, 1335–1355.

Natter, K., Leitner, P., Faschinger, A., Wolinski, H., McCraith, S., Fields, S., and Kohlwein, S.D. (2005). The spatial organization of lipid synthesis in the yeast Saccharomyces cerevisiae derived from large scale green fluorescent protein tagging and high resolution microscopy. Mol. Cell. Proteomics *4*, 662–672.

Neal, J.W., and Clipstone, N.A. (2002). Calcineurin mediates the calcium-dependent inhibition of adipocyte differentiation in 3T3-L1 cells. J. Biol. Chem. *277*, 49776–49781.

Norum, M., Tång, E., Chavoshi, T., Schwarz, H., Linke, D., Uv, A., and Moussian, B. (2010). Trafficking through COPII stabilises cell polarity and drives secretion during Drosophila epidermal differentiation. PLoS One *5*, e10802.

Noyes, B.E., Katz, F.N., and Schaffer, M.H. (1995). Identification and expression of the Drosophila adipokinetic hormone gene. Mol. Cell. Endocrinol. *109*, 133–141.

Ntambi, J.M., and Takova, T. (1996). Role of Ca2+ in the early stages of murine adipocyte differentiation as evidenced by calcium mobilizing agents. Differentiation. *60*, 151–158.

Oldham, S., Stocker, H., Laffargue, M., Wittwer, F., Wymann, M., and Hafen, E. (2002). The Drosophila insulin/IGF receptor controls growth and size by modulating PtdInsP(3) levels. Development *129*, 4103–4109.

Orchard, I., Carlisle, J.A., Loughton, B.G., Gole, J.W., and Downer, R.G. (1982). In vitro studies on the effects of octopamine on locust fat body. Gen. Comp. Endocrinol. *48*, 7–13.

Ostlund, G., Schmitt, T., Forslund, K., Köstler, T., Messina, D.N., Roopra, S., Frings, O., and Sonnhammer, E.L.L. (2010). InParanoid 7: new algorithms and tools for eukaryotic orthology analysis. Nucleic Acids Res. *38*, D196–203.

Palanker, L., Tennessen, J., Lam, G., and Thummel, C. (2009). Drosophila HNF4 Regulates Lipid Mobilization and β-Oxidation. Cell Metab. *9*, 228–239.

Patel, R.T., Soulages, J.L., Hariharasundaram, B., and Arrese, E.L. (2005). Activation of the lipid droplet controls the rate of lipolysis of triglycerides in the insect fat body. J. Biol. Chem. *280*, 22624–22631.

Piccin, a, Salameh, A., Benna, C., Sandrelli, F., Mazzotta, G., Zordan, M., Rosato, E., Kyriacou, C.P., and Costa, R. (2001). Efficient and heritable functional knock-out of an adult phenotype in Drosophila using a GAL4-driven hairpin RNA incorporating a heterologous spacer. Nucleic Acids Res. *29*, E55.

References

Pignoni, F., and Zipursky, S.L. (1997). Induction of Drosophila eye development by decapentaplegic. Development *124*, 271–278.

Pizzo, P., Lissandron, V., Capitanio, P., and Pozzan, T. (2011). Ca(2+) signalling in the Golgi apparatus. Cell Calcium *50*, 184–192.

Ponton, F., Chapuis, M.-P., Pernice, M., Sword, G. a, and Simpson, S.J. (2011). Evaluation of potential reference genes for reverse transcription-qPCR studies of physiological responses in Drosophila melanogaster. J. Insect Physiol. *57*, 840–850.

Pospisilik, J.A., Schramek, D., Schnidar, H., Cronin, S.J.F., Nehme, N.T., Zhang, X., Knauf, C., Cani, P.D., Aumayr, K., Todoric, J., *et al.* (2010). Drosophila genome-wide obesity screen reveals hedgehog as a determinant of brown versus white adipose cell fate. Cell *140*, 148–160.

Puig, O., Marr, M.T., Ruhf, M.L., and Tjian, R. (2003). Control of cell number by Drosophila FOXO: downstream and feedback regulation of the insulin receptor pathway. Genes Dev. *17*, 2006–2020.

Puseenam, A., Yoshioka, Y., Nagai, R., Hashimoto, R., Suyari, O., Itoh, M., Enomoto, A., Takahashi, M., and Yamaguchi, M. (2009). A novel Drosophila Girdin-like protein is involved in Akt pathway control of cell size. Exp. Cell Res. *315*, 3370–3380.

Rajan, A., and Perrimon, N. (2012). Drosophila cytokine unpaired 2 regulates physiological homeostasis by remotely controlling insulin secretion. Cell *151*, 123–137.

Reis, T., Van Gilst, M.R., and Hariharan, I.K. (2010). A buoyancy-based screen of Drosophila larvae for fat-storage mutants reveals a role for Sir2 in coupling fat storage to nutrient availability. PLoS Genet. *6*, e1001206.

Reiter, L.T., Potocki, L., Chien, S., Gribskov, M., and Bier, E. (2001). A systematic analysis of human disease-associated gene sequences in Drosophila melanogaster. Genome Res. *11*, 1114–1125.

Renault, a D., Sigal, Y.J., Morris, a J., and Lehmann, R. (2004). Soma-germ line competition for lipid phosphate uptake regulates germ cell migration and survival. Science *305*, 1963–1966.

Rizzuto, R., Pinton, P., Ferrari, D., Chami, M., Szabadkai, G., Magalhães, P.J., Di Virgilio, F., and Pozzan, T. (2003). Calcium and apoptosis: facts and hypotheses. Oncogene *22*, 8619–8627.

Roman, G., Endo, K., Zong, L., and Davis, R.L. (2001). P[Switch], a system for spatial and temporal control of gene expression in Drosophila melanogaster. Proc. Natl. Acad. Sci. U. S. A. *98*, 12602–12607.

Roos, J., DiGregorio, P.J., Yeromin, A. V, Ohlsen, K., Lioudyno, M., Zhang, S., Safrina, O., Kozak, J.A., Wagner, S.L., Cahalan, M.D., *et al.* (2005). STIM1, an essential and conserved component of store-operated Ca2+ channel function. J. Cell Biol. *169*, 435–445.

Rulifson, E.J., Kim, S.K., and Nusse, R. (2002). Ablation of insulin-producing neurons in flies: growth and diabetic phenotypes. Science *296*, 1118–1120.

Screaton, R.A., Conkright, M.D., Katoh, Y., Best, J.L., Canettieri, G., Jeffries, S., Guzman, E., Niessen, S., Yates, J.R., Takemori, H., *et al.* (2004). The CREB coactivator TORC2 functions as a calcium- and cAMP-sensitive coincidence detector. Cell *119*, 61–74.

References

Seegmiller, A.C., Dobrosotskaya, I., Goldstein, J.L., Ho, Y.K., Brown, M.S., and Rawson, R.B. (2002). The SREBP pathway in Drosophila: regulation by palmitate, not sterols. Dev. Cell *2*, 229–238.

Shi, H., Halvorsen, Y.D., Ellis, P.N., Wilkison, W.O., and Zemel, M.B. (2000). Role of intracellular calcium in human adipocyte differentiation. Physiol Genomics *3*, 75–82.

Shiga, Y., Tanaka-Matakatsu, M., and Hayashi, S. (1996). A nuclear GFP/ß-galactoside fusion protein as a marker for morphogenesis in living Drosophila. Dev. Growth Differ. *38*, 99–106.

Short, S.M., and Lazzaro, B.P. (2013). Reproductive status alters transcriptomic response to infection in female Drosophila melanogaster. G3 (Bethesda). *3*, 827–840.

Singh, R., Kaushik, S., Wang, Y., Xiang, Y., Novak, I., Komatsu, M., Tanaka, K., Cuervo, A.M., and Czaja, M.J. (2009). Autophagy regulates lipid metabolism. Nature *458*, 1131–1135.

Singh, R.K., Fullerton, M.D., Vine, D., and Bakovic, M. (2012). Mechanism of hypertriglyceridemia in CTP:phosphoethanolamine cytidylyltransferase-deficient mice. J. Lipid Res. *53*, 1811–1822.

Skorupa, D.A., Dervisefendic, A., Zwiener, J., and Pletcher, S.D. (2008). Dietary composition specifies consumption, obesity, and lifespan in Drosophila melanogaster. Aging Cell *7*, 478–490.

Smith, R.K., Carroll, P.M., Allard, J.D., and Simon, M. a (2002). MASK, a large ankyrin repeat and KH domain-containing protein involved in Drosophila receptor tyrosine kinase signaling. Development *129*, 71–82.

Smith, S.J., Cases, S., Jensen, D.R., Chen, H.C., Sande, E., Tow, B., Sanan, D.A., Raber, J., Eckel, R.H., and Farese, R. V (2000). Obesity resistance and multiple mechanisms of triglyceride synthesis in mice lacking Dgat. Nat. Genet. *25*, 87–90.

Smyth, J.T., and Putney, J.W. (2012). Regulation of store-operated calcium entry during cell division. Biochem. Soc. Trans. *40*, 119–123.

Soboloff, J., Rothberg, B.S., Madesh, M., and Gill, D.L. (2012). STIM proteins: dynamic calcium signal transducers. Nat. Rev. Mol. Cell Biol. *13*, 549–565.

Song, W., Ren, D., Li, W., Jiang, L., Cho, K.W., Huang, P., Fan, C., Song, Y., Liu, Y., and Rui, L. (2010). SH2B regulation of growth, metabolism, and longevity in both insects and mammals. Cell Metab. *11*, 427–437.

Spandl, J., White, D.J., Peychl, J., and Thiele, C. (2009). Live cell multicolor imaging of lipid droplets with a new dye, LD540. Traffic *10*, 1579–1584.

Speakman, J. (2004). Obesity: the integrated roles of environment and genetics. J. Nutr. *JN*, 2090–2105.

Speakman, J.R. (2013). Evolutionary perspectives on the obesity epidemic: adaptive, maladaptive, and neutral viewpoints. Annu. Rev. Nutr. *33*, 289–317.

Spencer, I.M., and Candy, D.J. (1976). Hormonal control of diacyl glycerol mobilization from fat body of the desert locust, Schistocerca gregaria. Insect Biochem. *6*, 289–296.

References

Spradling, A.C., and Rubin, G.M. (1982). Transposition of cloned P elements into Drosophila germ line chromosomes. Science *218*, 341–347.

Srikanth, S., Banerjee, S., and Hasan, G. (2006). Ectopic expression of a Drosophila InsP(3)R channel mutant has dominant-negative effects in vivo. Cell Calcium *39*, 187–196.

Stanisz, H., Saul, S., Müller, C.S.L., Kappl, R., Niemeyer, B.A., Vogt, T., Hoth, M., Roesch, A., and Bogeski, I. (2014). Inverse regulation of melanoma growth and migration by Orai1/STIM2-dependent calcium entry. Pigment Cell Melanoma Res.

Starz-Gaiano, M., Cho, N.K., Forbes, a, and Lehmann, R. (2001). Spatially restricted activity of a Drosophila lipid phosphatase guides migrating germ cells. Development *128*, 983–991.

Stathopulos, P.B., Zheng, L., Li, G.-Y., Plevin, M.J., and Ikura, M. (2008). Structural and mechanistic insights into STIM1-mediated initiation of store-operated calcium entry. Cell *135*, 110–122.

Staubli, F., Jorgensen, T.J.D., Cazzamali, G., Williamson, M., Lenz, C., Sondergaard, L., Roepstorff, P., and Grimmelikhuijzen, C.J.P. (2002). Molecular identification of the insect adipokinetic hormone receptors. Proc. Natl. Acad. Sci. U. S. A. *99*, 3446–3451.

Stone, J. V, Mordue, W., Batley, K.E., and Morris, H.R. (1976). Structure of locust adipokinetic hormone, a neurohormone that regulates lipid utilisation during flight. Nature *263*, 207–211.

Streb H, Irvine RF, Berridge MJ, S.I. (1983). Release of Ca2+ from a nonmitochondrial intracellular store in pancreatic acinar cells by inositol-1,4,5-trisphosphate. Nature *3-9*, 67–9.

Stryer, L., Berg, J.M., and Tymoczko, J.L. (2012). Biochemistry (New York: W. H. Freeman and Company).

Subramanian, M., Metya, S.K., Sadaf, S., Kumar, S., Schwudke, D., and Hasan, G. (2013). Altered lipid homeostasis in Drosophila InsP3 receptor mutants leads to obesity and hyperphagia. Dis. Model. Mech. *6*, 734–744.

Suh, J., Zeve, D., McKay, R., Seo, J., Salo, Z., and Li, R. (2007). Adipose Is a Conserved Dosage-Sensitive Antiobesity Gene. Cell Metab. *6*, 195–207.

Sujkowski, A., Saunders, S., Tinkerhess, M., Piazza, N., Jennens, J., Healy, L., Zheng, L., and Wessells, R. (2012). dFatp regulates nutrient distribution and long-term physiology in Drosophila. Aging Cell *11*, 921–932.

Talamillo, A., Herboso, L., Pirone, L., Pérez, C., González, M., Sánchez, J., Mayor, U., Lopitz-Otsoa, F., Rodriguez, M.S., Sutherland, J.D., *et al.* (2013). Scavenger receptors mediate the role of SUMO and Ftz-f1 in Drosophila steroidogenesis. PLoS Genet. *9*, e1003473.

Tatar, M., Kopelman, A., Epstein, D., Tu, M.P., Yin, C.M., and Garofalo, R.S. (2001). A mutant Drosophila insulin receptor homolog that extends life-span and impairs neuroendocrine function. Science *292*, 107–110.

Thomenius, M., Freel, C.D., Horn, S., Krieser, R., Abdelwahid, E., Cannon, R., Balasundaram, S., White, K., and Kornbluth, S. (2011). Mitochondrial fusion is regulated by Reaper to modulate Drosophila programmed cell death. Cell Death Differ. *18*, 1640–1650.

References

Umlauf, E., Csaszar, E., Moertelmaier, M., Schuetz, G.J., Parton, R.G., and Prohaska, R. (2004). Association of stomatin with lipid bodies. J. Biol. Chem. *279*, 23699–23709.

Venkiteswaran, G., and Hasan, G. (2009). Intracellular Ca2+ signaling and store-operated Ca2+ entry are required in Drosophila neurons for flight. Proc. Natl. Acad. Sci. U. S. A. *106*, 10326–10331.

Vig, M., Peinelt, C., Beck, a, Koomoa, D.L., Rabah, D., Koblan-Huberson, M., Kraft, S., Turner, H., Fleig, a, Penner, R., *et al.* (2006). CRACM1 is a plasma membrane protein essential for store-operated Ca2+ entry. Science *312*, 1220–1223.

Vroemen, S.F., Van Marrewijk, W.J., Schepers, C.C., and Van der Horst, D.J. (1995). Signal transduction of adipokinetic hormones involves Ca2+ fluxes and depends on extracellular Ca2+ to potentiate cAMP-induced activation of glycogen phosphorylase. Cell Calcium *17*, 459–467.

Wang, B., Goode, J., Best, J., Meltzer, J., Schilman, P.E., Chen, J., Garza, D., Thomas, J.B., and Montminy, M. (2008). The insulin-regulated CREB coactivator TORC promotes stress resistance in Drosophila. Cell Metab. *7*, 434–444.

Wang, B., Moya, N., Niessen, S., Hoover, H., Mihaylova, M.M., Shaw, R.J., Yates, J.R., Fischer, W.H., Thomas, J.B., and Montminy, M. (2011). A hormone-dependent module regulating energy balance. Cell *145*, 596–606.

Wang, C., Liu, Z., and Huang, X. (2012a). Rab32 Is Important for Autophagy and Lipid Storage in Drosophila. PLoS One *7*, e32086.

Wang, W., Sacher, M., and Ferro-Novick, S. (2000). TRAPP stimulates guanine nucleotide exchange on Ypt1p. J. Cell Biol. *151*, 289–296.

Wang, Y., Li, G., Goode, J., Paz, J.C., Ouyang, K., Screaton, R., Fischer, W.H., Chen, J., Tabas, I., and Montminy, M. (2012b). Inositol-1,4,5-trisphosphate receptor regulates hepatic gluconeogenesis in fasting and diabetes. Nature *485*, 128–132.

Wang, Z., Hayakawa, Y., and Downer, R.G.H. (1990). Factors influeincing cyclic AMP and diacylglycerol levels in fat body of Locusta migratoria. Insect Biochem. *20*, 325–330.

Welte, M.A., Gross, S.P., Postner, M., Block, S.M., and Wieschaus, E.F. (1998). Developmental Regulation of Vesicle Transport in Drosophila Embryos: Forces and Kinetics. Cell *92*, 547–557.

White, J.D., Olchovsky, D., Kershaw, M., and Berelowitz, M. (1990). Increased hypothalamic content of preproneuropeptide-Y messenger ribonucleic acid in streptozotocin-diabetic rats. Endocrinology *126*, 765–772.

Wolber, P.K., Collins, P.J., Lucas, A.B., De Witte, A., and Shannon, K.W. (2006). The Agilent in situ-synthesized microarray platform. Methods Enzymol. *410*, 28–57.

Wu, C.C., Howell, K.E., Neville, M.C., Yates, J.R., and McManaman, J.L. (2000). Proteomics reveal a link between the endoplasmic reticulum and lipid secretory mechanisms in mammary epithelial cells. Electrophoresis *21*, 3470–3482.

Wu, Q., Zhang, Y., Xu, J., and Shen, P. (2005). Regulation of hunger-driven behaviors by neural ribosomal S6 kinase in Drosophila. Proc. Natl. Acad. Sci. U. S. A. *102*, 13289–13294.

References

Xue, B., Moustaid-N, Wilkison, W.O., and Zemel, M.B. (1998). The agouti gene product inhibits lipolysis in human adipocytes via a Ca2+-dependent mechanism. FASEB J. *12*, 1391–1396.

Yang, H., He, X., Yang, J., Deng, X., Liao, Y., Zhang, Z., Zhu, C., Shi, Y., and Zhou, N. (2013). Activation of cAMP-response element-binding protein is positively regulated by PKA and calcium-sensitive calcineurin and negatively byPKC in insect. Insect Biochem. Mol. Biol. *43*, 1028–1036.

Yang, T.T.C., Suk, H.Y., Yang, X., Olabisi, O., Yu, R.Y.L., Durand, J., Jelicks, L.A., Kim, J.-Y., Scherer, P.E., Wang, Y., *et al.* (2006). Role of transcription factor NFAT in glucose and insulin homeostasis. Mol. Cell. Biol. *26*, 7372–7387.

Yuan, J.P., Zeng, W., Dorwart, M.R., Choi, Y.-J., Worley, P.F., and Muallem, S. (2009). SOAR and the polybasic STIM1 domains gate and regulate Orai channels. Nat. Cell Biol. *11*, 337–343.

Zechner, R., Zimmermann, R., Eichmann, T.O., Kohlwein, S.D., Haemmerle, G., Lass, A., and Madeo, F. (2012). FAT SIGNALS--lipases and lipolysis in lipid metabolism and signaling. Cell Metab. *15*, 279–291.

Zhang, L.L., Yan Liu, D., Ma, L.Q., Luo, Z.D., Cao, T.B., Zhong, J., Yan, Z.C., Wang, L.J., Zhao, Z.G., Zhu, S.J., *et al.* (2007). Activation of transient receptor potential vanilloid type-1 channel prevents adipogenesis and obesity. Circ. Res. *100*, 1063–1070.

Zhang, S.L., Yeromin, A. V, Zhang, X.H.-F., Yu, Y., Safrina, O., Penna, A., Roos, J., Stauderman, K. a, and Cahalan, M.D. (2006). Genome-wide RNAi screen of Ca(2+) influx identifies genes that regulate Ca(2+) release-activated Ca(2+) channel activity. Proc. Natl. Acad. Sci. U. S. A. *103*, 9357–9362.

Ziegler, R., Jasensky, R.D., and Morimoto, H. (1995). Characterization of the adipokinetic hormone receptor form the fat body of Manduca sexta. Regul. Pept. *57*, 329–338.

Zimmermann, R., Strauss, J.G., Haemmerle, G., Schoiswohl, G., Birner-Gruenberger, R., Riederer, M., Lass, A., Neuberger, G., Eisenhaber, F., Hermetter, A., *et al.* (2004). Fat mobilization in adipose tissue is promoted by adipose triglyceride lipase. Science *306*, 1383–1386.

Zinke, I., Schütz, C.S., Katzenberger, J.D., Bauer, M., and Pankratz, M.J. (2002). Nutrient control of gene expression in Drosophila: microarray analysis of starvation and sugar-dependent response. EMBO J. *21*, 6162–6173.

Zoog, S.J., Bertin, J., and Friesen, P.D. (1999). Caspase inhibition by baculovirus P35 requires interaction between the reactive site loop and the beta-sheet core. J. Biol. Chem. *274*, 25995–26002.

7 Summary

One main goal for all organisms, in order to survive under environmental changes, is to maintain energy homeostasis. Energy homeostasis depends mainly on three processes, the energy uptake, energy storage and energy consumption, respectively. An impairment of energy homeostasis or the lipid metabolism can cause body fat accumulation, which could finally lead to obesity. Since the outspread of obesity widely increased over the last years, the need to unveil new regulators of body fat storage rises. In order to identify novel body fat storage regulators, we used the fruit fly *Drosophila melanogaster* to do a conditional *in vivo* RNAi knockdown (KD) screen in the fat storage tissue of adult flies. Hereby, lethality due to developmental impairment can be excluded, which allows to screen for novel regulators in adult flies. By this approach, 6796 genes were down-regulated directly in the fat storage tissue of the fly and the body fat levels were determined. By further validations, I was able to identify 77 gene KDs, which resulted in obese or lean flies. Notably, most of the identified genes and processes are conserved up to humans. A Gene Ontology analysis of these genes revealed several processes, including store-operated calcium entry (SOCE), which was so far unrelated to body fat storage control. Interestingly, modulations of SOCE genes, which resulted in decreased intracellular Ca^{2+} levels (iCa^{2+}) causes obesity in flies. Controversial, modulations that leads to increased iCa^{2+} resulted in lean flies. In order to reveal the role of SOCE for body fat storage control, I characterized the effects of the central component known as the Stromal interaction molecule (Stim). A *Stim* KD in the fat storage tissue of mature adult flies resulted in decreased iCa^{2+} and obese flies, which also showed an increase in fat cell mass, likely driven through hypertrophy and hyperplasia. Further characterization of these flies revealed no effects on the activity or the metabolic rate, indicating that the body fat accumulation is independent from the energy expenditure. On the other hand, *Stim* KD flies show hyperphagia, which is driven by up-regulation of the orexigenic short neuropeptide F (sNPF) in the central nervous system of the fly. This regulation and the enriched energy intake drives an obesogenic program in the fat storage tissue of *Stim* KD flies, by up-regulation of the lipogenic *mdy/DmDGAT1* and down-regulation of the lipolytic *bmm/DmATGL* genes. These findings suggest a control of the energy storage, which is driven by SOCE *via* an inter-organ communication signaling pathway.

8 Lebenslauf

<u>Persönliche Daten</u>

Name:	Baumbach, Jens
Geburtstag/-ort:	17.08.1982 in Soltau
Wohnort/Strasse/Nr.:	37077 Göttingen, Hannoversche Str 152, WE 61
Tel. Nr.:	0175-1112159
Email-Adresse:	jbaumba@gmail.com
Konfession:	Evangelisch
Staatsangehörigkeit:	Deutsch

<u>Schulausbildung</u>

Sept. 1989 – Juni 1993:	Grundschule am Süllberg, Munster
Aug. 1993 – Juni 1995:	Orientierungsstufe Munster, Munster
Aug. 1995 – Juni 2003:	Gymnasium Munster, Munster
Schulabschluss:	Abitur
Sprachen:	Englisch, 9 Jahre (Schulwissen), 3 Jahre (angewandtes Wissen)
	Latein, 5 Jahre (Schulwissen)

<u>Beruflicher Werdegang</u>

Juli. 2003 – Juli 2005:	Bundeswehr, Zeitsoldat (Offizier der Reserve) bei PzPiLKp 90 in Munster
Okt. 2005 – März 2010:	Biologiestudium (Dipl.), Georg-August-Universität, Göttingen:

> Vordiplom (Okt, 2007)
> Diplomprüfung (08.07.2009)
> > Hauptfach: Mikrobiologie
> > 1. Nebenfach: Biochemie
> > 2. Nebenfach: Genetik
>
> Diplomarbeit (Abgabe: 31.03.2010)
> > "Auswirkungen von Wirtsmolekülen auf die Wirts-Pathogen Wechselwirkung" am Institut für Mikrobiolgie und Genetik bei Dr. Petra Neumann-Staubitz, Göttingen

Seit Mai 2010:	Promotion (Dr. rer. nat.), Max-Planck-Institut für biophysikalische Chemie, Abt. Molekulare Entwicklungsbiologie (Prof. Dr. H. Jäckle), Arbeitsgruppe Molekulare Physiologie (PD Dr. R. P. Kühnlein), Göttingen